

CHEMICAL AND PHYSICAL PROPERTIES OF
STARCH HYDROLYSIS PRODUCTS: A POLYMERIC PERSPECTIVE

A Thesis
Submitted to the Faculty
of
Graduate Studies
The University of Manitoba
by
Robert Stewart Swan

In Partial Fulfillment of the
Requirements for the Degree

of
Master of Science

Food Science Department

October, 1989



National Library
of Canada

Bibliothèque nationale
du Canada

Canadian Theses Service Service des thèses canadiennes

Ottawa, Canada
K1A 0N4

The author has granted an irrevocable non-exclusive licence allowing the National Library of Canada to reproduce, loan, distribute or sell copies of his/her thesis by any means and in any form or format, making this thesis available to interested persons.

The author retains ownership of the copyright in his/her thesis. Neither the thesis nor substantial extracts from it may be printed or otherwise reproduced without his/her permission.

L'auteur a accordé une licence irrévocable et non exclusive permettant à la Bibliothèque nationale du Canada de reproduire, prêter, distribuer ou vendre des copies de sa thèse de quelque manière et sous quelque forme que ce soit pour mettre des exemplaires de cette thèse à la disposition des personnes intéressées.

L'auteur conserve la propriété du droit d'auteur qui protège sa thèse. Ni la thèse ni des extraits substantiels de celle-ci ne doivent être imprimés ou autrement reproduits sans son autorisation.

ISBN 0-315-54932-7

Canada

CHEMICAL AND PHYSICAL PROPERTIES OF STARCH
HYDROLYSIS PRODUCTS:
A POLYMERIC PERSPECTIVE

BY

ROBERT STEWART SWAN

A thesis submitted to the Faculty of Graduate Studies of
the University of Manitoba in partial fulfillment of the requirements
of the degree of

MASTER OF SCIENCE

© 1989

Permission has been granted to the LIBRARY OF THE UNIVERSITY OF MANITOBA to lend or sell copies of this thesis, to the NATIONAL LIBRARY OF CANADA to microfilm this thesis and to lend or sell copies of the film, and UNIVERSITY MICROFILMS to publish an abstract of this thesis.

The author reserves other publication rights, and neither the thesis nor extensive extracts from it may be printed or otherwise reproduced without the author's written permission.

TO MY PARENTS

ACKNOWLEDGEMENTS

I would like to express my sincere gratitude to Dr. C.G. Biliaderis for his guidance and support throughout the course of my studies. His patience and understanding, as well as, his unlimited enthusiasm for the subject area instilled in me the drive required to complete this project.

I am also very grateful to Dr. E.D. Murray for his encouragement and support, J. Rogers for his technical assistance in the operation of the HPLC, P. Stephen for his computer expertise and to all other staff members and students of the Food Science Department, University of Manitoba for their friendship.

The financial assistance provided by Agriculture Canada is gratefully acknowledged.

Finally, special thanks are extended to my parents, brother and sister whose love has carried me through the rough times and helped me enjoy the good.

TABLE OF CONTENTS

	<u>PAGE</u>
TABLE OF CONTENTS	iii
LIST OF TABLES.	vi
LIST OF FIGURES	viii
ABSTRACT.	xi
1 INTRODUCTION	1
2 REVIEW OF LITERATURE	3
2.1 General Aspects Of Starch Chemistry	3
2.1.1 Major Starch Components.	3
A) Amylose	4
B) Amylopectin	4
2.1.2 The Starch Granule	9
A) Structure and Properties.	9
B) Gelatinization.	11
C) Gelation and Retrogradation	14
2.2 Starch Hydrolysis Products: Production And Properties	15
2.2.1 Introduction.	15
2.2.2 Commercial Production.	16
A) Acid Conversion	16
B) Enzymic Conversions	19
C) Final Processing	21
2.2.3 Characterization And Analysis	24

2.2.4	Properties And Applications.	25
2.3	Phase Transitions Of Polymeric Materials.	36
2.3.1	Glass Transition	36
2.3.2	Crystallization And Melting.	41
2.3.3	Factors Affecting T_g And T_m	42
	A) Chemical Structure.	45
	B) Molecular Weight And Chain Entanglement	48
	C) Branching	49
	D) Plasticizers And Polymer Blends	49
	E) Crosslinking And Crystallinity.	50
2.3.4	Methodologies Used To Probe Phase Transitions.	50
2.4	Phase Transition Behaviour Of Carbohydrate Materials.	55
2.4.1	Subzero Temperature Behaviour Of Frozen Aqueous-Carbohydrate Systems	55
2.4.2	Phase Behaviour Of Dry Carbohydrate Materials.	61
3	EXPERIMENTAL	63
3.1	Materials	63
3.2	Methods	63
3.2.1	Compositional Analysis Of SHPs	63
3.2.2	Evaluation Of The Thermal Behaviour Of Frozen Aqueous-SHP By DSC.	64
	A) General Procedures.	64
	B) Evaluation Of Thermal Parameters.	65
3.2.3	Kinetic Studies Of L-Ascorbic Acid Oxidation In Aqueous-SHPs.	66
3.2.4	Rheological Characterization Of SHPs	68
	A) Viscometry Studies.	68

B) Dynamic Rheometry Studies	68
3.2.5 Statistical Analyses	69
4 RESULTS AND DISCUSSION	70
4.1 Physico-chemical Properties Of Commercial SHPs.	70
4.2 Technological Implications Of Using SHPs In Food Formulations.	120
4.2.1 Reaction Kinetics Of Ascorbic Acid Oxidation.	125
4.2.2 Antistaling Properties Of SHPs	136
5 CONCLUSIONS AND RECOMMENDATIONS.	146
REFERENCES CITED.	151

LIST OF TABLES

<u>TABLE</u>	<u>PAGE</u>
1. Oligosaccharide composition of acid converted glucose syrups	26
2. Oligosaccharide composition of acid-enzyme converted glucose syrups	27
3. Oligosaccharide composition of enzyme-enzyme converted glucose syrups.	28
4. Functionality as a function of DE for commercial SHPs.	29
5. Tg' values for monodisperse glucose monomer and oligomer standards	73
6. Tg' values for commercial starch hydrolysates.	77
7. Viscosity of commercial starch hydrolysates at 20 and 40% (w/v) concentration.	83
8. Unfreezable water of glucose-based oligomers and commercial starch hydrolysates	96
9. Tg' values for monodisperse glucose-based oligomers and commercial starch hydrolysates at various concentrations	98
10. Oligosaccharide composition of various commercial starch hydrolysates.	111
11. Oligosaccharide composition of various debranched commercial starch hydrolysates	121
12. Effect of SHP incorporation on the oxidation kinetics of frozen ascorbic acid solutions stored at subzero temperatures	129
13. Effect of SHP incorporation on the oxidation kinetics of ascorbic acid solutions stored at above zero ($^{\circ}\text{C}$) temperatures	134
14. Effect of SHP on the retrogradation of gelatinized wheat starch (WS) samples.	140

15. Effect of SHP on the retrogradation of gelatinized
waxy maize (WM) starch samples 144

LIST OF FIGURES

<u>FIGURE</u>	<u>PAGE</u>
1. Chemical structure of amylose and amylopectin.	6
2. Proposed molecular structure for amylopectin	8
3. Schematic representation of the arrangement of amylopectin molecules within a growth ring of a starch granule	13
4. Generalized schematic for the manufacture of commercial SHPs	18
5. Generalized schematic for the final processing of commercial SHPs.	23
6. Relationship between viscosity and temperature for DE 42 glucose syrups manufactured by different conversion methods	32
7. Freezing point depression as a function of DE for glucose syrup fractions and commercial glucose syrups.	35
8. Generalized response of specific heat and specific volume as a function of temperature for three idealized polymers in the glass transition and melting temperature regions.	39
9. Molecular structure of a microcrystalline polymer.	44
10. Sources of free volume for plasticization: main chain "crankshaft" motion; chain end motion; side chain motion; and external plasticizer motion.	47
11. Phase changes from amorphous to crystalline in an idealized polymer.	53
12. Liquid-solid state diagram for a water-sucrose system.	58
13. Typical DSC thermal curve and its first derivative for an aqueous SHP (30% w/w)	72
14. Effect of molecular weight on the Tg' of aqueous monodisperse glucose monomer and oligomers at 30% w/w.	75

15.	Relationship between DE and Tg' of various polydisperse aqueous SHPs at 20% w/w.	80
16.	Viscosity as a function of shear rate for SHPs (40% w/v) of varying DE.	86
17.	Viscosity as a function of shear rate for 40% w/v Star-Dri 1 (DE 1.0).	88
18.	Viscosity as a function of DE of starch hydrolysates at 20% and 40% w/v	91
19.	Relationship between sample viscosity and Tg' for polydisperse aqueous starch hydrolysates at 20% w/w.	93
20.	Determination of unfreezable water for an aqueous starch hydrolysate (DE 20).	95
21.	Effect of solute concentration on Tg' for commercial SHPs of varying DE	102
22.	Effect of heating rate on Tg' for commercial SHPs of varying DE	105
23.	Prediction of Tg' for binary mixtures: maltose/maltoheptaose and Fro-Dex 42/Lo-Dex 5; 30% w/w total solids at various weight fractions for the two components.	108
24.	Typical HPLC chromatogram of a commercial SHP (Amaizo 42).	110
25.	Comparison between Tg'-predicted (Flory-Fox equation) and Tg'-measured (DSC) for polydisperse SHPs of varying DE	115
26.	Comparison between Tg'-predicted (Flory Fox equation) and Tg'-measured (DSC) for binary mixtures of monodisperse maltoheptaose + monodisperse glucose monomer and oligomers (1:1 w/w; 30% w/w total solids/H ₂ O).	117
27.	Comparison between Tg'-predicted (Flory-Fox equation) and Tg'-measured (DSC) for binary mixtures of Maltrin M040 + monodisperse glucose and maltose, and commercial SHPs (1:1 w/w; 30% w/w total solids/H ₂ O)	119
28.	Comparison between Tg'-predicted (Flory-Fox equation) and Tg'-measured for debranched polydisperse commercial SHPs of varying DE	124
29.	Ascorbic acid oxidation in a solution of acetate buffered (0.02M, pH 5.5) ascorbic acid (2.5 mg mL ⁻¹) containing H ₂ O ₂ (1500 ppm) and Maltrin M150 (20% w/v), stored at -4°C.	128

30. Effect of temperature on ascorbic acid oxidation kinetics
in frozen aqueous SHPs of varying DE 132
31. Effect of commercial SHPs on the gel strength (storage
modulus, G') of gelatinized wheat starch
(WS) samples 139
32. Effect of commercial SHPs on the gel strength (storage
modulus, G') of gelatinized waxy maize (WM) starch
samples. 143

ABSTRACT

The thermal and rheological properties of 35 commercial polydisperse starch hydrolysis products (SHPs), from corn and potato starch sources, in aqueous solution were studied. Starch hydrolysates ranged in dextrose equivalent (DE) from 0.5 to 42. Monodisperse glucose oligomers were used for comparative purposes.

A low temperature differential scanning calorimetry (DSC) technique was employed for determination of the glass transition temperature (T_g') of the concentrated solute in frozen aqueous SHP (20% w/v). An inverse linear correlation was observed between T_g' and DE for polydisperse SHPs ($r=-0.991$, $p<0.001$), and T_g' and reciprocal molecular weight for monodisperse oligosaccharide standards ($r=-0.990$, $p<0.001$). An upper T_g' limit, corresponding to the onset of polymer chain entanglement was attained at 257.23 K. For D-glucose and Star-Dri 42X, T_g' was independent of initial solute concentration, suggesting that a glass of constant composition was attained under equilibrium conditions where water was allowed to freeze. However, for all other carbohydrate samples tested, T_g' was depressed at high (>50% w/v) concentrations, possibly due to the plasticizing effect of additional water entrapped in the glass during non-equilibrium freezing.

Binary monodisperse and polydisperse mixtures exhibited single T_g' for the respective composite aqueous glasses. Using the Flory-Fox theory, predictive equations were derived to calculate T_g' of composite

carbohydrate mixtures in aqueous solutions. Similarly, a generalized form of the Flory-Fox equation was used to predict the T_g' of 21 commercial starch hydrolysates from their oligosaccharide composition, as determined by high performance liquid chromatography (HPLC), and the experimentally determined T_g' of the respective individual glucose oligomer standards. Oligosaccharides with a DP of 1-7 were effectively separated by HPLC. Differences in oligosaccharide distribution were obvious among samples of varying DE and from different suppliers. A linear relationship between T_g' -predicted (calculated from the Flory-Fox equation) and T_g' -measured (determined by DSC) was observed ($r=0.987$, $p<0.001$). However, it was noted that the measured values of T_g' deviated from what the theory predicted, particularly for high DE samples; i.e. in the presence of low molecular weight material the composite glass appeared to vitrify at a much lower temperature than that predicted assuming the Flory-Fox equation. Debranching of the starch hydrolysates, using a purified pullulanase preparation, did not significantly alter their oligosaccharide distribution, nor did it affect the linear relationship between T_g' -predicted and T_g' -measured.

Unfreezable water values, as determined by DSC, ranged from 0.12-0.35 g H₂O g⁻¹ solute for the starch hydrolysates examined. However, no apparent relationship between molecular size and unfreezable water content was found.

The rheological behaviour of aqueous solutions of SHPs was studied over a wide range of shear rates (9-1465 s⁻¹) and at concentrations of 20 and 40% w/v. Solution viscosity increased exponentially with decreasing solute DE. Viscosity values ranged from 2.90×10^3 - 3.94×10^4 Pa.s for

20% w/v samples and 6.92×10^3 - 2.72×10^6 Pa.s for 40% w/v solutions. The majority of SHPs tested, at 40% w/v, exhibited Newtonian behaviour. Star-Dri 1 (DE 1), was the only sample that demonstrated pseudoplastic (shear thinning) behaviour.

The performance of SHPs as stabilizing agents was assessed by monitoring the rate of oxidation of L-ascorbic acid in acetate buffer solutions containing starch hydrolysates at 20% and 40% w/v using UV spectroscopy. Samples were held under subzero (-4 to -16°C) and above zero (5-25°C) isothermal temperature storage regimes. Values for the reaction rate constant, k , varied between 1.30-13.90 min^{-1} for control samples and 0.04-10.10 min^{-1} for solutions containing SHP. Reaction rates at subzero temperatures appeared to be governed by Williams-Landel-Ferry kinetics.

The antistaling properties of SHPs in starch gels were examined by oscillatory rheological measurements using wheat and waxy maize starches. The observed pseudoplateau modulus, G' , values for wheat starch-SHP composite gels, after 10 hr storage, were up to 4X lower (0.76 kPa) than the values obtained for control (starch alone) samples (3.27 kPa). These results suggested that small molecular weight oligosaccharides inhibit interchain associations among amylose molecules exuded from the starch granules. On the other hand, incorporation of SHP into amylopectin gels did not seem to disrupt the gel network of this polysaccharide.

1 INTRODUCTION

The term starch hydrolysis products (SHPs) applies to a wide range of hydrolysates produced by treating granular starches with either acids or enzymes or combination of the two (Murray and Luft, 1973). A class of SHPs having a low degree of conversion is often referred to as maltodextrins. In the food industry, maltodextrins find use in a variety of applications. Being non-hygroscopic and having good solubility properties, they are used in spray-drying of seasonings, instant beverages (coffee, tea, fruit drinks), spices, flavours, enzymes as well as in fruit and vegetable concentrates (To and Flink, 1978a). Because of their body-imparting properties, they are also used as thickeners/stabilizers in puddings, creams, soups and ice cream mixes. Furthermore, maltodextrin gels are characterized by a neutral taste as well as their consistency and melting behaviour in the mouth that comes close to natural fats. Therefore, they can be used as fat substitutes wherever the fat acts in a conventional manner as a consistency former; e.g. in mayonnaise, cream cheeses, bread spreads, meat and sausage products, and whipped cream. With regard to freezer-storage stabilization of fabricated frozen foods, maltodextrins are effective against ice crystal growth ("grain growth") over time, lactose crystallization ("sandiness") in dairy products and enzymic activity at subzero ($^{\circ}\text{C}$) temperatures (Bevilacqua and Zaritsky, 1982; Flink, 1983; Harper and Shoemaker, 1983). The physico-chemical properties of commercial SHPs thus represent an important subject within the food industry. Surprisingly, though, the overall

area is poorly researched mainly because of the variability in carbohydrate composition and properties of SHPs which depend upon the method of manufacturing and the nature of the raw material. Thus even though SHPs are essentially homopolymers of α -D-glucose, due to the various sources of molecular heterogeneity (linear and branched molecules, highly polydispersed systems) their characterization is never an easy task, particularly if one wants to relate molecular structure to product functionality.

However, despite the complex nature of these products, much can be learned about their functional attributes by looking at these systems from a polymer science perspective. In view of the well known relationships between molecular weight/structure and thermomechanical properties (glass-rubber transition temperatures, gelation behaviour, etc.) of synthetic polymeric materials (Ferry, 1980), it appears highly probable that similar trends would exist for SHPs. The possibility of predicting the functional properties of starch hydrolysates from such relationships would have important implications for understanding the role of SHPs as ingredients in various food formulations and ultimately controlling the quality of processed foods.

In view of the above considerations, the objectives of this study were:

- A) To identify relationships between molecular parameters and thermophysical behaviour of polydisperse SHPs of varying composition in frozen aqueous systems.
- B) To explore and assess the feasibility of utilizing commercial SHPs to modify and control the physico-chemical behaviour of food systems.

2 REVIEW OF LITERATURE

2.1 General Aspects of Starch Chemistry

Starch is a reserve polysaccharide occurring in granular form in the organs of higher plants. Starch granules are synthesized in the chloroplasts and amyloplasts of plant cells as transitory and storage carbohydrates, respectively. Chemically and physically, the starch granule is heterogeneous in that it contains amylose (linear) and amylopectin (branched) molecules that are arranged into both crystalline and amorphous phases. The ratio of these two major fractions and their structural organization within the granule greatly affects the physico-chemical behaviour and, hence, functionality of starch (Banks and Greenwood, 1975).

2.1.1 Major Starch Components

The basic repeating unit of starch is anhydro- α -D-glucopyranose, which, in the synthesis of common starches, is polymerized into either amylose or amylopectin. A third component, thought to consist of short chain amylose (Banks et al., 1971), has been identified in some starches and is referred to as the intermediate fraction (Hood, 1982). Common starches contain 14-27% amylose and 73-86% amylopectin depending on their botanical source (Tegge, 1984). Starches extracted from certain mutant plant varieties consist entirely of amylopectin and are described as "waxy"; e.g. waxy maize. In contrast, high-amylose varieties, such as

amylomaize, have been developed through specific breeding programs.

A) Amylose. Amylose consists of anhydro-glucose units linked in series through α -1,4 bonds (figure 1a). It is essentially a linear polymer, although limited long chain branching involving α -1,6 linkages has been reported (Banks and Greenwood, 1975). Amylose has a molecular weight of $1.5-10.0 \times 10^5$ and a DP of 200-5000 depending on its biological origin (Swinkels, 1985).

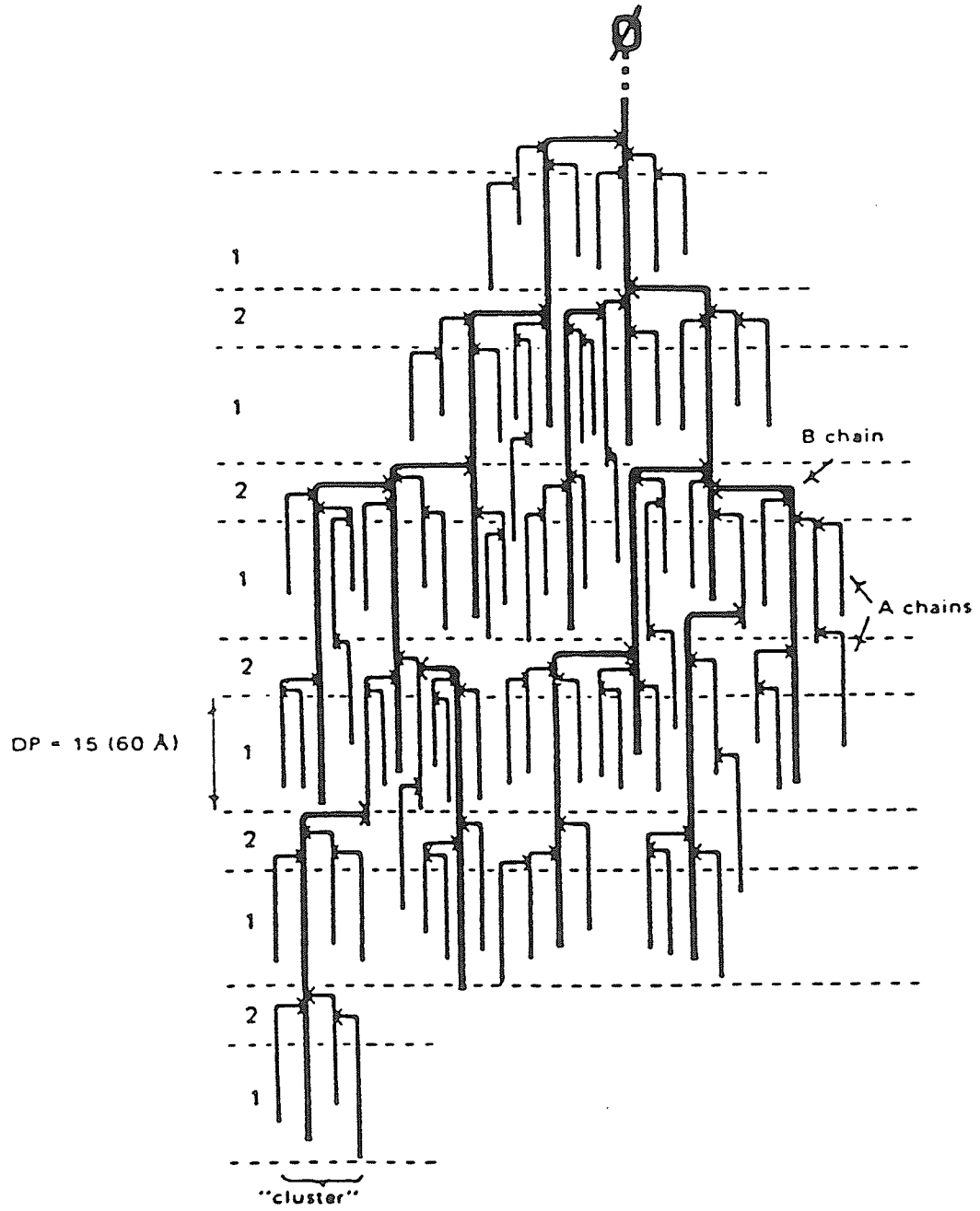
In solution, amylose readily complexes with iodine and various organic compounds by forming a helix around the complexing agent (Tegge, 1984). The complex of amylose with iodine gives a characteristic deep blue colour. The iodine binding capacity (IBC) is a measure of amylose content in starches and of purity in amylose isolates. In cereal starches, amylose typically complexes with naturally occurring fatty acids and phospholipids. Amylose molecules also contribute to the high degree of order in native starch granules by forming double helices with the linear regions of the amylopectin molecules (Hood, 1984). Light scattering studies show that, in neutral aqueous solutions, amylose adopts the conformation of a flexible coil (Banks and Greenwood, 1975).

B) Amylopectin. Amylopectin is a highly branched macromolecule consisting of short α -1,4 glucan chains linked to one another through α -1,6 and, occasionally, α -1,3 branch points (figure 1b). With a DP of over one million and a molecular weight on the order of 10^7-10^8 , amylopectin is one of the largest molecules in nature (Hood, 1984).

The most widely accepted model of amylopectin structure is the "cluster model" in which single and multiply branched glucan chains (DP 15) are arranged as clusters around longer (DP 45) glucan chains, which are themselves linked together (Robin et al., 1975) (figure 2).

Figure 1. Chemical structure of a) amylose and b) amylopectin.

Figure 2. Proposed molecular structure for amylopectin: 1 = crystalline area; 2 = amorphous area; θ = reducing end group; \rightarrow = α -(1,6) branch points; $-$ = α -(1,4)-glucan. Source: Robin et al. (1975).



According to this model, the structure has alternating crystalline and amorphous regions. The linear portions of both the short and long chains (the last 12-16 glucose units of each chain) form double helices with one another, and with the linear amylose molecules, and are responsible for the crystalline regions within the starch granule. The intercrystalline (amorphous) regions occur at 60-70 angstrom intervals and contain the majority of the branch points (Kassenbeck, 1978; French, 1984).

2.1.2 The Starch Granule

A) Structure and Properties. In their native state, starch molecules are organized into dense, water-insoluble, semi-crystalline granules, the size and shape of which are specific for each plant variety (French, 1984). Granules range in size from $2\mu\text{m}$ for rice starch to $100\mu\text{m}$ for potato starch. Characteristic shapes develop as the starch granules grow. In spite of these varietal differences in granule size and shape, all starches have a similar fine, submicroscopic structure (Lineback, 1984).

When viewed under polarized light, starch granules exhibit a well defined birefringence pattern termed the "Maltese Cross", which intersects at the original growth point of the granule (hilum). The positive sign of birefringence indicates that the starch molecules are oriented in a radial fashion or, more accurately, perpendicular to the granule surface (French, 1984).

Within the starch granule, the amylose/amylopectin double helices are organized into crystal lattices (Zobel, 1988). Distinctive X-ray diffraction patterns indicate the packing arrangement of the double helices in the different starches. In general, cereal starches yield A

patterns; tubers and fruit starches, B patterns; and certain root and seed starches, C patterns. Levels of crystallinity in granular starches range from 33-45% for the A type, 15-28% for the B type and 37-45% for the C type (Zobel, 1988). Amylopectin appears to be the principal crystalline component since waxy starches, with essentially no amylose, exhibit X-ray diffraction patterns very similar to those of "normal" starches, while high amylose maize starches show weaker, more dispersed patterns (Lineback, 1984).

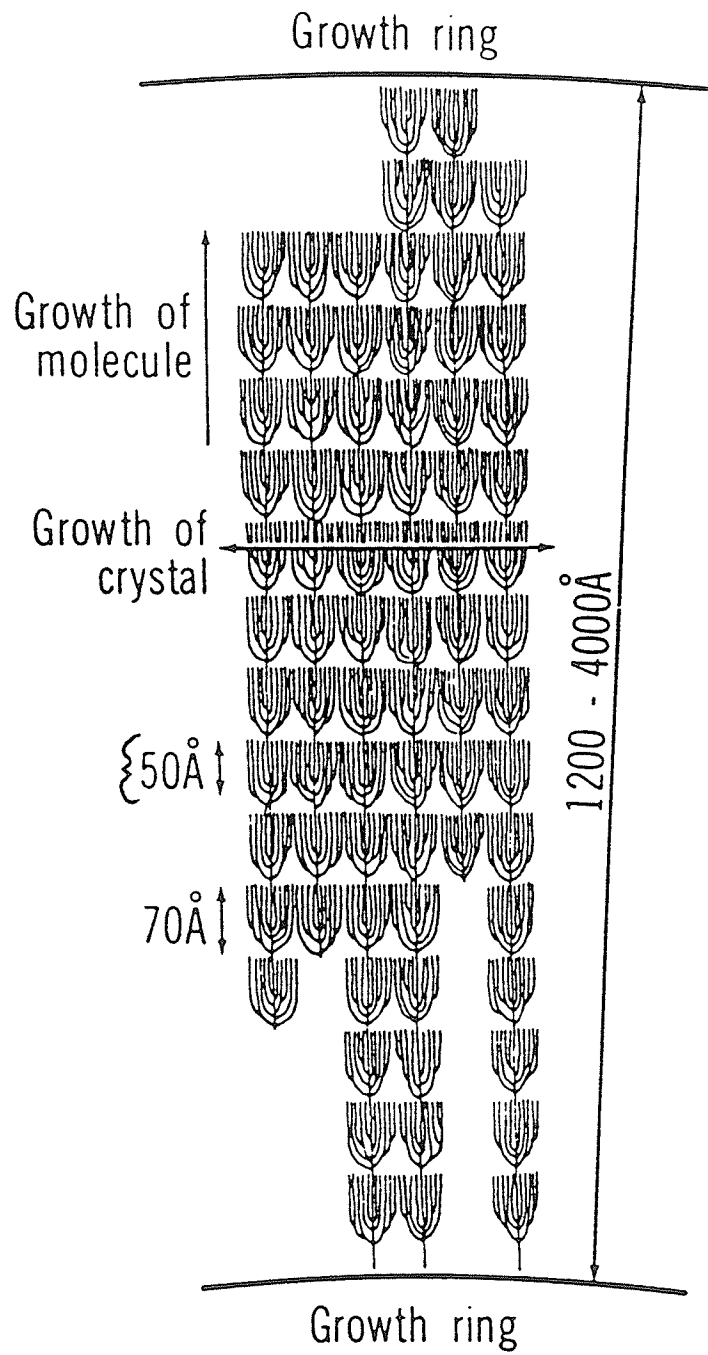
Light microscopy studies on large, hydrated starch granules (e.g. those of potato and canna) (French, 1984), as well as transmission and scanning electron microscopy studies on smaller, enzyme or acid eroded starch granules (Mussulman and Wagoner, 1968; Chabot et al., 1978) have revealed concentric or eccentric layers surrounding the hilum. French (1984) coined the term "growth rings" to describe these layers since they reflect periodic growth or, more specifically, fluctuations in carbohydrate available for starch deposition. The growth rings represent layers of alternating high and low refractive index, density, crystallinity and resistance or susceptibility to chemical or enzymic attack (French, 1984). The presence of growth rings fits with the theory that starch granules grow by apposition to produce an "onion-like" layered structure (Hood, 1984). Each ring is comprised of concentrically oriented, alternating crystalline and amorphous layers. In the crystalline region starch double helices are hydrogen-bonded to one another forming a micelle, which holds the granular structure together. Amorphous regions are formed by the branched portions of the amylopectin and low-molecular weight amylose (Tegge, 1984). There is a gradual transition from the amorphous to the crystalline regions of the growth ring sug-

gesting that some or all the starch molecules run continuously from one region to another (figure 3) (French, 1984). Yamaguchi and co-workers (1979) noted that the rings occur at irregular 1200-4000 angstrom intervals and probably represent the overall length of individual amylopectin molecules. They suggested that a single amylopectin molecule commences at one growth ring and terminates at the next.

B) Gelatinization. Native starch granules are insoluble in cold water and most organic solvents due to their compact, highly ordered, semi-crystalline structure. Limited reversible swelling (10-15% increase in diameter; Swinkels, 1985) is observed when starch granules are soaked in water at room temperature. At higher temperatures, the starch granules of an aqueous-starch suspension undergo hydration and profound, irreversible swelling. During heating, amylose preferentially leaches from the swollen granules and starch crystallites melt (i.e. the granules lose their native structure) forming a translucent paste. Collectively, these physico-chemical changes are known as gelatinization.

Starch gelatinization is manifested by a loss of birefringence and X-ray crystallinity and a sharp increase in sample viscosity. It occurs over a temperature range rather than at a single point suggesting that crystals of varying degrees of perfection are melted (Maurice et al., 1985). Biliaderis et al. (1986) proposed that during heating partial melting of the starch crystallites occurs followed by recrystallization of the metastable melt into more perfected and/or larger crystallites, and final melting. They and others (Slade and Levine, 1984; Maurice et al., 1985) have viewed starch gelatinization as a dynamic, nonequilibrium, process in which melting of starch crystallites and recrystalliza-

Figure 3. Schematic representation of the arrangement of amylopectin molecules within a growth ring of a starch granule. Source: French (1982).



tion are dependent on previous softening of the amorphous parts of the starch granule. In this regard, water plays an important role as a plasticizer, depressing the gelatinization temperature range (Biliaderis et al., 1986).

C) Gelation and Retrogradation. As a concentrated starch paste is cooled, it quickly develops into an opaque starch-gel, which becomes firmer on storage over several weeks (Miles et al., 1985). This return of a starch dispersion from a solvated, amorphous state to an insoluble, aggregated or crystalline condition is referred to as retrogradation (Swinkels, 1985). The changes taking place during retrogradation are of considerable importance to industrial users of starch. For example, retrogradation is believed to be an important factor in the staling of bread and in the textural changes of other starch containing foods (Ring, 1985).

The early stages of retrogradation (gelation) involve a reassociation of leached amylose chains at regions of local order or "junction zones" to produce a continuous three-dimensional network in which aqueous fluid and swollen or ruptured gelatinized starch granules are trapped. Gelation depends on amylose (and amylopectin) concentration, and amylose chain length. A critical amylose concentration C^* of $\geq 1.2\%$ w/w is required for chain entanglement, and thus network formation (Miles et al., 1985). Amylose molecules with a DP of 100-200 exhibit the highest rates of gelation. Longer molecules have greater difficulty in lining up with neighbouring amylose chains, while shorter molecules can not reassociate as completely (Clark et al., 1989). Amylopectin, because of its high degree of branching, forms gels only under extreme conditions of high starch concentrations or freezing temperatures (Ring et

al., 1987).

Subsequent to gelation, both amylose and amylopectin recrystallize, firming up the newly formed starch gel. Crystallization of the linear amylose molecules is completed within 24 hours. Conversely, the highly branched amylopectin molecules, for the most part still contained within the gelatinized starch granules, crystallize over several weeks. The less stable amylopectin crystallites are easily melted by heating to 100°C. This disordering of the amylopectin crystallinity accounts for the improved textural quality of stale bread that has been microwaved. Starch gels typically give X-ray diffraction patterns of the B-type. In cereal starch gels, V-patterns, characteristic of crystallization of amylose-lipid complexes, are also observed (Zobel, 1988).

2.2 Starch Hydrolysis Products: Production and Properties

2.2.1 Introduction

Starch hydrolysis products (SHPs) is the general term applied to those materials obtained by the hydrolytic degradation of starch. The hydrolysis of starch to glucose, maltose and maltodextrins involves the addition of water to D-glucosidic bonds at different points along the starch molecule. This first order reaction is acid and/or enzyme catalysed and can be further accelerated by heat (Tegge, 1984).

The extent of starch conversion, controlled to yield products of varying functionality, is usually measured in terms of dextrose equivalent (DE). Dextrose equivalent is defined as "the percentage of reducing sugars in the product, calculated as dextrose, on a dry weight basis" (Dziedzic and Kearsley, 1984). For example, a DE of 100 indicates that

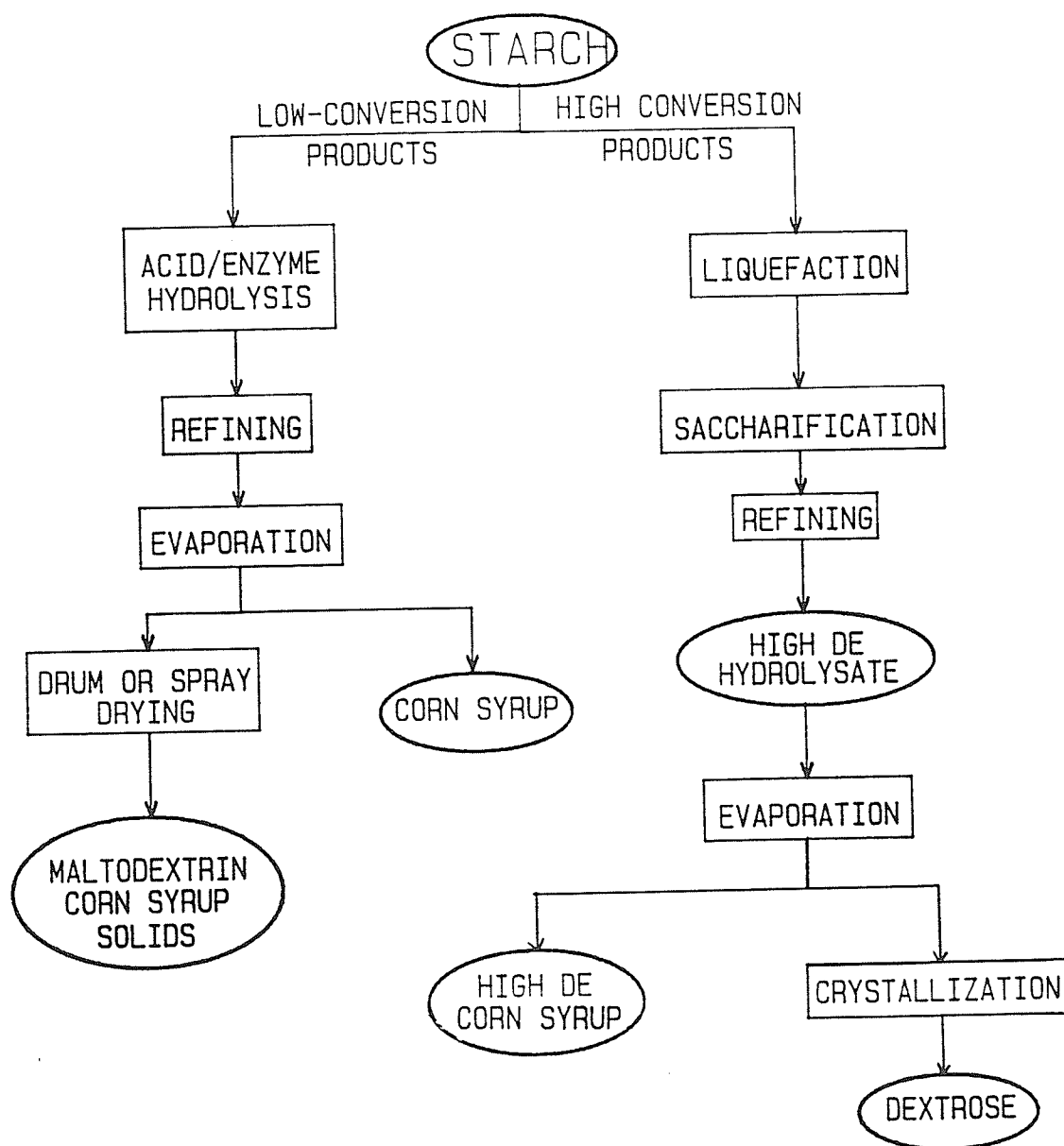
the starch molecule has been broken down completely to glucose. On the other hand, analysis of the original starch gives a DE of 0 since no conversion has taken place. In general, SHPs are classified according to their DE. Corn syrups, by definition, have a DE > 20, while maltodextrins have a DE < 20 (Pancoast and Junk, 1980). Both corn syrup and maltodextrins are marketed in various forms. Corn syrups are sold as such or as high-glucose or high-maltose syrups, or as corn syrup solids which have a moisture content of 3-4%. Dextrose obtained from the crystallization of high-glucose syrups is commercially available as anhydrous and monohydrate crystals. Maltodextrins are typically marketed as dried solids, although small amounts of product are sold as a concentrated syrup.

Currently, SHPs are manufactured by three different processes: acid hydrolysis; enzymic hydrolysis; and a two-step conversion, employing first acid and then enzyme(s). A generalized schematic for the manufacture of SHPs is shown in figure 4. The enzymic processes are more easily controlled and can produce SHPs of specific carbohydrate composition. Furthermore, enzymic hydrolysis, unlike acid conversion processes, enables production of non-retrograding maltodextrins and high DE (98) starch hydrolysates.

2.2.2 Commercial Production

A) Acid Conversion. Until the early 1960's starch hydrolysates were produced exclusively by the acid conversion method. In this process a 40% starch slurry was acidified to a pH of 2 using sulphuric or hydrochloric acid and, subsequently, pumped into a holding vessel (the converter) at elevated temperatures (140-160°C) and pressure. Initially,

Figure 4. Generalized schematic for the manufacture of commercial SHPs.
Modified from Fullbrook (1984).



the gelatinized starch is converted to the higher DP oligosaccharides. As the conversion proceeds, greater quantities of glucose, maltose and low molecular weight oligosaccharides are produced. Glucose is split off most quickly from the short chain linear oligomers; splitting from the nonreducing ends is faster than from the reducing ends (Tegge, 1984). Once the desired DE is reached, heating is discontinued and the hydrolysis quickly ended by the introduction of equivalent amounts of a neutralizing agent, usually soda ash (Pancoast and Junk, 1980).

Though still used today to produce high quality glucose syrups, the acid conversion method has two major drawbacks. First, since acid-catalysed starch hydrolysis is random, there is no way of influencing the carbohydrate distribution and, thus, functionality of SHPs (Katz, 1986). Second, using acid conversion, it is not possible to produce non-retrograding products below 30 DE or starch hydrolysates having DE values greater than 55 (Howling, 1979). The random nature of the attack of acid on the starch molecule is such that at DE levels below 30, some high molecular weight linear fractions of starch remain intact and retrograde into semi-crystalline aggregates. These retrograded fragments cause starch hydrolysate solutions to become hazy, a condition undesirable for some applications. Under the extreme conditions required to form high DE products, side reactions occur, yielding bitter tasting reversion products and undesirable colour precursors, such as 5-hydroxy methylfurfural and levulinic acid (Tegge, 1984).

B) Enzymic conversions. The limitations of the acid-hydrolysis process were, to a large extent, overcome with the industrial use of amylases. These starch-degrading enzymes occur in the digestive secre-

tions of animals, plants and microorganisms. They are divided into two main groups; those that hydrolyse the α -1,6 branch points (debranching enzymes) and those that cleave the α -1,4 linkages. The α -1,4 glucanases are further classified according to their action pattern. Endo-acting glucanases make random, internal cleavages, while exo-acting amylases hydrolyse in a step-wise manner from the non-reducing chain ends (Marshall, 1975).

The initial step in the enzymic process of starch hydrolysate production is the liquefaction of the gelatinised starch suspension. This may be accomplished using a combined acid-enzyme method or a two-step enzymic process. The former technique involves first thinning the starch slurry in acid, followed by adjusting the pH up to 6.0-6.5, and then dextrinisation at 85°C using bacterial α -amylase (Fullbrook, 1984). Alternatively, the all-enzyme process replaces acid with thermostable α -amylases at the thinning stage. Because of their endo-action pattern, α -amylases can quickly reduce the viscosity of the starch slurry. The end-products of α -amylase are low molecular weight sugars; mainly maltose, maltotriose and maltotetraose; as well as α -limit dextrans (since α -amylases are unable to hydrolyse α -1,6 branch points), all of which have the α -configuration at their reducing end groups. The advantages of both the acid-enzyme and enzyme-enzyme processes over the straight acid conversion is that they yield a liquefied product that is less likely to retrograde (since linear dextrans responsible for haze formation are hydrolysed in preference to branched dextrans) and that is more likely to lead to higher glucose yields (Fullbrook, 1984). Hydrolysis may be terminated at the liquefaction stage to give maltodextrins (DE 10-20) or

continued at the saccharification stage to yield higher DE products.

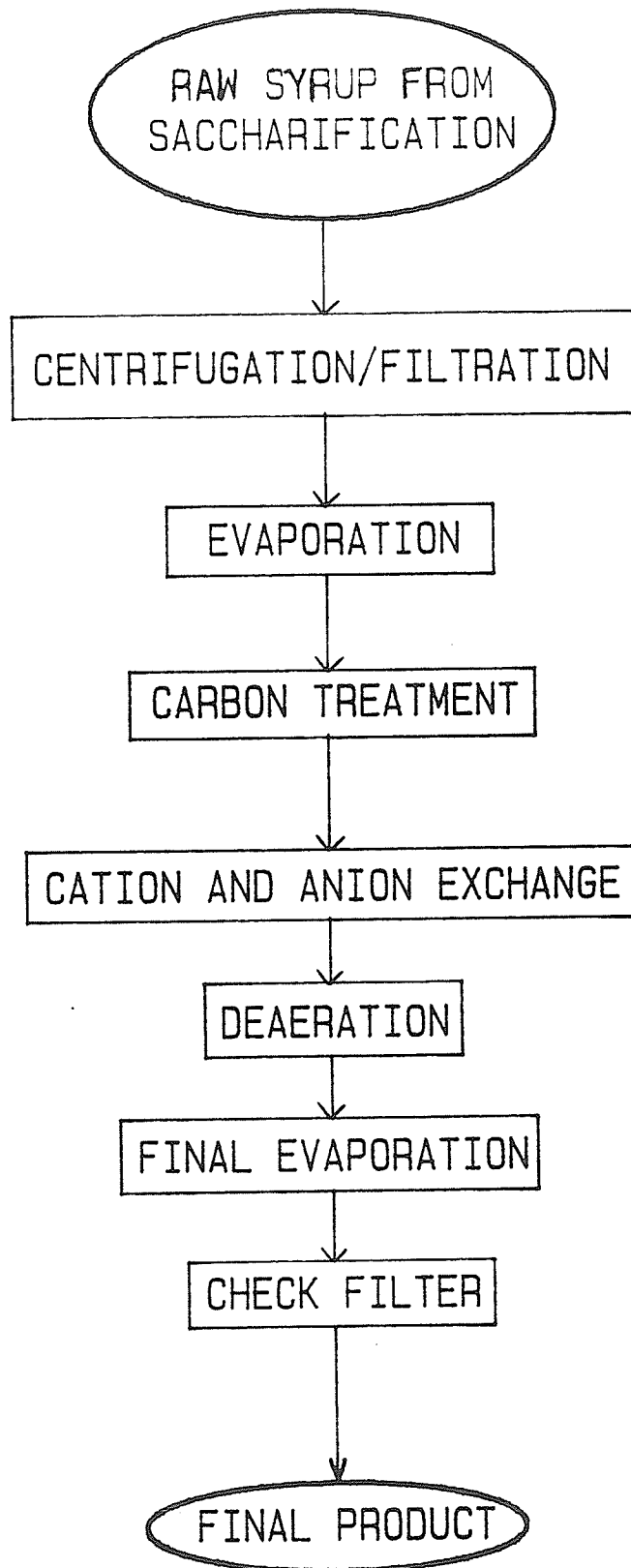
The exo- β -amylases are generally used at the saccharification stage to convert the partially hydrolysed starch intermediate into high maltose syrups (>50% maltose). β -amylases cleave every other α -1,4 glucosidic bond yielding β -maltose, but are unable to bypass the α -1,6 branch points. As a result, a high molecular weight " β -limit dextrin" containing all the original α -1,6 bonds is produced.

Starch or limit dextrans are first debranched to allow complete saccharification. The most important commercial debranching enzyme is pullulanase, which cleaves maltose and maltotriose side chains at the α -1,6 linkages. Its mode of action on branched polysaccharides, such as amylopectin, α - and β -dextrans, is predominantly exo (Marshall, 1975).

The exo-acting glucoamylases (amyloglucosidase) hydrolyse starch directly to α -D-glucose and, hence, are used to produce high DE (> 90) liquors from which dextrose can be crystallized. In this process α -1,4-glucosidic bonds are attacked preferentially to α -1,6 and α -1,3 bonds (Tegge, 1984). The main drawback associated with its use is the formation of reversion products, particularly isomaltose (Marshall, 1975). Also, compared to pullulanase, the debranching action of glucoamylase is relatively slow (Fullbrook, 1984). In this regard, Slominska and Maczynski (1985) have suggested the simultaneous use of glucoamylase and pullulanase for complete conversion of starch into glucose.

C) Final Processing. After the desired DE and carbohydrate profile have been attained, the raw starch hydrolysate liquor is further processed into a finished, commercial product (figure 5). Refining begins with the removal of suspended material (fatty substances, enzyme/protein residues, solid particles) from the liquor by centrifugation and rotary

Figure 5. Generalized schematic for final processing of commercial SHPs. Modified from Fullbrook (1984).



vacuum filtration. The filtrate is partially evaporated to approximately 60% solids and then passed through a three-stage bleaching/activated carbon treatment to remove colour and flavour compounds. Cation and anion exchange resins are used to remove trace amounts of colour and flavour bodies not removed by filtration or carbon treatment, as well as ash and soluble salts. After refining, the starch hydrolysate syrup is deaerated and evaporated to the desired solids level. As a final "check" the refined syrup is pumped through a very fine filter.

Maltodextrins and glucose syrup solids are obtained after liquefaction and saccharification by the removal of water to 95-97% dry solids. Moisture is removed by either spray or drum drying (Pancoast and Junk, 1980). Alternatively, maltodextrins are concentrated in vacuum evaporators to finished syrups containing about 75% dry solids.

2.2.3 Characterization and Analysis

Starch hydrolysates have traditionally been categorized according to their DE, which describes the average extent of starch conversion. This term is limited, however, in that two products of identical DE can have different carbohydrate profiles, and, hence, functional attributes. A more appropriate description of SHPs would be the determination of their oligosaccharide distribution.

Various chromatographic techniques have been employed in the compositional analysis of SHPs. Of these high performance liquid chromatography (HPLC) has become the method of choice. HPLC can provide good separation of oligosaccharides up to DP 12 in a relatively short analysis times and, unlike gas-liquid chromatography (GLC), does not require derivatization of the saccharides prior to analysis (Howling, 1979). As

well, through the development of robust column packing materials, HPLC has become suitable for extended, routine use (Folkes and Brookes, 1984).

The carbohydrate profile of a starch hydrolysate varies according to the conversion process used. Tables 1,2 and 3 list the carbohydrate composition of glucose syrups processed by the acid, acid-enzyme and enzyme-enzyme conversion methods. Differences in carbohydrate distribution reflect the different catalyst specificities of the three conversion processes. Acid-catalysed hydrolysis is a random process. Consequently, the different oligosaccharide fractions up to DP 5 (maltopentose) are distributed relatively evenly in the syrup (table 1). Conversely, the enzymic processes employ enzyme catalysts which have well defined action patterns and substrate specificities (e.g. amyloglucosidase and β -amylase) so that certain carbohydrate components, usually glucose or maltose, predominate (tables 2 and 3).

2.2.4 Properties and Applications

The functional properties of starch hydrolysates are largely dependent on their DE and carbohydrate composition. Table 4 shows the relationship between DE and functionality for various maltodextrins and corn syrup solids.

Properties that are dependent on structural development, such as viscosity and cohesiveness, increase with decreasing DE. Low DE hydrolysates contribute viscosity, body and "mouthfeel" to gravies, sauces, chewy candies and other foods. They are also used as binding agents in cereal bars, as encapsulators of flavours and essential oils, and as foam stabilizers and air retainers in instant whips, toppings, marshmal-

TABLE 1. Oligosaccharide composition¹ of acid converted glucose syrups²

	<u>Glucose syrup</u>			
	DE ³ 30	DE 34-36	DE 42-43	DE 55
Dextrose	10	13.5	19	31
Maltose	9	11.5	14	18
Maltotriose	10	10	12	13
Maltotetraose	8	9	10	10
Maltopentaose	7	8	8	7
Maltohexaose	6	6	7	5
Maltoheptaose	5	5.5	5	4
Higher sugars	45	36.5	25	12

¹ Data are expressed as percentage of total carbohydrate content.

² Source: Birch and Kearsley (1974).

³ Dextrose equivalent.

TABLE 2. Oligosaccharide composition¹ of acid-enzyme converted glucose syrups²

	<u>Type</u>			
	High maltose		High conversion (amyloglucosidase)	
DE ³	42	48	63	70
Dextrose	6	9	37	43
Maltose	45	52	32	30
Maltotriose	12	15	11	7
Maltotetraose	3	2	4	5
Maltopentaose	2	2	4	3
Maltohexaose	2	2	3	2
Higher sugars	30	18	9	10

¹ Data are expressed as percentage of total carbohydrate content.

² Source: Birch and Kearsley (1974).

³ Dextrose equivalent.

TABLE 3. Oligosaccharide composition¹
of enzyme-enzyme converted
glucose syrups²

	<u>Glucose Syrup</u>	
	DE ³ 42	DE 65
Dextrose	2.5	34.0
Maltose	56.0	47.0
Maltotriose	16.0	3.0
Maltotetraose	0.7	2.0
Maltopentaose	0.4	1.5
Maltohexaose	0.7	1.0
High sugars	23.7	11.5

¹ Data are expressed as percentage of total carbohydrate content.

² Source: Birch and Kearsley (1974).

³ Dextrose equivalent.

TABLE 4. Functionality as a function of DE for commercial SHPs¹

	Starch	Maltodextrins			Corn Syrup Solids		
	0	5	10	15	20	25	36
Dextrose Equivalent (D.E.)	0	5	10	15	20	25	36
Viscosity/Bodying Agent	←—————						
Browning Reaction	—————→						
Cohesiveness	←—————						
Freezing Point Depression	—————→						
Hygroscopicity	—————→						
Sweetness	—————→						
Prevention of Coarse Crystals	←—————						
Solubility	—————→						
Osmolality	—————→						

¹ Source: Anonymous (Bulletin 11005, GPC)

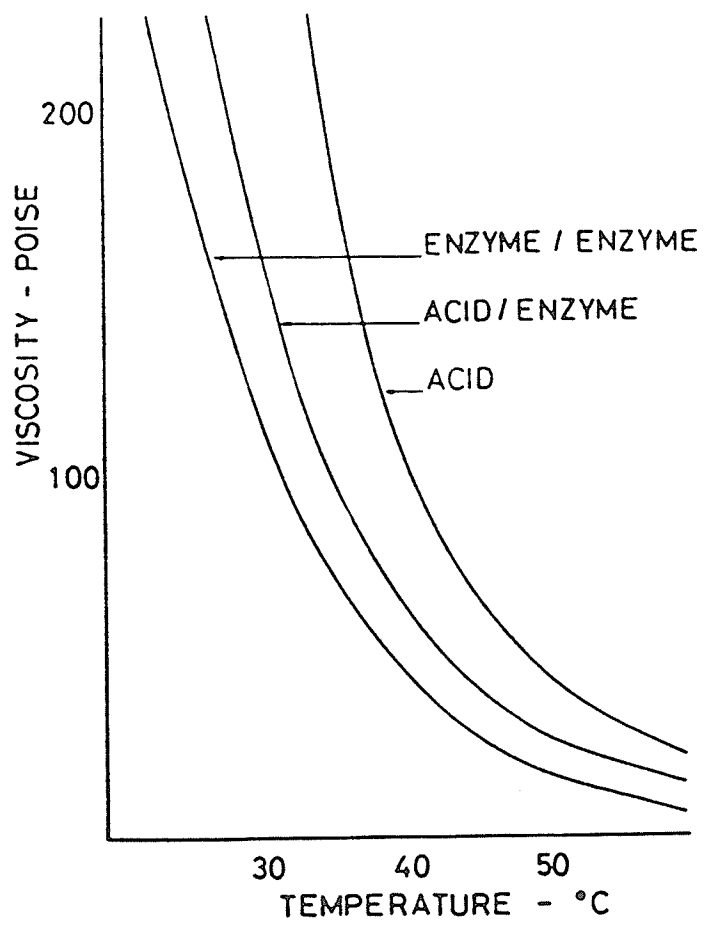
lows, etc.

At constant solids content the viscosity of a starch hydrolysate is also influenced by its carbohydrate profile. Figure 6 illustrates the effect of temperature on the viscosity of three glucose syrups of identical DE (42). Each syrup has been processed by a different method, giving each its own carbohydrate spectrum. The acid-converted syrup contains a higher concentration of high molecular weight components than either of the enzymically hydrolysed syrups and, consequently, has higher viscosity at any given temperature.

The applications of starch hydrolysates as drying aids and in the prevention of coarse crystal formation are closely related to their viscosity effects. Structural integrity is maintained in freeze-, spray-, and drum-dried foods if low DE maltodextrins are incorporated into the product prior to drying. The increased viscosity, contributed by the maltodextrin, sets the "natural" microstructure of the food. Control of crystallization increases with decreasing DE. Low DE starch hydrolysates are added to a food formulation to increase its viscosity to such an extent that crystal growth is significantly retarded. This principle is applied in the prevention of ice recrystallization in frozen food systems (Bevilacqua and Zaritzky, 1982; Harper and Shoemaker, 1983; Franks, 1985), lactose recrystallization in dairy products (White and Cakebread, 1966; Flink, 1983) and sucrose recrystallization in hard candies (McNulty and Flynn, 1977; Herrington and Branfield, 1984). Higher DE SHPs are included in ice cream formulations to promote the development of fine (as opposed to coarse) crystals and thus a smoother texture and better appearance (Levine and Slade, 1988).

The ability of a starch hydrolysate to absorb moisture (i.e. its

Figure 6. Relationship between viscosity and temperature for DE 42 glucose syrups manufactured by different conversion methods.
Source: Howling (1979).



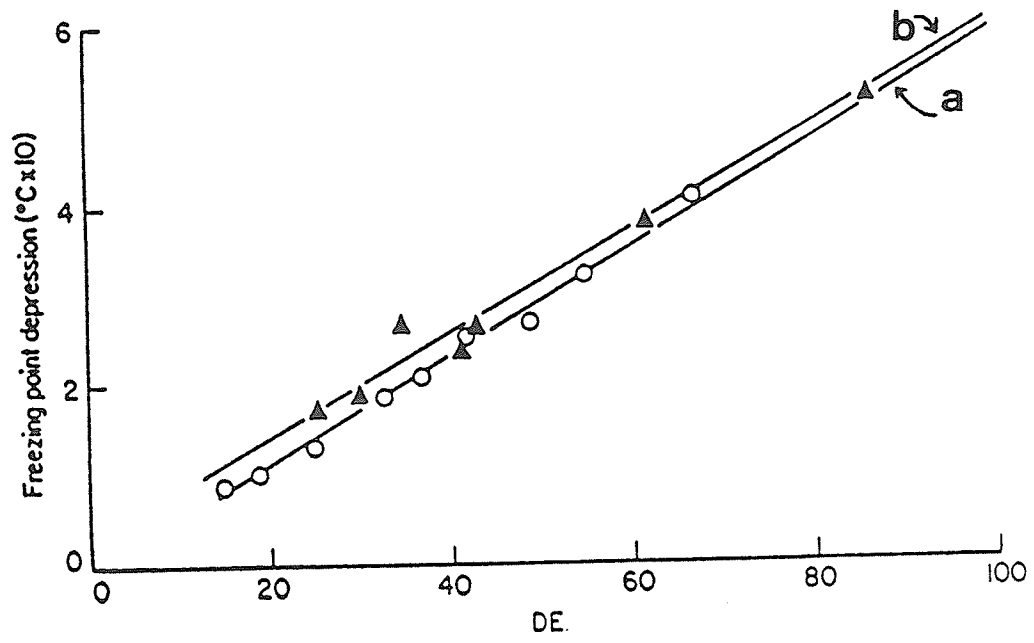
hygroscopicity) increases with increasing DE. Using starch hydrolysates of specific DE, the food processor can greatly prolong the shelf-life of a particular product. High DE starch hydrolysates, for example, are very hygroscopic and prevent foods, such as cakes, bread and icings, from drying out. On the other hand, for products such as hard candies, where absorption of moisture reduces quality, the required solids content can be attained by employing non-hygroscopic, low DE maltodextrins.

The oligosaccharide distribution of a starch hydrolysate especially affects its colligative properties. SHPs of high molecular concentration (i.e. those containing high quantities of glucose and maltose) will elevate the boiling point of a food system. This effect is important in the production of high boiled sugar confectionery. By careful choice of glucose syrup and glucose to sucrose ratio, the boiling point can be reduced by as much as 5°C resulting in less browning of the product and reduced energy costs (McDonald, 1984).

Similarly, a linear relationship exists between freezing point depression and DE; i.e., depression of the freezing point is greater with increasing DE (Kearsley and Birch, 1975) (figure 7). Normally, low DE SHPs are used in the manufacture of frozen dessert products, such as ice cream, in order to minimize freezing point depression, while at the same time adding body and mouthfeel, and controlling ice recrystallisation.

Another colligative property, osmotic pressure, is often manipulated to control microbial spoilage in jams and marmalades. High DE (high molecular concentration) glucose syrups are incorporated into the formulations of such products to increase their osmotic pressure beyond that at which spoilage organisms can survive.

Figure 7. Freezing point depression vs. DE for a) glucose syrup fractions and b) commercial glucose syrups. Source: Kearsley and Birch (1975).



When choosing a particular starch hydrolysate for any of the above mentioned applications, its other physico-chemical properties must be considered. For example, when used as a meat extender or as a body enhancer in gravy mixes, the SHP can not be overly sweet. Sweetness increases with increasing DE and thus a lower DE hydrolysate would be appropriate for these purposes.

Similarly, there is a linear relationship between solubility and DE. Certain applications require the SHP to be in true solution (e.g. boiling point elevation) while for others complete solubility is less important (e.g. bulk dilution, viscosity development).

Another factor to consider is the Maillard browning experienced by a starch hydrolysate as its reducing sugars can react with nitrogenous compounds. As the reducing sugars content increases (i.e. as DE increases) browning reaction rates increase. Where browning is undesirable (e.g. canned fruit) lower DE glucose syrups are used. In some cases browning is highly desirable (e.g. development of a brown crust in bread, manufacture of toffee) and thus high DE syrups are employed.

2.3 Phase Transitions of Polymeric Materials

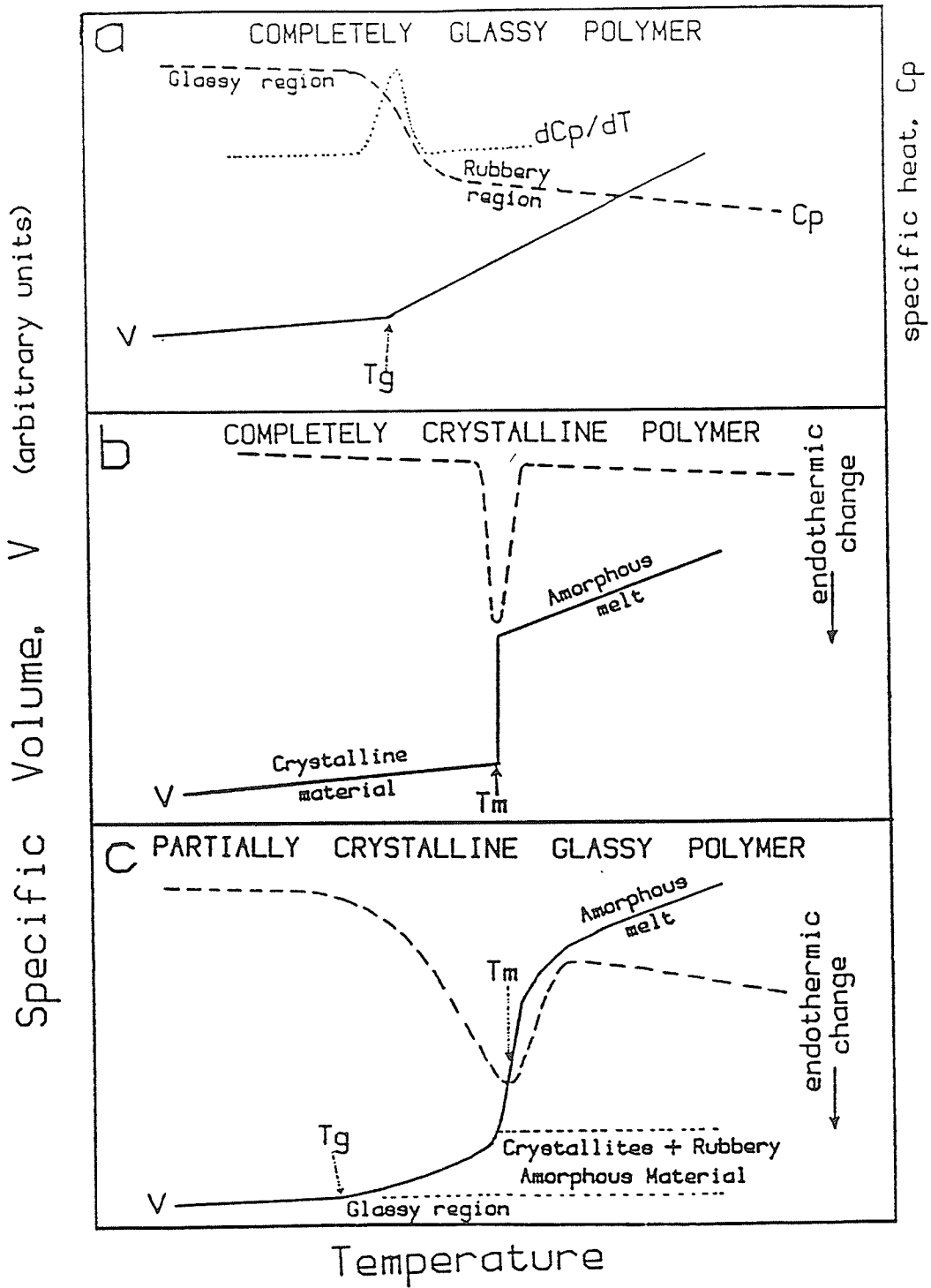
2.3.1 Glass Transition

Most polymers are either completely amorphous (i.e. randomly arranged) or have a partially-crystalline structure (Nielsen, 1974). When the melt of such materials is cooled, it gradually becomes more viscous and rubbery. If the temperature is reduced still further, below a certain point, the polymer abruptly changes from a soft, flexible rubber to a hard, rigid glass. This rubber to glass transformation is referred to as the glass transition. The temperature at which it occurs is called

the glass transition temperature, T_g , and is characteristic of each polymer. In many ways the glass transition resembles a second-order thermodynamic transition. For example, at T_g there is a discontinuous change in specific heat (C_p) and specific volume, as shown in figure 8 for glassy and partially-crystalline polymers (Biliaderis et al., 1986). Although the glass transition is associated with the changes in these second-order variables, it is considered to be a kinetic phenomenon (Eisenberg, 1984). In this regard, application of free volume theory has proved useful in analysing glass transition behaviour (Young, 1981). The free volume is the space in a solid or liquid sample which is not occupied by polymer molecules (Fox and Flory, 1950). It originates primarily from the inefficient packing of disordered chains in the amorphous regions of the polymer and, to a lesser extent, from the nonharmonic vibrations of the constituent atoms (Cowie, 1973; Sears and Darby, 1982). In the liquid state, where free volume is high, molecular motion takes place relatively easily since there is space for molecules to move about. As the melt is cooled, however, the free volume decreases and molecular motion becomes more restricted. Eventually a temperature is reached at which the free volume has a certain value, common to all polymers, which is so low that segmental motion no longer takes place. This temperature corresponds to T_g . Below T_g , the polymer chains are locked into a random network. Above this point, translational movement of the entire chain is possible (Billmeyer, 1984).

Changes in the extent of molecular motion of a polymer passing through its glass transition are manifested by equally abrupt changes in its physico-chemical properties. At T_g there are dramatic changes in

Figure 8. Generalized response of specific heat (dashed lines) and specific volume (solid line) as a function of temperature for three idealized polymers in the glass transition and melting temperature regions: T_m , melting temperature; T_g , glass transition temperature; V , specific volume; C_p , specific heat. Source: Biliaderis et al. (1986).



specific volume, specific heat (figure 8a), refractive index, permeability, dielectric constant, and electrical or thermal conductivity. As well, there is a sharp increase in modulus and viscosity as a glass-forming polymer is cooled below T_g ; thus, the reaction rates of diffusion-controlled processes, such as crystallization, drop significantly and abruptly at T_g .

The T_g is of considerable technological importance in that it defines the lower limit of usefulness of a non-crystallizing rubber and the upper limit of practical utility of a glass-like thermoplastic (Brydson, 1972). Within the temperature range for the rubbery state (i.e. from T_g to $T_g + 100^\circ\text{C}$), the viscoelastic properties of amorphous polymers have been shown to be empirically related to T_g by the Williams-Landel-Ferry (WLF) equation (Ferry, 1980):

$$\log_{10}(k_T/k_{T_g}) = 17.44 (T - T_g) [51.6 + (T - T_g)]^{-1} \quad (1)$$

where k is the reaction rate constant at a particular temperature. This equation describes the kinetic nature of the glass transition and defines the exponential temperature dependence of any diffusion-controlled relaxation process (Soesanto and Williams, 1981; Levine and Slade, 1986). The impact of WLF behaviour on polymeric systems can be illustrated as follows: for ΔT (i.e. $T - T_g$) = 0, 3, 7, 11 and 21°C , corresponding relative reaction rates would be 1, 10, 10^2 , 10^3 , and 10^5 , respectively (Levine and Slade, 1986). Thus the kinetics of diffusion-controlled processes such as crystallization and, blooming and bleeding of additives in composite products can be altered dramatically by even small temperature changes (Brydson, 1972; Levine and Slade, 1986).

2.3.2 Crystallization and Melting

Crystallization is a first-order thermodynamic process whereby an ordered structure is produced from a disordered phase (Young, 1981). As the temperature of a polymer melt is brought below the melting point (T_m) segmental motion of individual chains is greatly decreased. In this reduced energy environment hydrogen bonds, dipolar, van der Waals, and other attractive forces between adjacent polymer chains last longer and are thus able to stabilize the polymer into a highly ordered state. Crystallization is a two-step process. In the first step a stable nucleus, from which the crystal can grow, is formed. Nucleation is classified as being either homogeneous (spontaneous) or heterogeneous (catalytic) (Cowie, 1973). Homogeneous nucleation depends on the random, spontaneous orientation of polymer chains into a geometry conducive to crystallization. Heterogeneous nucleation results from the presence of foreign particles that are able to act as crystallization catalysts. The second step of crystallization involves the diffusion of molecules from the liquid to the solid/liquid interface created during nucleation. This step is termed crystal propagation. Under most practical conditions propagation is rapid compared to nucleation so that the latter is the rate determining step (Billmeyer, 1984).

The number, size and morphology of crystals formed depends heavily on the rate of supercooling and the temperature to which the material is cooled. At low cooling rates nucleation tends to be sporadic and a relatively small number of large spherulites are formed. On the other hand, high cooling rates result in the formation of many nuclei and a large number of small, imperfectly formed crystals are obtained (Young, 1981). The maximum rate of crystal growth occurs between ($T_m - 10K$) and

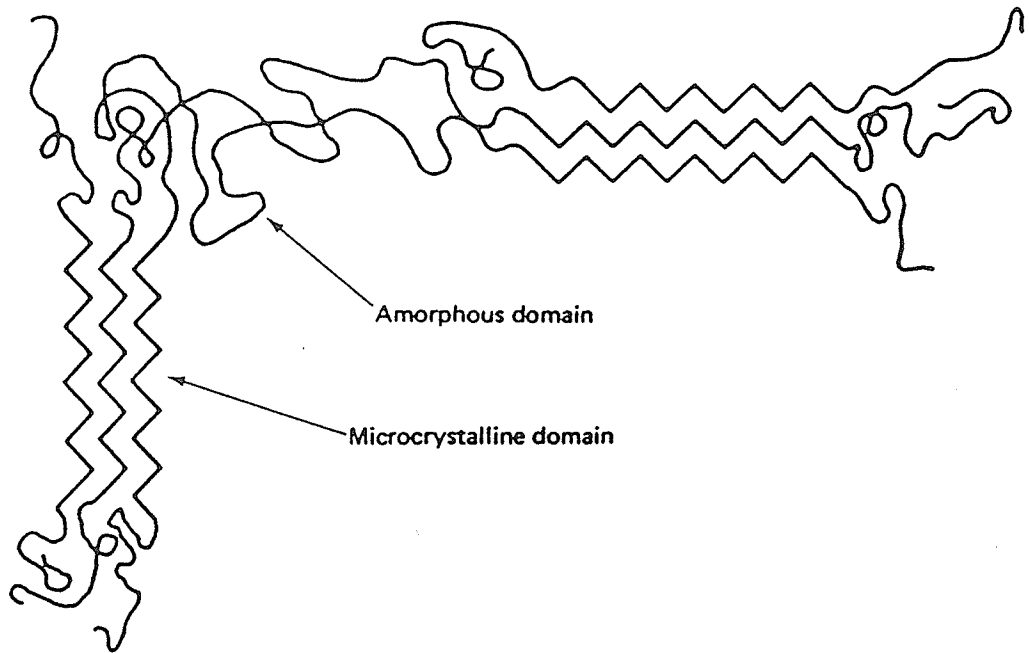
($T_g + 30K$) (Cowie, 1973). At temperatures close to T_m the segmental motion of individual chains is too great to allow many stable nuclei to form, while near T_g the viscosity of the polymer melt becomes so high that molecular diffusion is slowed significantly. If the melt of a crystallizable polymer is supercooled below T_g a glass is formed. On reheating above T_g , crystallization may occur. The degree of crystallinity greatly affects the mechanical properties of crystalline polymers (Allcock and Lampe, 1981). Most crystalline polymers consist of microcrystallites embedded in an amorphous matrix. These crystalline domains stiffen the polymer by functioning as crosslinks for the amorphous regions (figure 9) (Allcock and Lampe, 1981). As the degree of crystallinity increases the polymer becomes tougher and more leathery.

Melting is in effect the opposite of crystallization; i.e. a disordered phase is obtained by heating an ordered structure above its T_m . The melting of a perfectly crystalline polymer is characterized by marked changes in first-order thermodynamic functions such as volume and enthalpy, and by a well defined melting temperature, T_m (figure 8b). However, polymers are rarely completely crystalline and, as previously noted, the crystals that are formed vary in size and morphology. Thus melting of crystalline polymers normally takes place over a range of temperatures. This range reflects the variability of crystal size and perfection in the polymer.

2.3.3 Factors Affecting T_g and T_m

The use of polymers in practical applications depends heavily on their T_g and T_m (Young, 1981). Because of this, there has been considerable interest in determining the factors which control these tempera-

Figure 9. Molecular structure of a microcrystalline polymer.



tures. Based on the stipulated relationships between free volume, molecular motion and phase behaviour in polymeric systems, two important generalizations regarding the factors that control T_g and T_m can be made. First, the factors that raise or lower T_g tend to have a similar effect on T_m ; i.e. for homopolymers, it is not possible to control T_g and T_m independently (Billmeyer, 1984). Second, any factor that will reduce the free volume of a polymer will elevate its T_g and T_m . Conversely, any factor that will increase the free volume will depress both T_g and T_m .

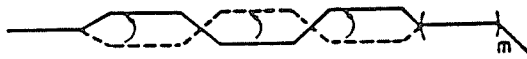
Factors affecting the T_g and T_m of a polymer can be categorized as follows:

- A) Chemical Structure
- B) Molecular Weight and Chain Entanglement
- C) Branching
- D) Polymer Composition and Plasticizers
- E) Crosslinking and Crystallinity

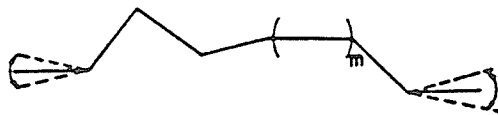
A) Chemical Structure. The overriding factor which determines the phase transition temperatures of a polymer is the chemical structure of its main chain and side groups. Chain flexibility is a measure of the ability of a chain to rotate about the constituent chain bonds (Cowie, 1973). Flexible main chains rotate in a "crankshaft" motion (figure 10a) and have a higher free volume than rigid (non-rotating chains) (Sears and Darby, 1982). Thus polymers containing groups such as Si-O, CH₂-CH₂ and CH₂-O that rotate easily about their bonds have correspondingly low T_m and T_g values. On the other hand, the presence of a phenyl group in the main chain increases stiffness (i.e. reduces free volume) and causes

Figure 10. Sources of free volume for plasticization: a) main chain "crankshaft" motion; b) chain end motion; c) side chain motion; and d) external plasticizer motion. Source: Sears and Darby (1982).

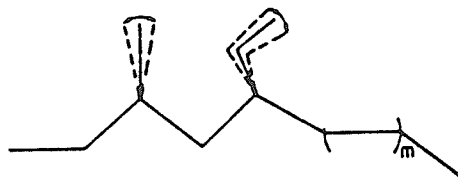
a



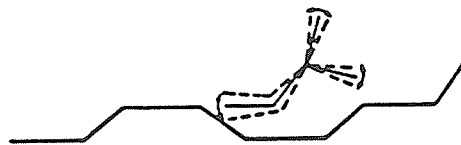
b



c



d



a large increase in both T_m and T_g (Cowie, 1973).

An additional restriction to main chain bond rotation is imposed by the steric effects of side groups. Polymers with large, bulky side groups have a low free volume and, hence, elevated T_g and T_m as compared to polymers with small or flexible side groups. Superimposed on this group size factor is the effect of polarity. The presence of polar side groups such as -Cl, -OH or -CN tends to raise the T_g and T_m more than non-polar groups of equivalent size. This is because the polar interactions restrict bond rotation (Young, 1981).

B) Molecular Weight and Chain Entanglement. Another source of free volume in polymers is chain end motion (figure 10b). The end of a chain is less restrained than a segment in the center of a chain and, therefore, more prone to violent motions, which create greater free volume (Brydson, 1972). Thus as the number of chain ends is reduced, the free volume decreases and T_g and T_m are elevated. Since molecular weight is inversely proportional to chain end concentration (Young, 1981), it follows that T_g increases with increasing molecular weight (Billmeyer, 1984). The relationship between the T_g and molecular weight (MW) of polymers is given by the expression:

$$T_g = T_g^\infty - K/MW \quad (2)$$

where K is a constant characteristic of each polymer and T_g^∞ is the glass transition temperature at infinite molecular weight (Fox and Flory, 1954). For polystyrene ($K= 1.75 \times 10^5$), the T_g increases from 83°C for a sample with $MW= 10^4$ to 100°C for a sample of infinite MW (Fox and Flory, 1954).

A similar relationship exists between T_m and molecular weight; i.e.

as molecular weight increases (and chain end concentration decreases) T_m is elevated. For example, polypropylene, with $MW = 2 \times 10^3$, has a $T_m = 114^\circ\text{C}$, whereas a sample with $MW = 3 \times 10^4$, has a $T_m = 170^\circ\text{C}$ (Cowie, 1973).

The effect of molecular weight on T_g , however, levels off at high molecular weight due to entanglement coupling of polymer chains; i.e. a limit is reached in which further increases in molecular weight have little or no effect on T_g (Billmeyer, 1984; Levine and Slade, 1986).

C) Branching. The effect of polymer branching on T_g and T_m is dependent on the degree of branching (Young, 1981). Low levels of branching effectively increase total free volume by introducing additional chain ends (figure 10c) and T_g is depressed (Brydson, 1972). In the case of crystalline polymers, branching reduces packing efficiency. Consequently the crystalline content is lowered and the polymer melts at a lower temperature (Cowie, 1973).

Conversely, a high density of branching will have the same effect as bulky side groups in restricting chain mobility and raise the transition temperatures.

D) Plasticizers and Polymer Blends. The T_g and T_m of a polymer are also influenced by its composition. For homopolymers, a single composite T_g is observed and can be predicted using the Flory-Fox equation (Fox and Flory, 1954):

$$\frac{1}{T_g} = \frac{W_1}{T_{g1}} + \frac{W_2}{T_{g2}} \quad (3)$$

where T_g , T_{g1} and T_{g2} are the glass transition temperature of the blend and the constituent polymers respectively, and w_1 and w_2 the correspond-

ing constituent weight fractions (Billmeyer, 1984). Thus, a polymer comprised mainly of a constituent with a low T_g will also have a low T_g .

An effective method of depressing the T_g and T_m of polymeric materials is to include compounds of lower molecular weight (figure 10d). These compounds, known as plasticizers or softeners, increase the free volume of the system by introducing additional chain ends. Their plasticizing effect is enhanced if they are slightly branched and free of side groups that may interact with the polymer. An example of a very effective plasticizer is water, which causes a large depression in the T_g of synthetic polymers (Jin et al., 1984) and biopolymers (Biliaderis et al., 1986; Hoseney et al., 1986; Levine and Slade, 1986).

E) Crosslinking and Crystallinity. Crosslinking raises T_g and T_m by introducing restrictions on the molecular motions of polymer chains. An example of this is the sulphur vulcanization (i.e. crosslinking) of natural rubber. At room temperature natural rubber is tacky and tends to flow. Vulcanization elevates the T_g of natural rubber such that it exhibits useful elastomeric properties (Young, 1981).

In crystalline polymers, microcrystallites act as crosslinks by tying segments of polymer chains together (figure 9). The crystalline structures reduce free volume in the polymer, effectively restrict chain motion and thereby increase T_g (Biliaderis et al., 1986).

2.3.4 Methodologies Used To Probe Phase Transitions

Considering the technological importance of phase transitions of polymeric materials, it is not surprising that so much attention has been paid to developing accurate, reliable methods for the detection of T_g and T_m and the assessment of related thermophysical changes. Method-

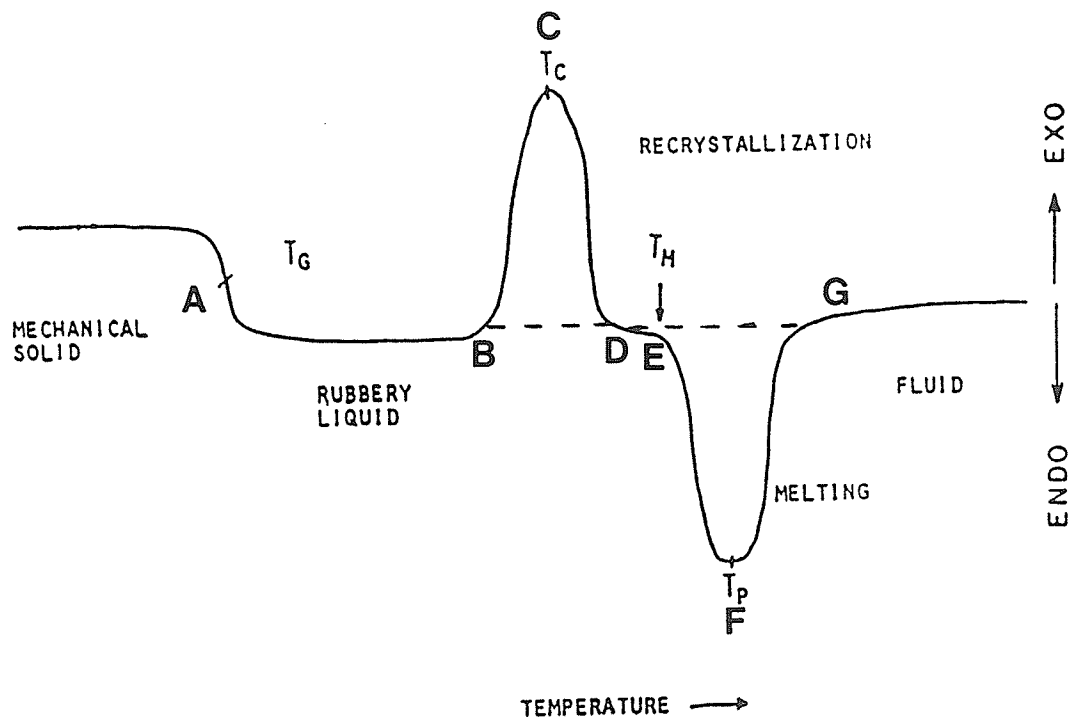
ologies used to probe phase transitions are defined by: a) the property they monitor and, b) whether the test sample is analysed directly or in comparison to a reference material. The methods used to examine phase behaviour of polymeric materials are thermomechanical analysis (TMA), differential thermal analysis (DTA), and differential scanning calorimetry (DSC).

TMA refers to the group of techniques that measure directly the mechanical response of a test material to temperature change. Examples of TMA include: thermodilatometry, which measures volume expansion or contraction as the sample is heated or cooled; density gradient techniques, which monitor sample density as a function of temperature; penetrometry, which measures the depth to which a weighted needle penetrates a polymer as it is heated; and torsional rigidity tests, which record the resistance of a polymer to torsional forces as it passes from one phase to another. In each case, phase transitions are characterized by marked changes in the property being monitored.

DTA measures the temperature difference between a substance and a reference material as a function of time or temperature. Phase transitions appear as peaks or gradual deviations from the baseline of a DTA curve; the temperature at which these changes occur represent T_m and T_g , respectively.

Conversely, with DSC, the temperature of the test sample is maintained equal to that of a reference material throughout the run. The amount of energy absorbed or emitted by the test sample in order to maintain this zero temperature difference with the reference material is monitored as a function of time or temperature. Figure 11 is a generalized DSC curve of a polymeric system illustrating the phase transitions

Figure 11. Phase changes from amorphous to crystalline in an idealized polymer; where T_g = the glass transition temperature, T_c = the crystallization temperature, T_p = the peak temperature of the melting endotherm, and T_m = the melting temperature.



it undergoes upon reheating. The glass transition is accompanied by a change in the heat capacity of the sample as shown by the baseline shift at point A. Recrystallization (i.e., the crystallization of previously vitrified crystallizable material) is evidenced by the exotherm (segment BCD). The area under the exothermic peak is proportional to the amount of heat released in the recrystallization process. The endothermic peak (segment EFG) is characteristic of the melting of sample crystallites. Both the onset temperature (point E) and the peak temperature (point F) of the endotherm have been used to represent the melting point. The enthalpy change associated with melting is calculated from the area of the endothermic melting peak.

Techniques for locating phase transition temperatures can be further categorized as static or dynamic according to the frequency or rate with which measurements are made. In static methods, such as thermilatometry and density gradient analysis, enough time is allowed between measurements to allow the sample to equilibrate and relax at each observation temperature. On the other hand, in dynamic methods measurements are conducted much faster and the sample is no longer allowed to come to equilibrium. Thus, for dynamic methods, the transition region is dependent on the rate of measurement. In general, it is observed that with an increasing rate of measurement, T_g and T_m increase. Examples of dynamic methods include DTA and DSC. While static methods are more accurate, dynamic methods provide reasonable estimates of T_g and T_m in a more practical time frame. Of the methods discussed, DSC has proven to be the most successful for the study of food materials. This is because it provides a relatively fast and reproducible estimate of the temperatures and heat quantities associated with phase

transitions using only small amounts of sample.

2.4 Phase Transition Behaviour of Carbohydrate Materials

Since the development of more sensitive thermal analytical techniques, the phase transition behaviour of carbohydrate materials has been researched extensively. Studies on both frozen aqueous-carbohydrate systems and dry carbohydrate materials have demonstrated the non-equilibrium nature of conventional food processing and storage methods, and the existence of various metastable states. In this section, the phase transition phenomena of carbohydrate materials and the thermodynamic and kinetic factors governing them are discussed with reference to their effects on food quality and stability.

2.4.1 Subzero Temperature Behaviour of Frozen Aqueous-Carbohydrate Systems

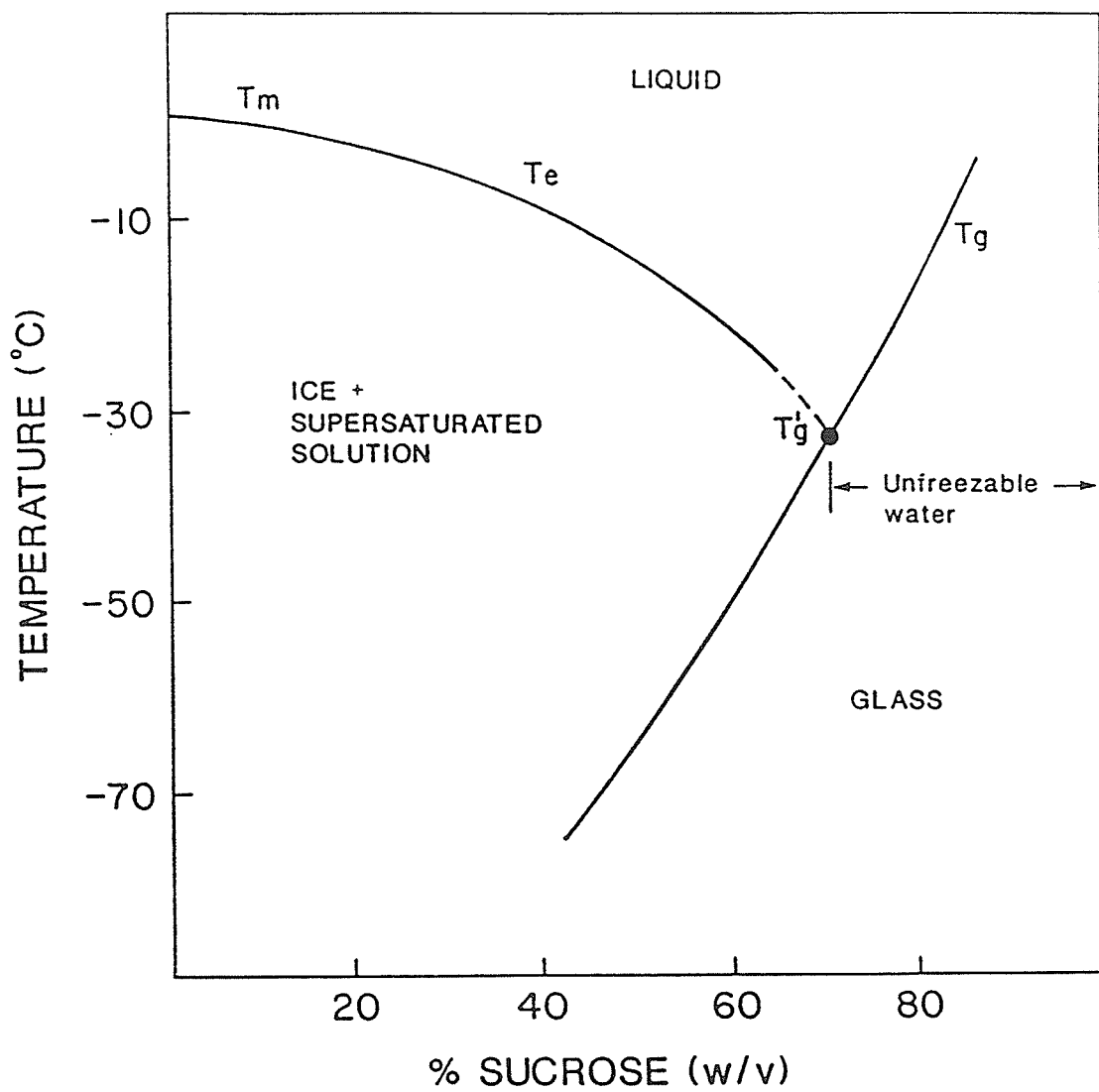
The physico-chemical properties of a solidified aqueous system are determined, to a large extent, by the manner in which it was transformed into the solid state. Two phenomena, freezing and vitrification (glass formation) are involved to varying degrees according to the rate and extent of cooling, and the concentration and nature of the solutes in the system. Under equilibrium conditions of slow cooling, aqueous solutions tend to the thermodynamic state of lowest free energy - the crystalline state (Angell and Choi, 1986). Thus during equilibrium freezing, large spherulitic ice crystals separate out as a pure phase. Conversely, a metastable state is produced if the aqueous solution is cooled below its equilibrium freezing point without crystallizing; i.e. if it is supercooled. This occurs when suitable nuclei have not been made avail-

able to the cooled liquid (MacKenzie, 1977; Franks, 1986). If supercooling proceeds below T_g , the supersaturated liquid vitrifies into an amorphous metastable solid (a glass). Even if nucleation (homogeneous or heterogeneous) occurs during cooling, the rate of cooling may be high enough to prevent significant crystal propagation within the experimental timeframe so that, instead, small irregularly shaped crystals are produced.

Both homogeneous nucleation and ice crystal propagation require diffusion of water molecules (Franks, 1985; Angell and Choi, 1986). Furthermore, the diffusion rate of solute molecules away from the advancing ice front affects the size, morphology and distribution of the ice crystals formed (Biliaderis, 1989). If in any way diffusion is retarded, the rate and extent of crystallization will decrease and a non-equilibrium state (a rubbery fluid if $T_g < T < T_m$ and a glass if $T < T_g$) will predominate. As discussed in section 2.3.1, the viscosity of a material increases with decreasing temperature, reaching an upper limit of 10^{14} Pa.s at its T_g . Since diffusion rates decrease with increasing viscosity, diffusion-controlled processes, such as ice crystallization, are prevented or, at least, greatly retarded if the aqueous system is rapidly cooled to temperatures approaching T_g . Metastability in frozen aqueous systems is thus based on the kinetic (as opposed to thermodynamic) control of freezing dynamics (Franks, 1982).

The low temperature phase transition behaviour of frozen aqueous-carbohydrate systems can be graphically represented in a liquid-solid state diagram which plots T_m and T_g values over a range of solute concentrations. An example of a typical phase diagram for a carbohydrate-water system is shown in figure 12 (Schenz et al., 1984; Biliaderis,

Figure 12. Liquid-solid state diagram for a water-sucrose system;
 T_m = melting temperature, T_g = glass transition temperature,
 T_g' = glass transition temperature of the maximally freeze
concentrated solute matrix. Source: Biliaderis (1989).



1989). Colligative depression of the equilibrium melting temperature, T_m , is observed down to a point on the melting (liquidus) curve corresponding to the eutectic temperature, T_e (Franks, 1986). However, most carbohydrates do not readily crystallize at T_e (Simatos et al. 1975; Franks, 1985). Instead, the solutions become supersaturated and the melting curve becomes progressively steeper towards lower temperatures with increasing solute concentration (Franks, 1985; Biliaderis, 1989). Figure 15 also illustrates the depression in T_g with decreasing sucrose concentration (and increasing % moisture). Water acting as a plasticizer increases the free movement of the solute molecules in the amorphous state such that a lower temperature is required for glass formation. The resulting glass curve defines the various temperature and composition combinations at which the aqueous-sucrose system is kinetically stable due to the intrinsic slowness of large-scale reorganization at temperatures below T_g (Franks, 1982; Angell and Choi, 1985). During cooling of an aqueous-carbohydrate solution, a point (T_g') is reached, corresponding to the intersection of the liquidus and glass curves, at which no more ice freezes out and the supersaturated solute matrix is vitrified (Levine and Slade, 1986; Biliaderis, 1988). For each solute, there is a characteristic maximum water content of the aqueous glass at T_g' which corresponds to the amount of unfrozen water; i.e. the composition of the freeze-concentrated solute phase is constant and independent of the initial concentration (Levine and Slade, 1986; Biliaderis, 1988). The "unfreezability" of this water fraction is due to the kinetic retardation of diffusion of water and solute molecules at the low temperatures approaching T_g , and not to tight equilibrium binding by solute (i.e. solute hydration) as implied by usage of the term "bound" water (Franks,

1985; Franks, 1986; Levine and Slade, 1988). Consequently, the unfrozen water is best regarded as a plasticizer for the amorphous solute matrix, depressing the T_g of the latter (Franks, 1985; Franks, 1986; Levine and Slade, 1988).

Food products prepared by conventional processing methods are generally found to be in a metastable state (To and Flink, 1978a). As such, these materials will strive to attain mechanical and thermodynamic equilibrium if stored at temperatures exceeding their respective T_g (or T_g'). The glass transition is thus the underlying and prerequisite phenomenon to all diffusion-controlled, relaxation related collapse processes which determine food stability and quality (Levine and Slade, 1986). Furthermore, as with the glass transition itself, these kinetic processes are controlled by the superposed dependent variables of time, temperature and, % moisture (Tsourouflis et al., 1976).

An example of the collapse phenomenon in a frozen food system is the recrystallization of ice (i.e. "grain growth") in frozen dessert products. Storage of these products at temperatures exceeding the recrystallization temperature, T_r , results in a resumption of the original ice crystallization process that was interrupted when the material assumed an amorphous solid state. Other manifestations of structural relaxation of frozen food systems going through their glass transition include: lactose recrystallization ("sandiness") in dairy products, shrinkage ("melt-back") of amorphous materials during freeze-drying, over-run loss in ice cream, and enzymatic activity at subzero temperatures.

2.4.2 Phase Behaviour of Dry Carbohydrate Materials

As with frozen aqueous-carbohydrate systems, the stability of dry carbohydrate materials is determined by a combination of thermodynamic (equilibrium) and kinetic (non-equilibrium) factors, which in turn are affected by the critical variables time, temperature and moisture content (Karel and Flink, 1983; Levine and Slade, 1986; Levine and Slade, 1988). For example, a freeze dried carbohydrate is maintained in a kinetically stable state if stored at temperatures below its characteristic collapse temperature, T_c . However, if the material is rewarmed above T_c or plasticized (with additional moisture) so that its T_c falls below the existing storage temperature, viscous flow is initiated, resulting in the structural collapse of the freeze dried amorphous matrix under its own weight (To and Flink, 1978b). This structural breakdown is most noticeable as a radial shrinkage ("melt-back") of the freeze dried "cake" (To and Flink, 1978b), but is also manifested by the loss of entrapped aroma and flavour volatiles and the oxidation of encapsulated lipids (Tsourouflis et al., 1976; To and Flink, 1978c).

Other examples of structural collapse of dried food products may be cited. The caking of amorphous powders that have been exposed to humid air or fluctuating temperatures is attributed to the structural collapse phenomenon (White and Cakebread, 1966; Moreyra and Peleg, 1981; Karel and Flink, 1983). In spray- or drum- drying operations, if the operating temperature or humidity in the chamber is too high, the "dried" powder will stick to the dryer walls (To and Flink, 1978b). The "sticky-point" temperature that marks the transition from a stable dry powder to a viscous state is thus related to collapse (Tsourouflis et al., 1976).

In certain processes limited structural relaxation is actually

desirable. For example, the instantising of powders by agglomeration involves a controlled raising of the moisture content so that a limited collapse of the powdered materials occurs. The partially collapsed particles stick together in clusters, which are then dried to the desired moisture content (Tsourouflis et al., 1976).

The term "collapse" is not limited to descriptions of structural breakdown, but rather is used in general to describe any of the relaxation-related, diffusion-controlled processes associated with the glass transition. Thus processes such as sugar recrystallization (e.g. sugar bloom in chocolate and graining in boiled sweets), plating of colour agents on the surfaces of amorphous powder particles, and enzymic activity in dry powders are also regarded as collapse phenomena. Levine and Slade (1986) observed that the same mechanism that drives the glass transition (i.e. viscous flow and diffusion at T_g) controls all collapse phenomena. Furthermore, they concluded that the various phenomenological threshold temperatures (e.g. $T_c = T_r = T_{\text{sticky point}}$) are all equal to the particular T_g (or T_g') which corresponds to the solute(s) concentration for the situation in question (Levine and Slade, 1986 and 1988).

3 EXPERIMENTAL

3.1 Materials

Thirty six commercial SHPs from corn and potato sources, provided by various suppliers [Grain Processing Co., Muscatine, Iowa; American Maize-Products Co. (Amaizo), Hammond, Indiana; A.E. Staley Manufacturing Co., Decatur, Illinois; AVEBE, Hopelawn, New Jersey] were used. Starch hydrolysates ranged in DE from 0.5 to 42. D-glucose and D-maltodextrin standards up to and including D-maltoheptaose were obtained from Boehringer Mannheim GmbH, West Germany. Waxy maize starch was provided by the St. Lawrence Starch Co., Mississauga, Ontario, and wheat starch by Ogilvie Mills, Medland, Ontario. Pullulanase (amylopectin 6-glucanohydrolase, E.C.3.2.1.41) was purchased from Hayashibara Biochemical Labs. Inc., Okayama, Japan. L-ascorbic acid was obtained from Fisher Scientific Co., Fair Lawn, New Jersey.

3.2 Methods

3.2.1 Compositional Analysis Of Starch Hydrolysates

The maltodextrin composition of the SHPs was determined using high performance liquid chromatography (HPLC). The chromatographic system consisted of a model M-6000A pump, a U6K injector, and a model 441 refractive index detector (Waters Associates, Milford, MA). The system was interfaced to a Vista data station (Varian 401) for data acquisition and peak area integration. Native (i.e. nondebranched) and debranched

samples (20 mg mL^{-1} , $50 \text{ }\mu\text{L}$ injection volume) were run isocratically at a flow rate of 0.6 mL min^{-1} through an Aminex HPX-42A ($300 \times 7.8 \text{ mm}$) column (Bio-Rad Labs., Richmond, CA) in conjunction with a guard column. The eluent was distilled water that had been filtered and degassed. The column temperature was 85°C . Column calibration was carried out with standard solutions of the homologous series of D-glucose up to and including D-maltoheptaose (4 mg mL^{-1} , $20 \text{ }\mu\text{L}$ injection volume). Prior to sample injection a standard cleanup procedure was applied by passing the sample through a SEP-PAK C18 cartridge (Waters Associates) and filtering through a $0.45 \text{ }\mu\text{m}$ cellulose acetate filter (Millipore Corp., Bedford, MA). All samples were analysed in triplicate.

Starch hydrolysates were debranched using pullulanase. Prior to use, the enzyme was dialysed (molecular weight cutoff 10^4) at 4°C for 12 hr against acetate buffer (0.025M , pH 5.7) to remove all salts. Solutions containing starch hydrolysate (100 mg) and dialyzed pullulanase (0.1 mL ; 40 IU) in acetate buffer (5 mL , 0.05M , pH 5.7) were incubated at 35°C for 24 hr and were then boiled for 15 min. Aliquots of 1 mL debranched digests were used for HPLC analysis. The remainder was concentrated (10X) in a Fisher isothermperature dry bath and kept for DSC analysis.

3.2.2 Evaluation Of The Thermal Behaviour of Frozen Aqueous-SHP By DSC

A) General Procedures. All DSC measurements were performed with a DuPont 9900 thermal analyzer equipped with a 910 DuPont cell base and a DSC ambient pressure cell. The cell base was operated at 10X sensitivity and calibrated with indium metal. Samples (20-70% w/w SHP in distilled water) of 10-15 mg total weight were hermetically sealed in an aluminum

coated pan, and scanned (against an empty reference pan) at a heating rate of $10^{\circ}\text{C min}^{-1}$, from -60°C (in all cases well below T_g') to $+30^{\circ}\text{C}$. Initial cooling to below -60°C , using liquid nitrogen, ensured maximal freeze concentration of the samples. Triplicate scans were made on all samples. Data were recorded as heat flow in mW mg^{-1} as a function of temperature at 1.0 s^{-1} time intervals and stored on floppy disks. Data analyses were performed using the DuPont software analysis program. The analogue derivative function on the DuPont 9900 allowed the precise determination of T_g' with a reproducibility of $\pm 1^{\circ}\text{C}$ for repeated analyses of the same sample. The analysis program was also used to quantify ice formation in the frozen aqueous system by measuring the enthalpy value (ΔH) for the melting endotherm.

B) Evaluation Of Thermal Parameters. In preliminary tests of both native and debranched starch hydrolysates, all sample solutions for T_g' determination consisted of 20% w/w hydrolysate solids in water.

Heat of fusion values for samples over a range of moisture levels (20-70% w/w) were used to determine the characteristic unfreezable water content of a frozen aqueous-carbohydrate system. By extrapolation to zero enthalpy, where no more freezable water is evident, an estimate of the unfreezable water ($\text{g H}_2\text{O g}^{-1}$ material) was obtained.

The T_g' of frozen aqueous binary mixtures of SHPs was predicted, according to the Flory-Fox equation (equation 3, section 2.3.3), on the basis of the T_g' of each of the constituent starch hydrolysates and their corresponding weight fractions. Sample composition ranged from 0%SH_{P1}:100%SH_{P2} to 100%SH_{P1}:0%SH_{P2}. All samples were prepared at a constant concentration of 30% w/w of total hydrolysate solids in water.

Similarly, the effective T_g' for each of the 21 polydisperse commercial SHPs analysed was predicted from their oligosaccharide composition, as determined by HPLC, and the experimentally determined T_g' of the respective individual oligosaccharide standards by employing the following generalized form of the Flory-Fox equation:

$$\frac{1}{T_g} = \sum_{i=0}^{i=n} \left(\frac{W_i}{T_{g_i}} \right) \quad (4)$$

where W_i and T_{g_i}' are the weight fractions and glass transition temperature of the i^{th} constituent.

The applicability of the Flory-Fox equation to frozen aqueous-carbohydrate systems was further tested by examining a series of binary mixtures, each of which had a common reference maltodextrin and a second maltodextrin of varying DE. The two components were combined in a 1:1 ratio by weight, while maintaining a total solids content of 30% w/w.

To study the effect of heating rate on T_g' , frozen starch hydrolysates of varying DE were heated at different rates and their T_g' was determined. Heating rates employed ranged between 1-20°C min⁻¹. For this analysis, the samples were prepared at a concentration of 20% w/w.

3.2.3 Kinetic Studies Of L-Ascorbic Acid Oxidation In Aqueous Starch Hydrolysates

The performance of SHPs as preservative agents was assessed by monitoring the effects of SHP incorporation on the oxidation kinetics of L-ascorbic acid solutions. Using UV spectroscopy, the rate of oxidation of ascorbic acid to dehydroascorbic acid was measured. Ascorbic acid was added to 20 and 40% w/v acetate buffered (0.02M, pH 5.5) starch hydrolysate solutions in a concentration of 2.5 mg ascorbic acid per 100 mL of

total liquid. The test mixture also contained excess hydrogen peroxide (1500 ppm) to ensure an adequate oxygen supply throughout the reaction. Samples were stored in both the liquid and frozen states; i.e. at temperatures above and below 0 °C. Duplicate tests were performed on all samples.

The absorbance of the reaction mixture was measured at 265 nm on a Hewlett Packard 8451 single beam, diode array spectrophotometer. For the above 0°C studies, the reaction mixture was stored directly in the sample cell of the spectrophotometer. Water was circulated from a Haake D1 water bath to maintain the sample cell at the desired storage temperature. Measurements were taken at time 0 and at subsequent intervals.

Samples for the below 0°C studies were prepared as follows. Aliquots of one mL of the reaction mixture were dispensed into test tubes. The tubes were tilted (to facilitate rapid cooling and thawing) and the liquid samples were frozen instantaneously using liquid nitrogen. The frozen samples were immediately transferred to an alcohol bath and held at the desired storage temperature. After a 5 min equilibration period, aliquots were removed at time 0 and at subsequent intervals. Each was thawed by addition of 10 mL of acetate buffer (0.02M, pH 5.5, 20°C) and subsequent storage at 20°C for 30 sec. Following 10 sec of mixing, the absorbance of the solution was read.

Reaction rate constants (k) were determined at each temperature assuming pseudo-first-order kinetics:

$$\log(a-x) = \log a - \frac{kt}{2.303} \quad (5)$$

where a is the initial concentration of ascorbic acid and x is the decrease in the concentration of ascorbic acid in time t.

3.2.4 Rheological Characterization Of Starch SHPs

A) Viscometry Studies. The viscosity of 20% and 40% w/v starch hydrolysate suspensions in water was measured by employing the Bohlin Rheometer System (Bohlin Reologi, Science Park Ideon, Lund, Sweden). The concentric cylinder 25 system with a bob diameter of 25 mm and an angle of 150° was used. All measurements were conducted at 20°C (well above the temperatures required for rubber and glass formation for any of the starch hydrolysates tested) and over a shear rate range of $9\text{-}1465\text{ s}^{-1}$. A torsion bar with a torque element of 93.2 g cm was employed. Measurements were taken at 10X sensitivity for samples with a $\text{DE} > 1$ and at 1X sensitivity for $\text{DE} = 1$ samples.

B) Dynamic Rheometry Studies. The antistaling behaviour of starch hydrolysates in polysaccharide gels was investigated using the Bohlin Rheometer System in the oscillatory mode. Starch hydrolysates were added at 20% w/w (basis) to 20% w/v solutions of wheat and waxy maize starches. After thorough mixing, the sample was encapsulated in a screwcap, metal cylinder (25 mm x 62 mm) and heated at 95°C for 15 min. The sample cylinder was then transferred to a waterbath at 6°C and equilibrated at this temperature for 15 min. For wheat starch gels, a thin slice (approximately 1 mm) of the gelatinized sample was placed on the lower, precooled plate of the parallel plate apparatus (plate diameter = 30 mm). The upper plate was lowered into the gel and excess material was trimmed from the periphery with a blade. Light paraffin oil was added to a level just covering the upper plate and held by a layer of masking tape surrounding the base of the measuring apparatus. Using this method, evaporation of the sample was prevented. Waxy maize samples were pre-

pared in an identical fashion, but had a more pastelike consistency; thus the cone and plate 5/30 system (cone angle = 5.4° , cone diameter = 30 mm) was employed.

All experiments were conducted at $6 \pm 0.1^\circ\text{C}$ using a torsion bar with a torque element of 93.2 g cm. Small amplitude oscillatory measurements were performed at 0.20 Hz and 10% amplitude (2% strain). Data were collected at 15 min intervals for up to 20 hr. Values for the storage (G'), loss (G'') and complex (G^*) moduli, as well as viscosity were obtained. Duplicate runs were performed on all samples.

3.2.5 Statistical Analyses

Where applied, data were analysed by standard statistical methods. The Duncan's multiple range test was used for comparing means among various treatments. Correlation analyses were performed using linear regression. Mean values and standard deviations were calculated for all replicates.

4 RESULTS AND DISCUSSION

4.1 Physico-chemical Properties Of Commercial SHPs

An example of the glass transition and melting phenomena as they are manifested in a typical thermal curve of a frozen starch hydrolysate is shown in figure 13. As previously noted (section 2.3.4), the glass transition is characterized by the shift in the heat capacity curve at T_g' , while melting of ice is evidenced by the large endothermic peak immediately following the glass to rubber transformation. Figure 13 also demonstrates the effective application of the derivative feature of the DuPont 9900 in precisely determining T_g' .

In table 5 the measured T_g' values for a homologous series of monodisperse carbohydrate standards, analysed by this method, are listed. The T_g' values range from 229.75 K for glucose itself (100 DE) to 259.65 K for maltoheptaose (1.56 DE). A direct plot of these results (T_g' as a function of molecular weight; curve A of figure 14) reveals a plateau region in which further increases in molecular weight have little or no effect on T_g' . As previously mentioned (section 2.3.3), Levine and Slade (1986) have attributed such behaviour to intermolecular entanglement of polymeric chains (leading to network formation) that occurs above the critical polymer concentration, C^* (Ferry, 1980). The limiting T_g' value defines the upper boundary with which one can effectively control T_g' by altering the molecular weight of the carbohydrate

Figure 13. Typical DSC thermal curve and its first derivative (broken line) for an aqueous SHP (30% w/w) showing the glass transition temperature (T_g') and the melting enthalpy (ΔH); heating rate = $10^\circ\text{C min}^{-1}$.

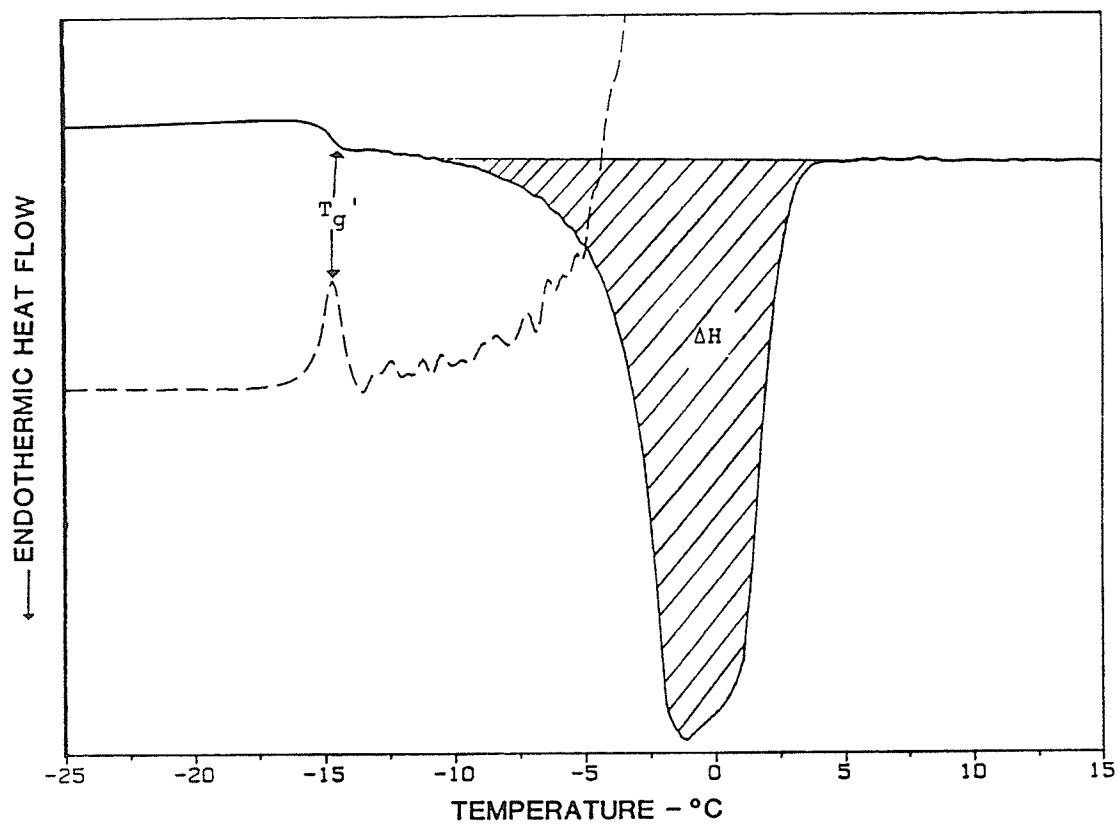
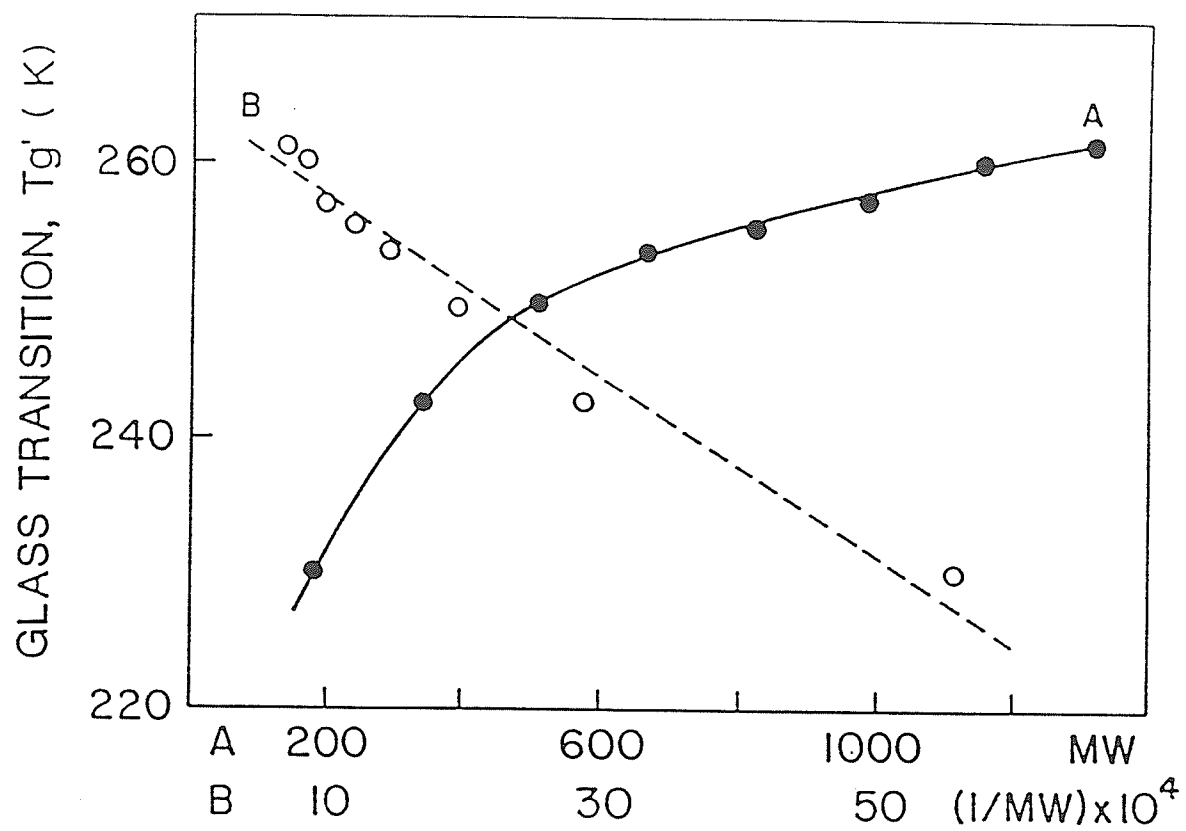


TABLE 5. T_g' values¹ for monodisperse glucose monomer and oligomer standards

Sample	Manufacturer	DE	T_g' (K)
D-Glucose	Boehringer	100	229.75 \pm 1.08
D-Maltose	Boehringer	50	242.22 \pm 0.40
D-Maltotriose	Boehringer	25	249.14 \pm 0.07
D-Maltotetraose	Boehringer	12.5	252.62 \pm 0.23
D-Maltopentaose	Boehringer	6.25	255.04 \pm 0.02
D-Maltohexaose	Boehringer	3.13	256.03 \pm 0.03
D-Maltoheptaose	Boehringer	1.56	259.65 \pm 0.05

¹ DSC analysis performed on 20% w/w samples as described in section 3.2.2.2; (n=3).

Figure 14. Effect of molecular weight on the T_g' of aqueous monodisperse glucose monomer and oligomers at 30% w/w.



solute. Curve B in figure 14, a plot of T_g' as a function of reciprocal molecular weight, shows an inverse linear relationship between the two parameters. This behaviour is consistent with the well known molecular weight dependence of T_g for synthetic polymers (equation 2, section 2.3.3.2) (Billmeyer, 1984; Levine and Slade, 1986) and, in the case of the present studies, is described by the following regression equation:

$$T_g' = 257.23 - 0.28 \text{ MW}^{-1} \quad (6)$$

where $r = -0.990$, $p < 0.001$. In this equation, the y intercept (257.23) corresponds to $T_g'^{\infty}$, and the slope (-0.28) equals the constant, K.

The T_g' values for the 35 commercial, polydisperse starch hydrolysates analysed are listed in table 6. These results, plotted in figure 15, show a similar inverse linear relationship between DE and T_g' (i.e., the greater the DE the lower the T_g') and are in agreement with the recently reported findings of Levine and Slade (1986). Measured T_g' values range from 245.58 K for Fro-dex 42 (coarse) and Star-Dri 42F to 267.05 K for Amaizo ARD2308 (table 6). In general, for the higher DE products (DE 35-42) the T_g' values at any given DE were similar among samples of different origin; a difference of no greater than 0.9 K was observed between samples of identical DE. Conversely, for the lower DE starch hydrolysates, the differences are much greater; e.g. Star-Dri 15 and Maltrin M150 have a difference of 2.36 K. For samples from similar starting materials (e.g., waxy maize, corn and dent corn) this variance can be attributed to the processing method used by the different manufacturers. Because different methods are used, the molecular polydispersity, the degree of branching, and thus the T_g' itself, would be expect-

TABLE 6. T_g' values¹ for commercial starch hydrolysates

Sample	Manufacturer	Source	DE ²	T_g' (K)
Fro-dex 42 (coarse)	Amaizo	Waxy maize	42	245.58±0.28
Fro-dex 42 (fine)	Amaizo	Waxy maize	42	246.42±0.16
Star-Dri 42C	Staley	Corn	42	246.33±0.88
Star-Dri 42F	Staley	Corn	42	245.58±0.20
Star-Dri 42R	Staley	Corn	42	245.94±0.04
Star-Dri 42X	Staley	Corn	42	245.65±0.29
Maltrin M365	GPC	Dent corn	36	248.72±0.08
Fro-dex 36	Amaizo	Waxy maize	36	249.64±0.11
Star-Dri 35F	Staley	Corn	35	249.03±0.01
Star-Dri 35R	Staley	Corn	35	248.83±0.02
Fro-dex 24D	Amaizo	Waxy maize	28	253.48±0.14
Fro-dex 24-924	Amaizo	Waxy maize	24	255.59±0.01
Star-Dri 24R	Staley	Corn	24	253.30±0.05
Maltrin M250	GPC	Dent corn	23.4	253.76±0.02
Star-Dri 20	Staley	Corn	20	259.50±0.13
Maltrin M200	GPC	Dent corn	20	255.97±0.03
Lo-dex 15	Amaizo	Waxy maize	18	257.56±0.10
Star-Dri 15	Staley	Dent corn	15	261.36±0.17
Maltrin M150	GPC	Dent corn	15	259.00±0.15
Lo-dex 10	Amaizo	Waxy maize	11	261.68±0.44

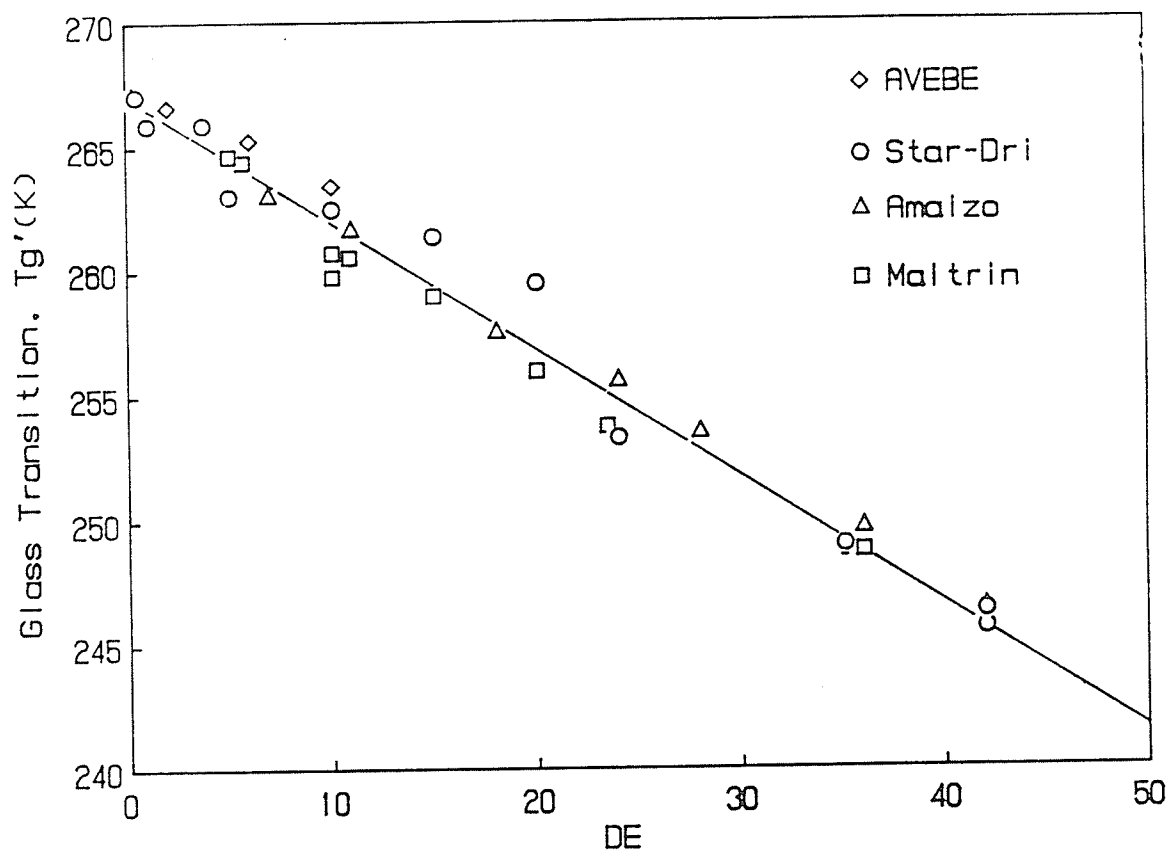
TABLE 6 cont.

Sample	Manufacturer	Source	DE	T _g ' (K)
Maltrin M100	GPC	Dent corn	10.9	260.55 _± 0.33
Maltrin M500	GPC	Dent corn	10	259.76 _± 0.71
Maltrin M700	GPC	Dent corn	10	260.77 _± 0.09
Star-Dri 10	Staley	Dent corn	10	262.50 _± 0.03
Lo-dex 5	Amaizo	Waxy maize	7	263.03 _± 0.25
Maltrin M050	GPC	Dent corn	5.7	264.40 _± 0.09
Maltrin M040	GPC	Dent corn	5	264.63 _± 0.08
Star-Dri 5	Staley	Dent corn	5	263.04 _± 0.21
Star-Dri 1	Staley	Dent corn	1	265.88 _± 0.28
ARD2308	Amaizo	Dent corn	0.3	267.05 _± 0.04
AVEBE 10	AVEBE	Potato	10	263.40 _± 0.11
AVEBE 6	AVEBE	Potato	6	265.26 _± 0.13
Staley 3.8	Staley	Potato	3.8	265.86 _± 0.03
AVEBE 2	AVEBE	Potato	2	266.61 _± 0.01
Staley 0.5	Staley	Potato	0.5	267.04 _± 0.14

¹ DSC analysis performed on 20% w/w samples as described in section 3.2.2.2; (n=3).

² DE values were provided by the manufacturer.

Figure 15. Relationship between DE and Tg' of various polydisperse aqueous SHPs at 20% w/w.



ed to vary from product to product. Variability in T_g' between SHPs of the same DE but from different plant sources might reflect the different chemical composition and structure of the respective starting starch materials. For example, SHPs from potato generally have T_g' values that are 1-3 K higher than that of corresponding corn based products. This is because SHPs manufactured from potato starch inherently have a higher hydrodynamic volume (due to the presence of phosphate groups; Swinkels, 1985) and thus are expected to show higher T_g' values than starch hydrolysates produced from corn. Differences in T_g' between the carbohydrate standards and commercial SHPs of similar DE (tables 5 and 6) could reflect differences in the levels of chain polydispersity. A polydisperse SHP is more likely to undergo chain entanglement than the corresponding monodisperse carbohydrate standard since the former is comprised of long oligomer chains (in mixture with short chains), while the latter contains a homogeneous mixture of oligomers of identical chain lengths. From tables 5 and 6 it is seen that the carbohydrate standards consistently have T_g' values that are 2-10 K lower than those observed for SHPs of comparable DE.

The relationships presented in figures 14 and 15 provide a physico-chemical basis for cryostabilization technology. A controlled elevation of T_g' in a frozen food system to temperatures approaching or even exceeding the conventional freezer temperature, T_f , through the inclusion of carbohydrate solutes of specific molecular weight or DE, would improve storageability of low-temperature preserved products. Furthermore, the linear relationship shown in figure 15 may be used as a calibration curve to predict the T_g' of a SHP by knowing its DE value.

The equation describing the regression line in figure 15 is:

$$T_g' = 267.00 - 0.50(DE) \quad (7)$$

where $r = -0.991$, $p < 0.001$.

Elevation of T_g' with decreasing solute DE, as observed in figures 14 and 15, can be attributed directly to the parallel increase in solution viscosity. As a solution becomes more viscous with the addition of higher molecular weight materials, its free volume decreases, allowing its transition from a liquid to a rubber and then to a glassy state to occur at a higher temperature. To investigate the effect of solution viscosity on T_g' , shear rate sweeps were performed on 29 commercial SHPs at both 20 and 40% w/v concentrations. The viscosity values obtained at the maximum shear rate of $1.47 \times 10^3 \text{ s}^{-1}$ are given in table 7. All samples but one (Star-Dri 1 40% w/v) exhibited classical Newtonian behaviour; i.e. a constant viscosity over a broad range of shear rates, as illustrated by figure 16 for a number of representative samples. In contrast, Star-Dri 1 (DE 1) was the only sample that demonstrated pseudoplastic (shear-thinning) behaviour (figure 17). These findings support the distinction made by Levine and Slade (1986) in identifying high molecular weight polymers from oligomers by their capacity for molecular chain entanglement coupling. Solutions of high molecular weight polymers thus behave as rubber-like viscoelastic networks at concentrations above the critical polymer concentration. As shown by the viscosity as a function of shear rate profile for Star-Dri 1 (40% w/v) (figure 17), at very high shear rates this network exhibits shear thinning behaviour, presumably due to disentanglement of the polymeric chains. The shear thinning behaviour shown by Star-Dri 1 is typical of all pseudoplastic materials

TABLE 7. Viscosity¹ of commercial starch hydrolysates at 20 and 40% (w/v) concentration

Sample	Viscosity (kPa.s)	
	20%	40%
Amaizo 42 (coarse)	2.90 \pm 0.06	7.07 \pm 0.67
Amaizo 42 (fine)	3.00 \pm 0.23	7.62 \pm 1.06
Star-Dri 42C	3.15 \pm 0.02	7.87 \pm 0.18
Star-Dri 42F	3.23 \pm 0.04	7.94 \pm 0.10
Star-Dri 42R	3.06 \pm 0.10	6.92 \pm 0.27
Star-Dri 42X	2.99 \pm 0.02	7.53 \pm 0.17
Maltrin M365	3.08 \pm 0.02	8.52 \pm 0.09
Amaizo 36	3.67 \pm 0.07	11.40 \pm 0.22
Star-Dri 35F	3.03 \pm 0.17	8.01 \pm 0.79
Star-Dri 35R	3.22 \pm 0.06	8.38 \pm 0.15
Amaizo 24D	3.69 \pm 0.20	13.89 \pm 0.77
Amaizo 24-924	4.15 \pm 0.13	13.56 \pm 0.24
Star-Dri 24R	3.33 \pm 0.13	10.73 \pm 0.28
Maltrin M250	3.58 \pm 0.08	11.74 \pm 0.13
Star-Dri 20	4.05 \pm 0.23	12.75 \pm 0.04
Maltrin M200	3.82 \pm 0.05	14.31 \pm 0.42
Amaizo 15	4.27 \pm 0.07	16.91 \pm 0.28
Star-Dri 15	4.44 \pm 0.06	21.54 \pm 0.41
Maltrin M150	4.86 \pm 0.08	20.85 \pm 0.33

TABLE 7 cont.

Sample	Viscosity (kPa.s)	
	20%	40%
Amaizo 10	6.28 \pm 0.09	36.25 \pm 0.85
Maltrin M100	5.64 \pm 0.06	31.51 \pm 1.52
Maltrin M500	5.51 \pm 0.12	30.54 \pm 1.34
Maltrin M700	5.88 \pm 0.17	28.30 \pm 0.77
Star-Dri 10	6.39 \pm 0.07	36.11 \pm 0.72
Amaizo 5	9.08 \pm 0.15	67.19 \pm 1.94
Maltrin M040	12.65 \pm 0.62	98.14 \pm 6.55
Star-Dri 5	15.83 \pm 0.15	175.0 \pm 1.0
Star-Dri 1 ²	39.36 \pm 0.55	2718 \pm 174

¹ Viscosity determined at a shear rate of $1.47 \times 10^3 \text{ s}^{-1}$ as described in section 3.2.4.1; (n=2).

² Viscosity for Star-Dri 1 was determined at a shear rate of only 58 s^{-1} due to limitations of the measuring system in handling solutions of very high viscosity.

Figure 16. Viscosity as a function of shear rate for SHPs (40% w/v) of varying DE.

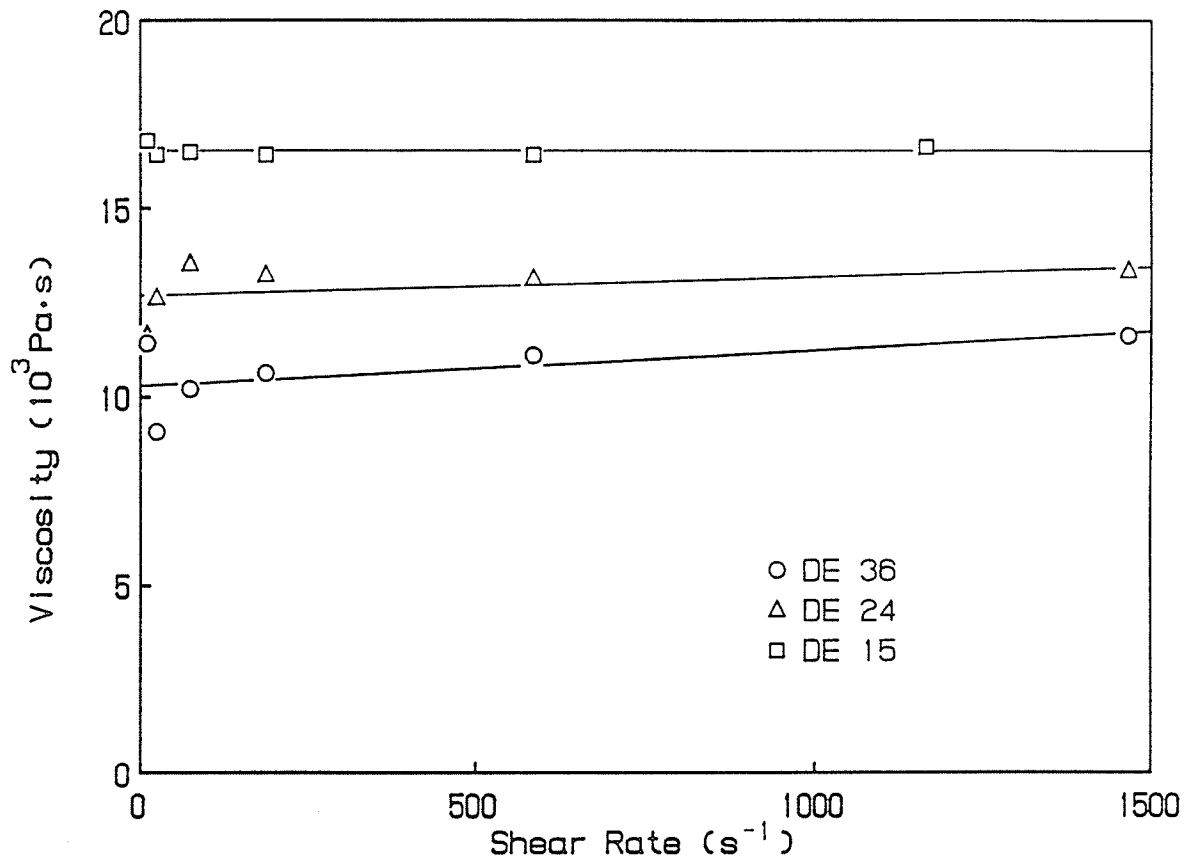
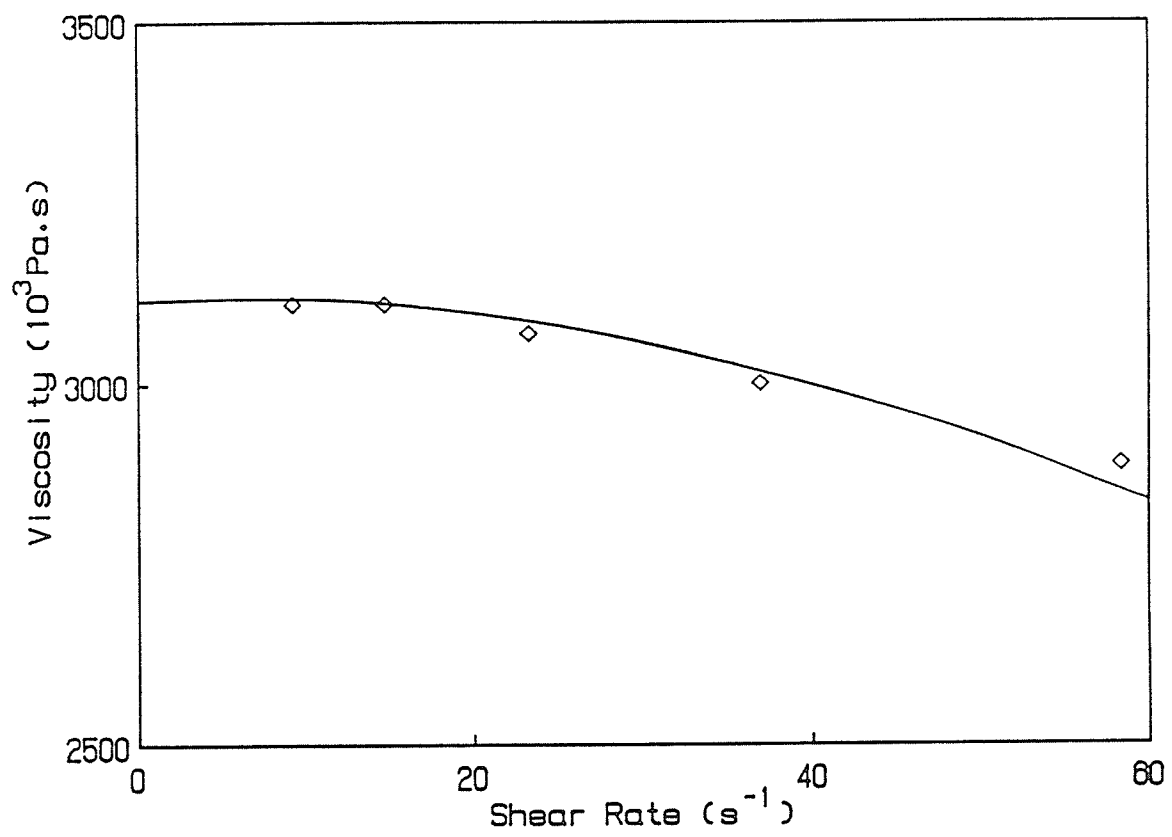


Figure 17. Viscosity as a function of shear rate for 40% w/v Star-Dri
1 (DE 1.0).



(Tung, 1988).

Figures 18a and b represent relationships between DE and solution viscosity for the starch hydrolysates at 20 and 40% w/v respectively. As seen by these plots, at both solute concentrations, solution viscosity increases exponentially with decreasing solute DE. In the context of free volume theory, the relationships between viscosity and T_g' , for 20% (w/v) samples is shown in figure 19. An upper T_g' limit, corresponding to the onset of chain entanglement, is attained at approximately 265 K. Beyond this value, further increases in solute molecular weight have little or no effect on T_g' , but continue to dramatically influence the viscoelastic properties of the sample network; i.e. increase gel strength at constant temperature, as reflected by increases in viscosity (figure 19). Ferry (1980) has observed similar behaviour for synthetic polymers. Figure 19 emphasizes the importance of choosing the correct starch hydrolysate for a particular food system. Choosing a SHP with a DE even slightly lower than ideal will offer little protection to the food system; i.e. T_g' will remain much lower than T_{storage} . The relationships presented in figures 14, 15 and 19 should aid the manufacturer/processor in selecting the appropriate starch hydrolysate for specific formulations.

Unfreezable water was also quantified by measuring the heat of fusion, ΔH (figure 13), for samples over a broad range of moisture contents. Figure 20 is a plot of melting enthalpy of ice as a function of water content in the sample for a typical starch hydrolysate (DE 20). By extrapolating to zero enthalpy, where no more freezable water exists, the amount of unfreezable water can be recorded. Unfreezable water values for the starch hydrolysates examined (table 8) ranged from 0.18-

Figure 18. Viscosity as a function of DE of starch hydrolysates at a) 20% w/v and b) 40% w/v.

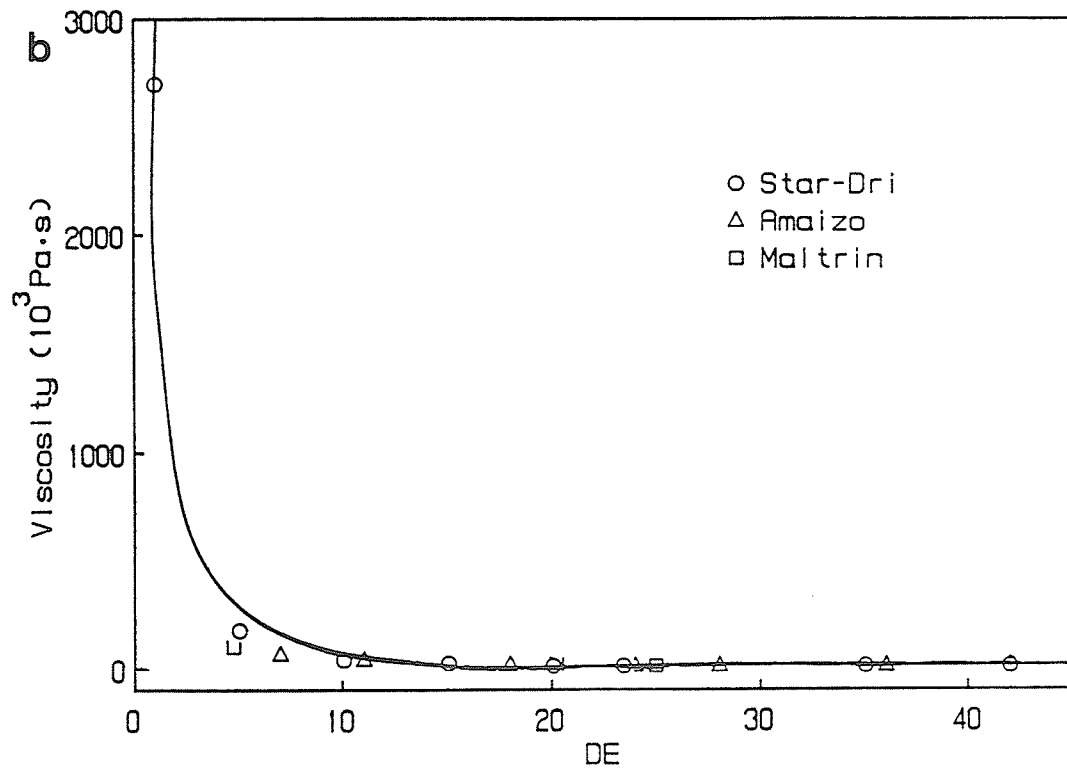
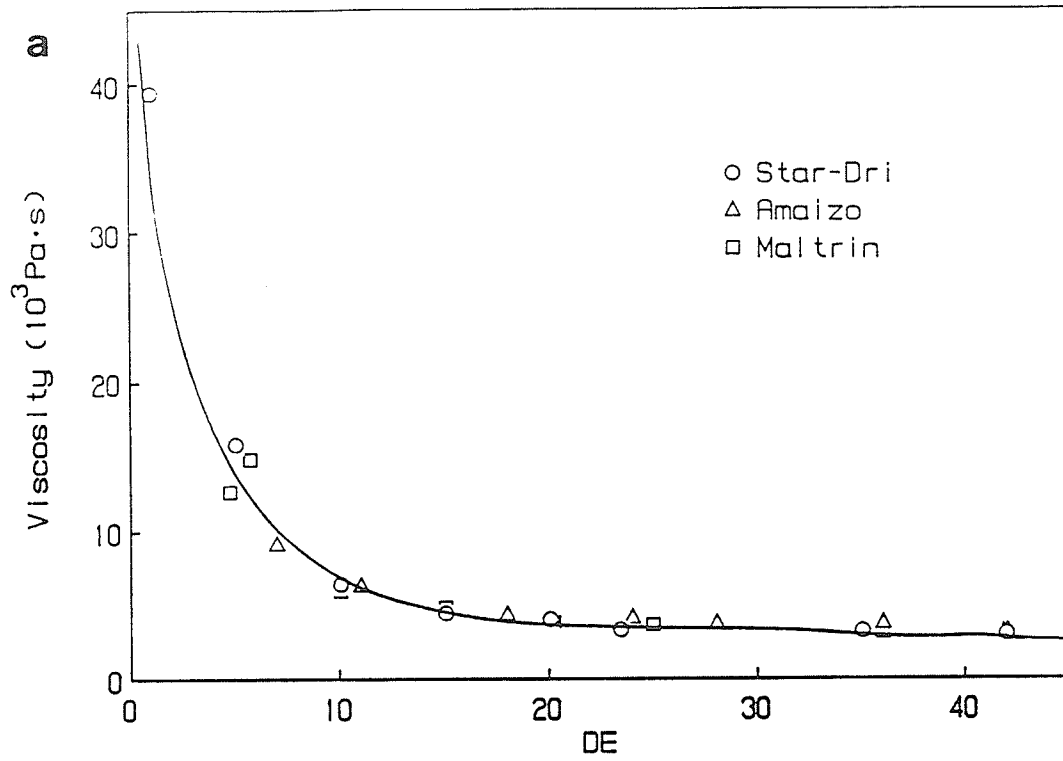


Figure 19. Relationship between sample viscosity and Tg' for polydisperse aqueous starch hydrolysates at 20% w/w; points represent SHPs of varying DE.

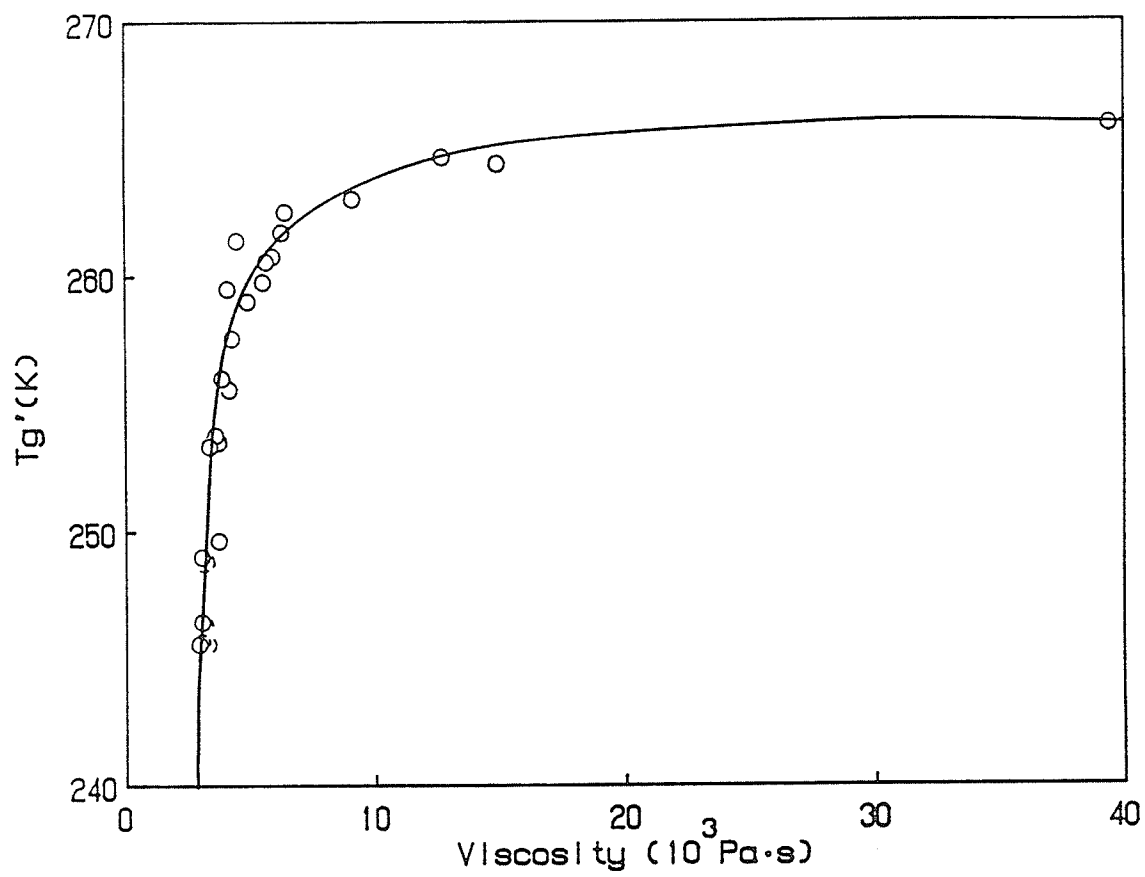


Figure 20. Determination of unfreezable water for an aqueous starch hydrolysate (DE 20).

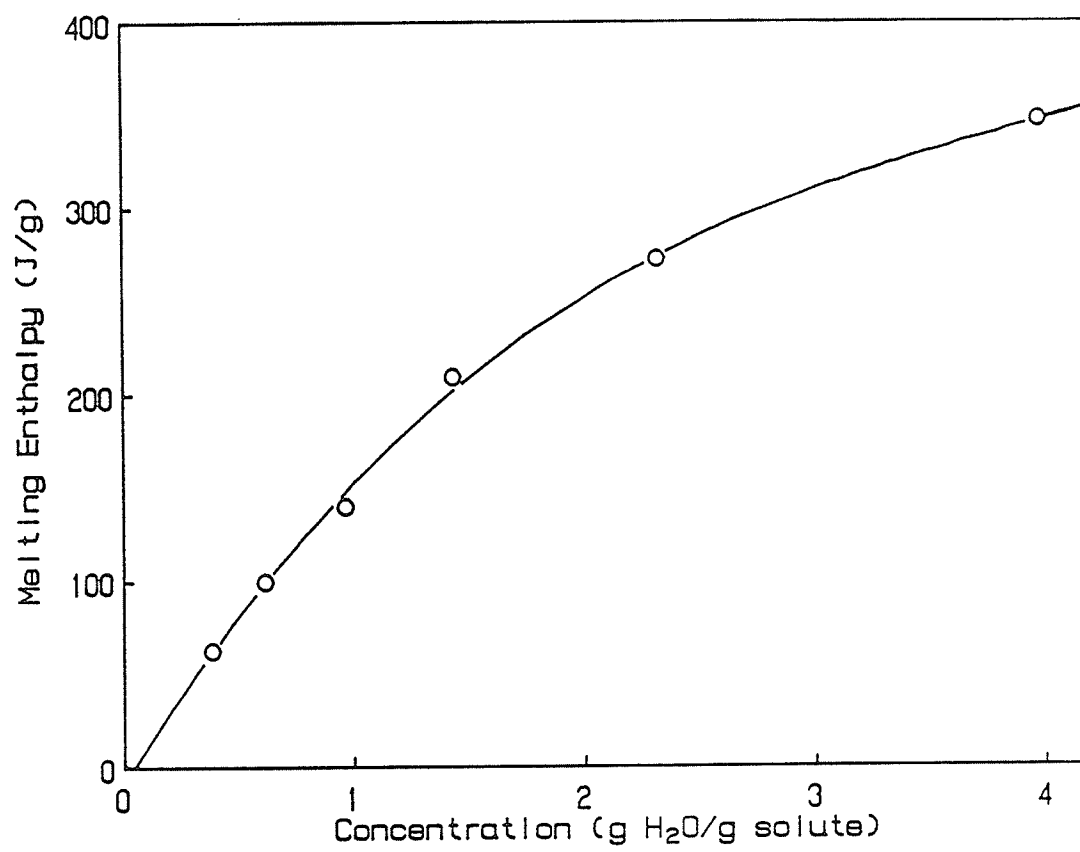


TABLE 8. Unfreezable water¹ of glucose-based oligomers and commercial starch hydrolysates

Sample	Unfreezable Water (g H ₂ O g ⁻¹ solid)
D-glucose	0.18
D-maltose	0.25
D-maltotriose	0.28
D-maltotetraose	0.14
D-maltopentaose	0.23
D-maltohexaose	0.24
D-maltoheptaose	0.27
Star-Dri 42X	0.35
Star-Dri 35R	0.15
Amaizo 24D	0.30
Star-Dri 20	0.25
Maltrin M150	0.20
Amaizo 10	0.30
AVEBE 6	0.25
Star-Dri 5	0.12
Star-Dri 1	0.29

¹ Determined by extrapolation to zero enthalpy as described in section 3.2.2.

0.35 g H₂O g⁻¹ solute. Any relationship between molecular size and unfreezable water content was not observed. Levine and Slade, however, determined unfreezable water contents for a homologous series of commercial corn syrups (1986) and a less homologous group of sugar solids (1987) and found that there is an inverse linear relationship between T_g' and unfreezable water with correlation coefficients of -0.91 and -0.89 respectively. Based on these results, their conclusion was that for a homologous set of glucose oligomers, the fraction of total water unfrozen in the glass at T_g' decreases with increasing molecular weight of the solute. On the other hand, these researchers found a poor correlation (r=-0.47) between unfreezable water and reciprocal molecular weight for a group of diverse polyhydroxy compounds. These findings, as well as our own (presented in table 8), confirm the observations of Franks (1985), who noted that among the (non-homologous) sugars and polyols, most widely used as "water binders" in fabricated foods, the amount of unfreezable water does not show a simple dependence on molecular weight of the solute. As Levine and Slade (1988) have recently pointed out, the critical importance of the unfreezable water as a plasticizer necessitates further investigation into the relationships between T_g', viscosity, solute structure/concentration/ molecular weight, and unfreezable water.

In this context, T_g' values for monodisperse glucose oligomers and starch hydrolysates, prepared at concentrations ranging from 20-70% w/v and analysed by DSC, are shown in table 9. When these results were plotted for a number of representative samples (figure 21) it was seen that T_g' was independent of initial solute concentration for low molecular weight samples (e.g. glucose, Star-Dri 42X). This finding suggests

TABLE 9. Tg' values¹ for monodisperse glucose-based oligomers and commercial starch hydrolysates at various concentrations

Sample	Concentration (% w/v)	Tg' (K) ²
D-Glucose	20.08	230.64±0.75 ^a
	30.00	231.31±0.38 ^a
	40.66	234.05±0.35 ^b
	50.40	232.31±0.14 ^{ab}
	60.36	231.69±0.84 ^a
	70.00	231.06±0.95 ^a
D-Maltose	20.51	243.76±0.70 ^a
	30.16	242.90±0.63 ^{ab}
	40.00	243.25±0.08 ^a
	50.83	241.91±0.39 ^b
	60.00	242.54±0.05 ^{ab}
	72.86	240.20±0.24 ^c
D-Maltotriose	20.00	250.22±0.06 ^a
	30.00	250.00±0.05 ^a
	40.00	249.67±0.00 ^a
	52.74	248.17±0.42 ^b
	60.00	243.85±0.28 ^c
D-Maltotetraose	20.00	251.37±0.03 ^a
	30.45	250.43±0.06 ^b
	40.74	250.69±0.05 ^b
	51.28	248.81±0.17 ^c
	60.35	247.96±0.11 ^d
D-Maltopentaose	20.41	255.74±0.00 ^a
	30.00	255.84±0.13 ^a
	40.45	255.77±0.04 ^a
	51.78	254.04±0.09 ^b
	60.06	252.01±0.12 ^c
D-Maltohexaose	20.16	256.38±0.14 ^a
	30.48	257.05±0.03 ^b
	41.56	256.90±0.01 ^b
	51.15	254.30±0.03 ^c
	60.59	254.97±0.08 ^d

TABLE 9. cont.

Sample	Concentration (% w/v)	Tg' (K)
D-Maltoheptaose	20.41	259.92±0.03 ^a
	30.39	259.61±0.14 ^a
	40.00	259.20±0.01 ^b
	50.00	257.63±0.07 ^c
	62.30	255.82±0.18 ^d
Star-Dri 42X	20.00	246.15±0.30 ^a
	25.00	246.36±0.01 ^a
	30.00	246.11±0.40 ^a
	39.80	245.78±0.08 ^a
	50.00	245.69±0.01 ^a
	60.00	243.35±0.01 ^b
Star-Dri 35R	20.00	248.82±0.24 ^a
	30.00	249.45±0.03 ^b
	40.00	249.61±0.05 ^b
	50.00	248.89±0.09 ^a
	60.00	248.76±0.14 ^a
Amaizo 24D	20.00	253.48±0.08 ^a
	30.00	253.44±0.02 ^a
	40.00	253.60±0.03 ^a
	50.00	252.69±0.04 ^b
	60.00	249.08±0.32 ^c
Star-Dri 20	20.13	259.49±0.00 ^a
	30.18	259.51±0.03 ^a
	41.11	259.38±0.03 ^a
	51.13	258.72±0.23 ^b
	61.94	255.80±0.19 ^c
Maltrin M150	20.00	259.16±0.05 ^a
	30.46	259.27±0.07 ^a
	40.31	259.02±0.08 ^a
	50.54	259.06±0.01 ^a
	59.34	255.84±0.69 ^b
Amaizo 10	19.95	261.43±0.05 ^a
	30.95	261.45±0.14 ^a
	40.14	261.30±0.02 ^a
	51.75	259.62±0.13 ^b

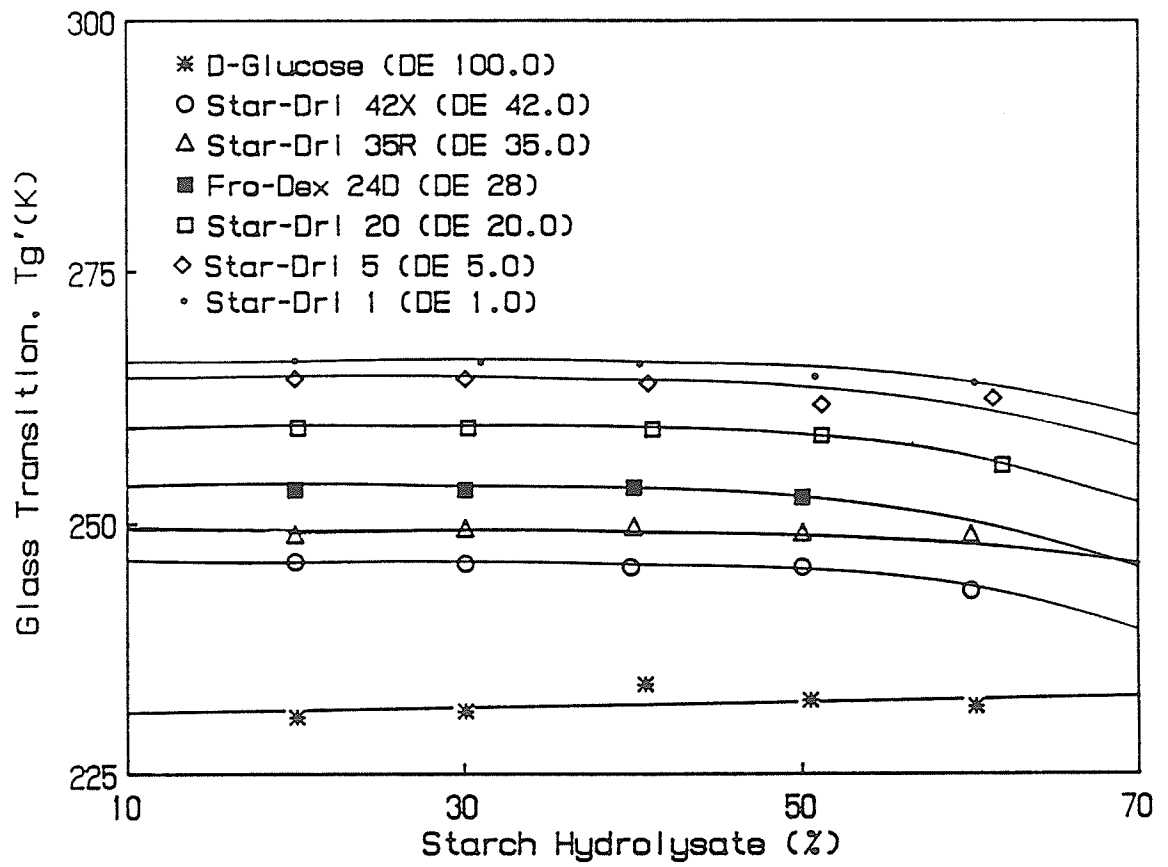
TABLE 9. cont.

Sample	Concentration (% w/v)	T _g ' (K)
AVEBE 6	20.20	265.27±0.05 ^a
	29.88	265.62±0.08 ^b
	42.38	265.41±0.10 ^{ab}
	52.10	264.48±0.02 ^c
	61.40	263.14±0.05 ^d
Star-Dri 5	20.00	264.32±0.05 ^a
	30.07	264.39±0.04 ^a
	40.88	263.84±0.14 ^a
	51.09	261.42±0.03 ^b
	61.36	262.41±0.50 ^c
Star-Dri 3.8	20.00	266.38±0.18 ^a
	30.00	266.23±0.10 ^a
Star-Dri 1	20.00	266.18±0.18 ^a
	30.95	265.92±0.03 ^a
	40.33	265.84±0.22 ^a
	50.68	264.45±0.04 ^b
	60.19	263.79±0.32 ^c

¹ DSC analysis as described in section 3.2.2.2.

² For each sample, T_g' values followed by the same letter are not significantly different (p≤0.05).

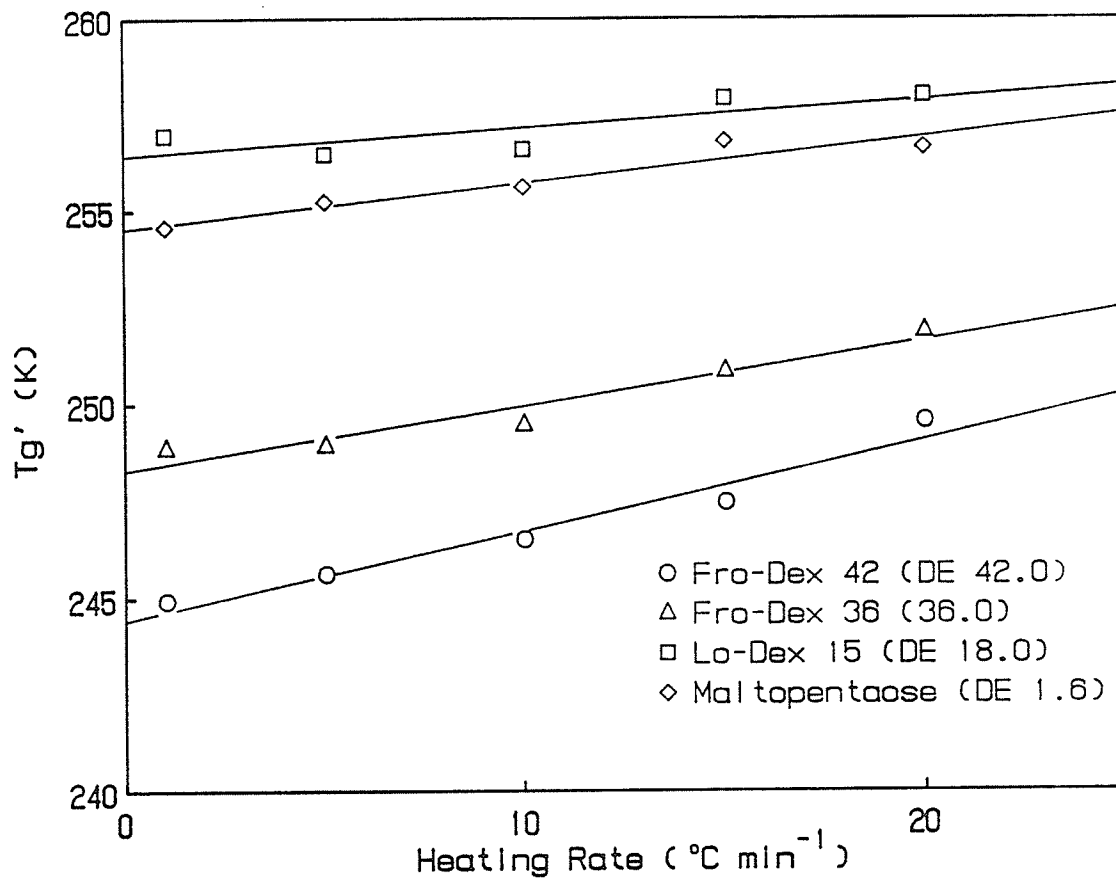
Figure 21. Effect of solute concentration on T_g' for commercial SHPs of varying DE; heating rate $10^\circ\text{C min}^{-1}$.



that a glass of constant composition is attained under equilibrium conditions where water is allowed to freeze. As reported by Simatos et al. (1975), various researchers have made similar observations for fish, egg white and yolk, beef muscle, different proteins, casein, plasma, and dough systems using older DTA methodologies. However, in the present study, it was noted that, aside from glucose and Star-Dri 42X, all other carbohydrate materials exhibited depressed T_g' at high concentrations ($\geq 50\%$ w/v), under the freezing protocol used. It appears that the elevated viscosities, as a result of high solute concentrations, are responsible for incomplete phase separation during freezing; i.e. some of the freezable water remains in the amorphous state rather than freezing out as ice. This additional water present in the glass exerts a plasticizing effect and could explain the depression in T_g' for these samples. Moreover, for all carbohydrate dispersions exhibiting depressed T_g' values at high solute concentration, ice recrystallization (an exothermic effect) was observed. This provided additional evidence that these particular samples were cooled at a relatively rapid rate (i.e. non-equilibrium freezing process), so that some of the freezable water did not have adequate time to crystallize into ice, and, instead, remained in the amorphous phase surrounding the ice crystals. Simatos et al. (1975) has reported similar behaviour (i.e. depressed T_g' values and ice recrystallization) in plasma solutions that have been rapidly cooled.

The effect of heating rate on the apparent T_g' values is illustrated in figure 22. For all samples tested, there is consistently a slight increase in the calorimetrically measured T_g' with increasing heating rate; this is a direct reflection of the dynamic character of DSC analysis in determining phase transition temperatures. As a result of these

Figure 22. Effect of heating rate on T_g' for commercial SHPs (20% w/v) of varying DE.



findings, a constant intermediate heating rate of $10^{\circ}\text{C min}^{-1}$ was adopted to obtain a reasonable estimate of T_g' over a practical experimental time frame.

A further aspect of the behaviour of frozen hydrolysates examined in this study was the identification of predictive equations that would allow assessment of T_g' on the basis of oligosaccharide composition and their respective T_g' . The Flory-Fox equation (equation 3, section 2.3.3), originally developed to describe the T_g of binary mixtures of synthetic polymers (Fox and Flory, 1954), was tested with the frozen aqueous carbohydrate systems of this study. To and Flink (1978b) first employed this equation in predicting the characteristic collapse temperature (T_c), of freeze dried carbohydrate mixtures of known composition. Following this approach and working with frozen aqueous binary mixtures of SHPs, we observed that similar relationships exist. Figure 23 illustrates the dependence of T_g' on composition of the carbohydrate mixtures; both the DSC measured and the predicted (using the Flory-Fox equation) T_g' values are given for monodisperse (figure 23a) and polydisperse (figure 23b) carbohydrate systems respectively. As can be seen from these figures, the Flory-Fox equation provides estimates of T_g' that are very close to the experimentally observed values.

The above rationale was further extended to polydisperse systems for 21 starch hydrolysates in an attempt to predict their effective T_g' from their oligosaccharide composition as determined by HPLC. A typical chromatogram for the analysis of one of the SHPs (Amaizo 42) is shown in figure 24. Under the outlined operating conditions for the HPLC analysis (section 3.2.1), good separation was obtained for oligosaccharides with DP of 1-7. Table 10 summarizes the oligosaccharide composition of the

Figure 23. Prediction of T_g' for binary mixtures: a) maltose/maltoheptaose and b) Fro-Dex 42/Lo-Dex 5; 30% w/w total solids at various weight fractions for the two components.

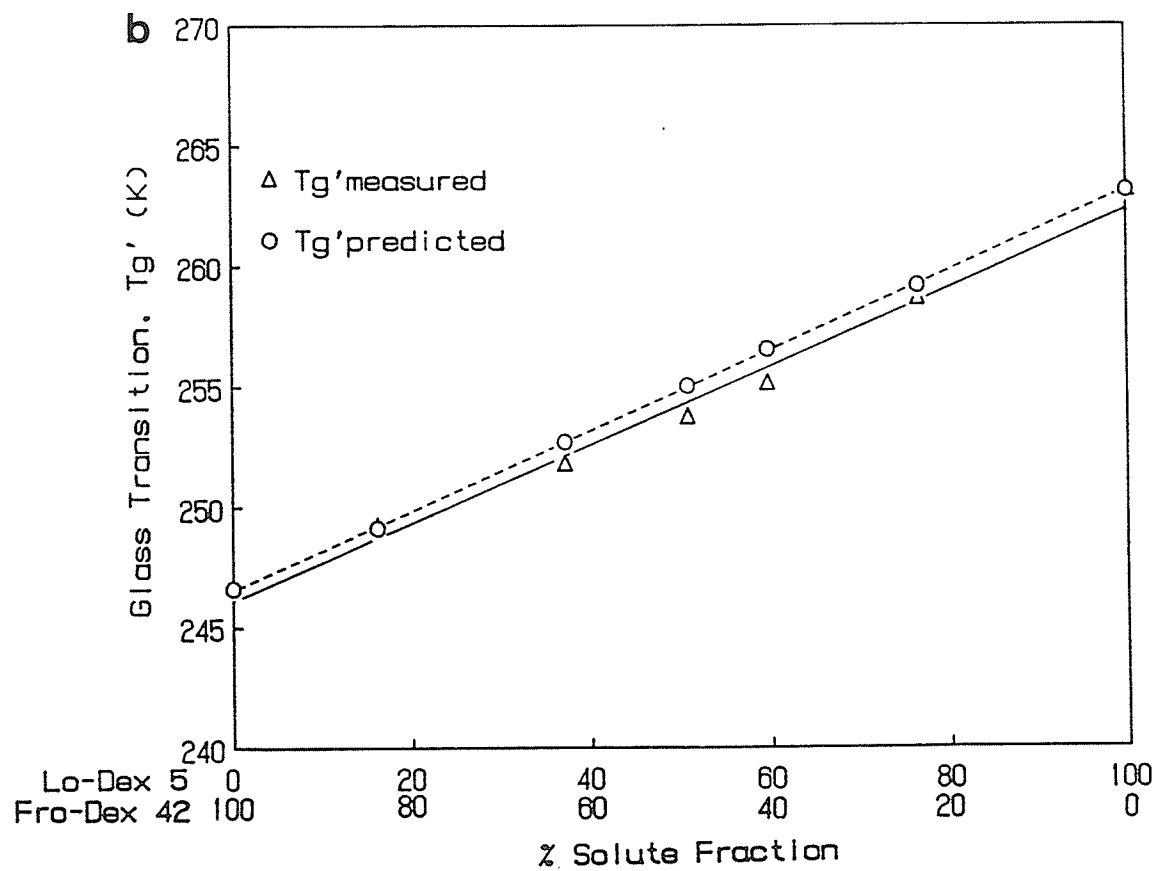
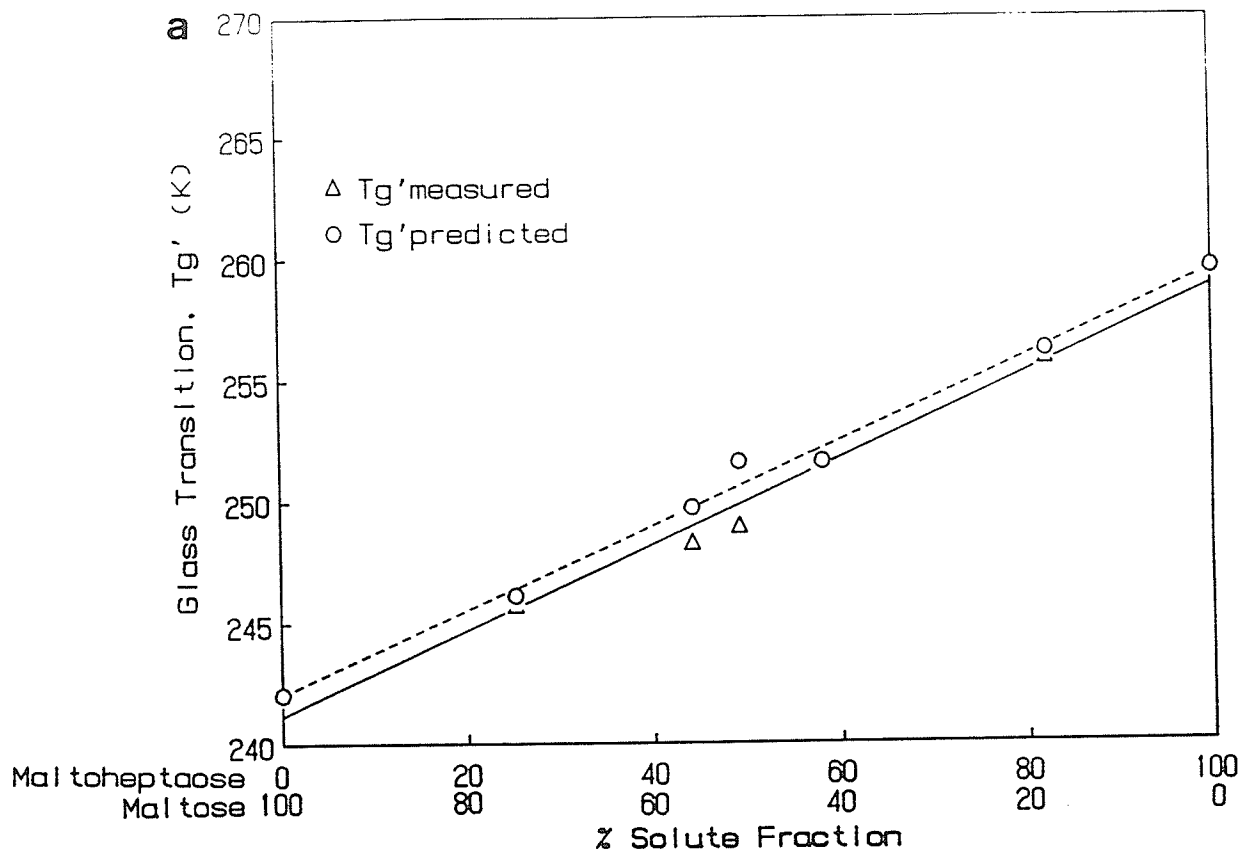


Figure 24. Typical HPLC chromatogram of a commercial SHP (Amaizo 42, 20 mg mL⁻¹). Column: Aminex HPX-42A oligosaccharide analysis. Eluent: DDI H₂O. Injection volume: 50 μL. Temperature: 85°C. Detection: refractive index; attenuation 16X.

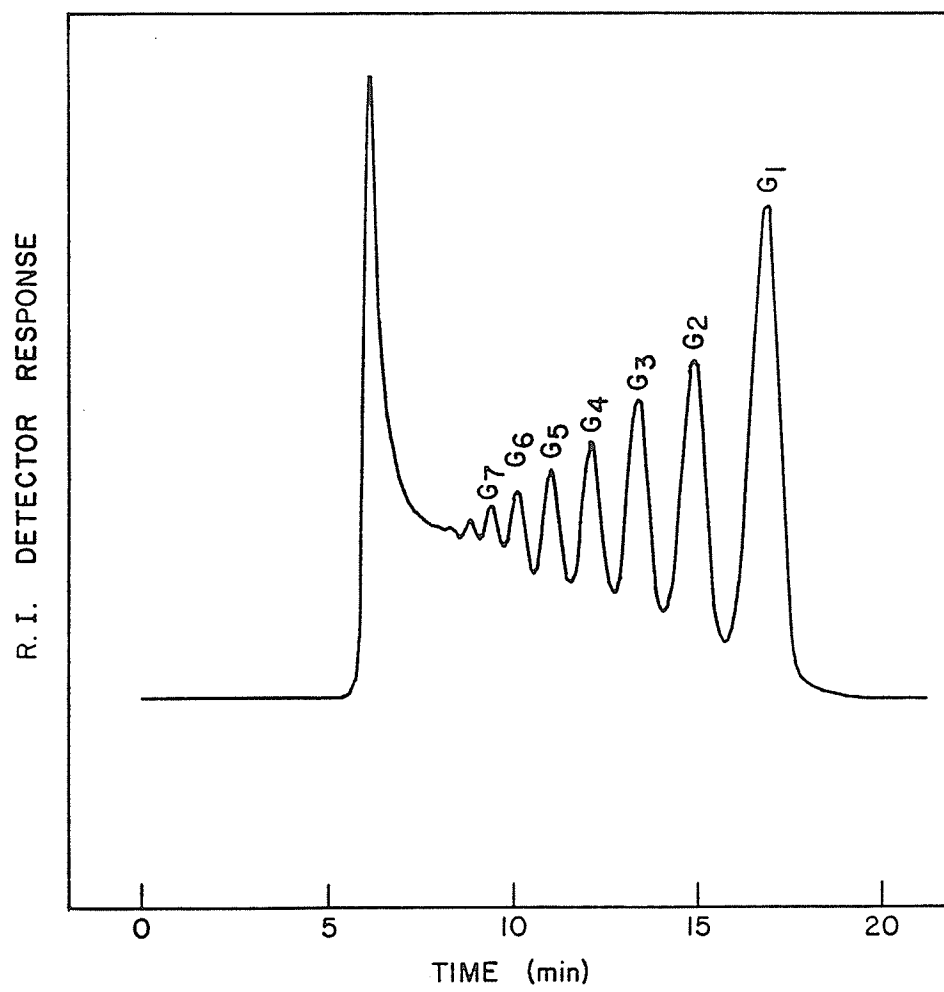


TABLE 10. Oligosaccharide composition¹ of various commercial starch hydrolysates²

Sample	Composition (%)								>DP ₇ ³
	DP ₁	DP ₂	DP ₃	DP ₄	DP ₅	DP ₆	DP ₇		
Amaizo 42	19.50±0.33	13.25±0.20	10.35±0.19	8.45±0.18	7.11±0.19	6.05±0.05	4.67±0.13	30.62	
Star-Dri 42F	21.11±0.36	15.53±0.28	12.30±0.22	10.22±0.26	8.61±0.23	6.68±0.15	5.24±0.28	20.31	
Amaizo 36	14.39±0.52	10.26±0.38	8.38±0.33	7.16±0.25	6.31±0.29	5.42±0.10	4.29±0.20	43.79	
Maltrin M365	6.52±0.20	27.86±0.35	16.75±0.19	6.84±0.07	5.01±0.06	4.36±0.14	3.44±0.10	29.27	
Star-Dri 35R	14.29±0.05	11.49±0.05	9.97±0.03	8.66±0.04	7.76±0.04	6.74±0.07	5.43±0.02	35.66	
Amaizo 24D	9.22±0.40	7.47±0.29	6.79±0.23	6.28±0.23	5.77±0.29	5.24±0.25	4.47±0.07	54.76	
Amaizo 24924	6.31±0.23	5.57±0.19	5.34±0.19	5.24±0.13	5.15±0.16	4.65±0.07	4.04±0.19	63.76	
Star-Dri 24R	6.71±0.09	7.18±0.02	8.23±0.05	7.20±0.10	6.78±0.02	8.69±0.13	8.54±0.05	46.67	
Maltrin M250	7.52±0.10	7.20±0.10	7.04±0.11	6.89±0.07	6.67±0.11	5.96±0.12	5.05±0.02	53.67	
Maltrin M200	2.46±0.15	7.99±0.10	9.32±0.11	6.84±0.15	6.65±0.12	13.80±0.25	12.63±0.26	40.31	
Star-Dri 20	2.10±0.02	7.17±0.09	8.33±0.09	5.34±0.08	6.06±0.09	14.91±0.18	10.37±0.15	45.77	
Amaizo 15	4.98±0.17	4.88±0.16	4.92±0.17	5.02±0.18	5.06±0.18	4.65±0.21	4.17±0.05	66.32	

TABLE 10 cont.

Sample	Composition (%)							DP ₇	>DP ₇
	DP ₁	DP ₂	DP ₃	DP ₄	DP ₅	DP ₆	DP ₇		
Maltrin M150	0.98±0.18	4.20±0.13	5.87±0.07	4.89±0.06	4.24±0.13	8.62±0.18	-	-	71.20
Star-Dri 15	1.25±0.05	3.92±0.05	5.65±0.06	4.11±0.04	3.63±0.08	8.92±0.11	12.83±0.11	12.83±0.11	59.69
Anaizo 10	0.70±0.09	2.77±0.14	3.88±0.07	3.20±0.02	2.67±0.07	5.56±0.07	6.55±0.09	6.55±0.09	74.67
Maltrin M100	0.99±0.22	3.07±0.22	4.51±0.15	3.86±0.10	3.38±0.14	6.28±0.11	7.70±0.28	7.70±0.28	70.21
Maltrin M500	0.60±0.04	2.51±0.08	3.99±0.06	3.45±0.04	3.14±0.04	5.50±0.09	6.84±0.10	6.84±0.10	73.97
Star-Dri 10	0.85±0.06	1.89±0.10	3.13±0.05	2.48±0.06	2.45±0.09	4.78±0.15	6.01±0.02	6.01±0.02	78.41
Maltrin M050	0.66±0.12	0.83±0.11	1.03±0.06	1.19±0.08	1.05±0.33	1.48±0.03	1.49±0.01	1.49±0.01	92.27
Anaizo 5	0.39±0.02	1.65±0.01	2.72±0.02	2.14±0.02	1.86±0.11	4.26±0.05	5.72±0.01	5.72±0.01	81.26
Star-Dri 5	1.07±0.15	1.62±0.03	1.98±0.13	1.59±0.08	1.76±0.12	2.68±0.03	2.31±0.16	2.31±0.16	86.99
Maltrin M040	-	0.54±0.18	1.04±0.15	0.99±0.07	1.06±0.15	1.56±0.04	1.92±0.13	1.92±0.13	92.89
Avebe 10	-	1.59±0.07	2.96±0.02	2.29±0.04	1.96±0.03	3.95±0.01	5.68±0.03	5.68±0.03	81.57
Avebe 6	-	0.94±0.08	1.65±0.02	1.25±0.01	1.06±0.07	2.24±0.07	3.05±0.21	3.05±0.21	89.81

¹ Data are expressed as percentage of total carbohydrate content (\bar{x} ±SD, n=3).

² HPLC analysis of starch hydrolysates as described in section 3.2.1.

³ Determined by difference: 100 - Σ (DP_i).

starch hydrolysates analysed. Differences in oligosaccharide distribution were not only evident among samples of varying DE, but also among samples of identical DE provided by different suppliers. The compositional data obtained for all Maltrin products were, in each case, in very close agreement with both the manufacturer's specifications (Maltrin: Maltodextrins and Corn Syrup Solids; Grain Processing Corp., Muscatine, Iowa) and the results of Brooks and Griffin (1987) as determined by HPLC. The oligosaccharide profiles for all other starch hydrolysates compared favourably to the compositional data supplied by the Corn Refiners Association as reported by Hobbs (1986). Based on the oligosaccharide composition and the experimentally determined T_g' of the respective individual oligosaccharide standards, predictions of T_g' for polydisperse hydrolysates were made by employing the generalized form of the Flory-Fox equation, as described in section 3.2.2. A comparison between the DSC measured glass transition temperatures and those predicted by the Flory-Fox equation is illustrated in figure 25. Assuming that this theory holds, T_g' predicted should equal T_g' measured (by DSC), as represented by the solid line. Although a linear relationship between the two temperatures was found ($y = 1.22x - 59.82$; $r = 0.987$, $p < 0.001$), there seemed to be a deviation of the measured values from what the theory predicts, particularly for high DE samples; i.e. in the presence of low molecular weight material the composite glass appears to vitrify at a much lower temperature than that predicted assuming the Flory-Fox formalism.

This departure from ideality was confirmed by similar tests on a series of binary mixtures, each of which had a common reference maltodextrin and a second maltodextrin of varying DE combined in a 1:1 ratio.

Figure 25. Comparison between T_g' -predicted (Flory-Fox equation) and T_g' -measured (DSC) (shown by broken line) for polydisperse SHPs of varying DE. Solid line refers to the theoretically predicted relationship.

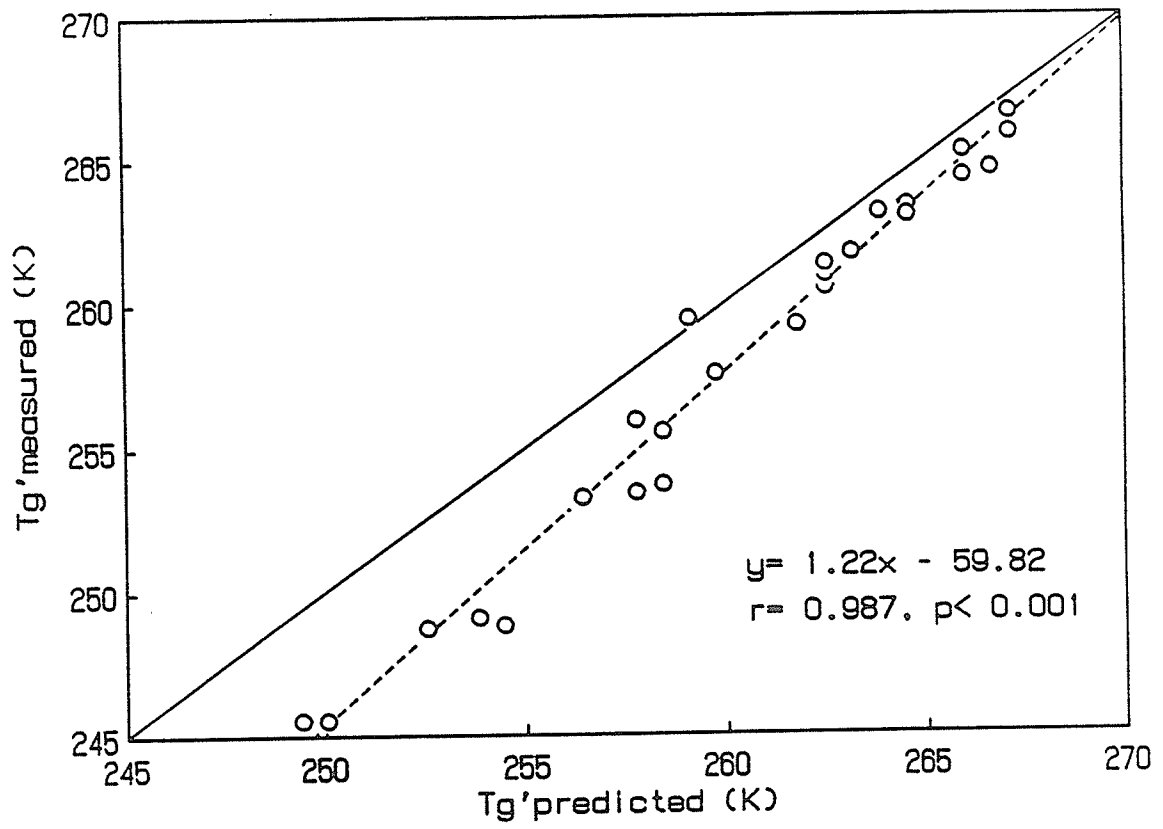


Figure 26. Comparison between T_g' -predicted (Flory Fox equation) and T_g' -measured (DSC) (shown by broken line) for binary mixtures of monodisperse maltoheptaose + monodisperse glucose monomer and oligomers (1:1 w/w; 30% w/w total solids/H₂O): a) glucose; b) maltose; c) maltotriose; d) maltotetraose; e) maltopentaose; f) maltohexaose; g) maltoheptaose. Solid line refers to the theoretically predicted relationship.

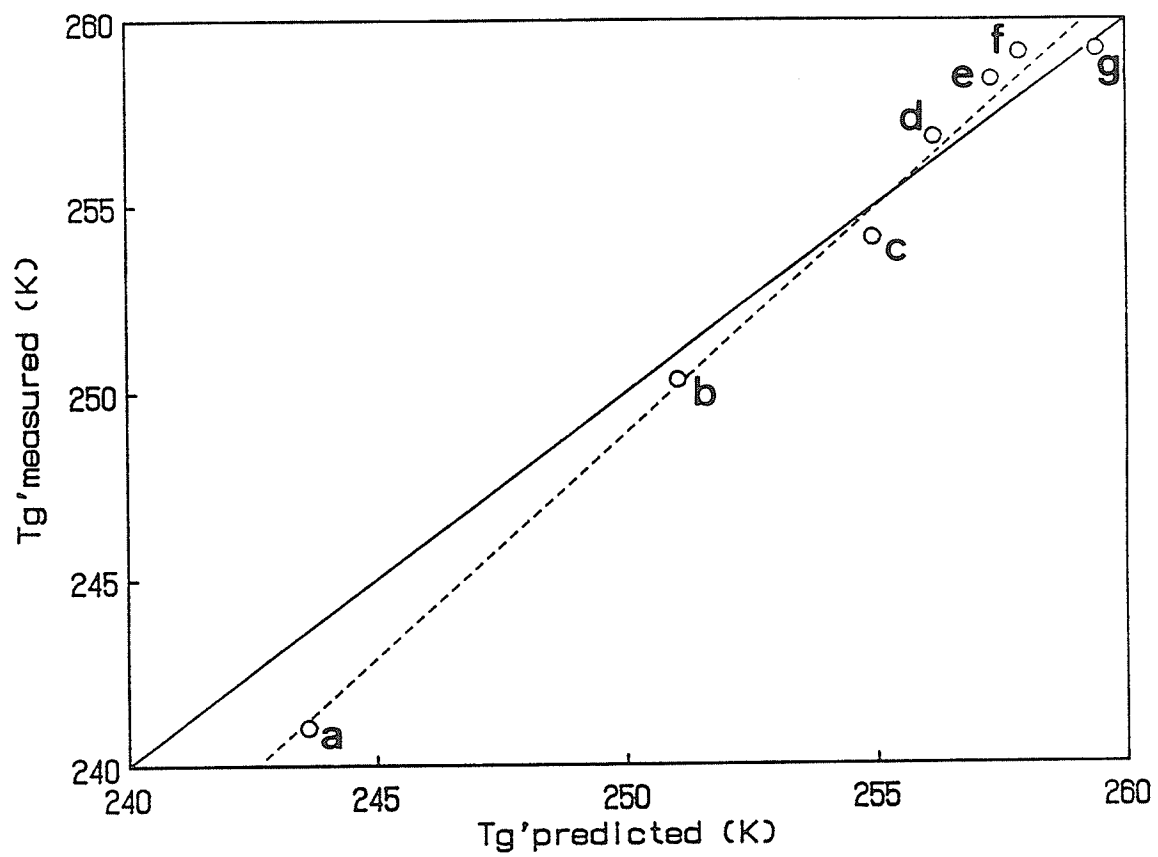
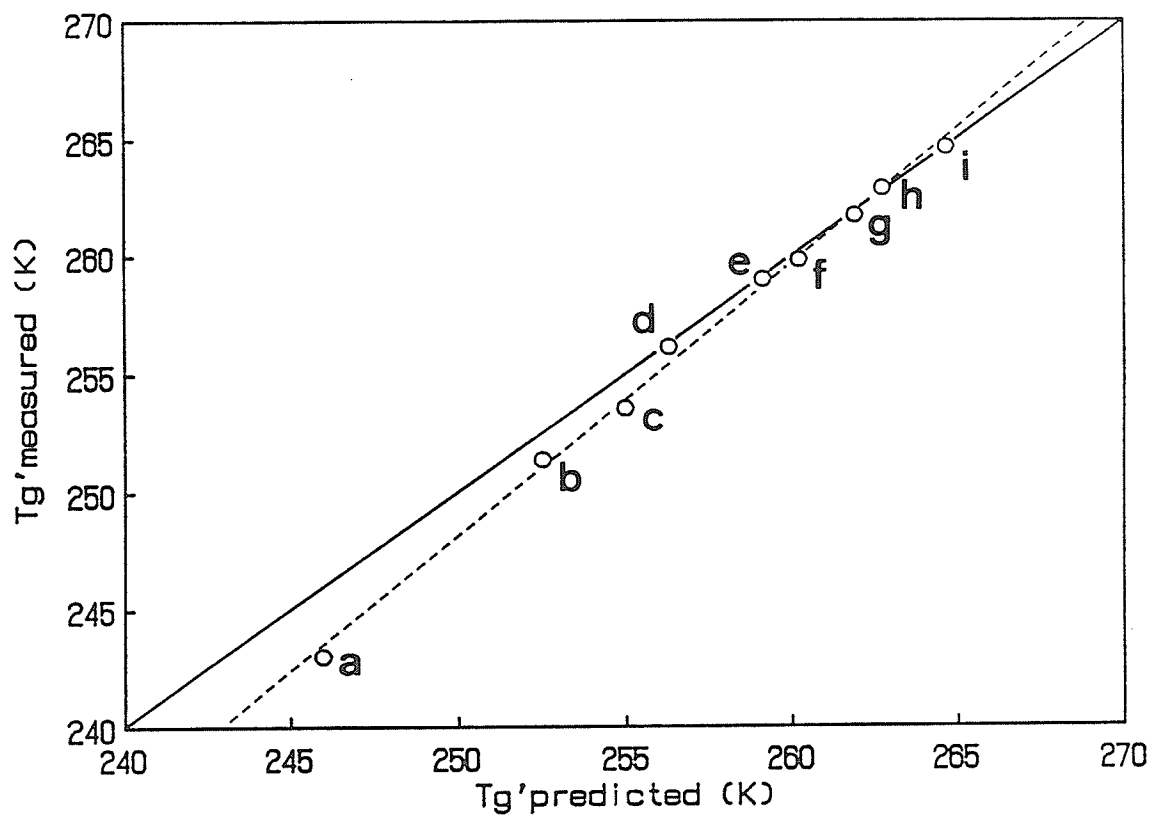


Figure 27. Comparison between T_g' -predicted (Flory-Fox equation) and T_g' -measured (DSC) (shown by broken line) for binary mixtures of Maltrin M040 + monodisperse glucose and maltose, and commercial SHPs (1:1 w/w; 30% w/w total solids/H₂O): a) glucose; b) maltose; c) Fro-Dex 42; d) Maltrin M365; e) Maltrin M250; f) Maltrin M200; g) Maltrin M150; h) Maltrin M100; and i) Maltrin M040. Solid line refers to the theoretically predicted relationship.



For both monodisperse and polydisperse binary systems (figures 26 and 27 respectively), the mixtures containing high DE maltodextrins also exhibited a more depressed T_g' value than that predicted by the Flory-Fox equation. Thus it appears that in the presence of low molecular weight constituents the effective free volume of the mixture is much greater than that theoretically anticipated.

To test the possibility of having greater free volume effects due to the presence of branched oligosaccharides, as it is known for branched synthetic polymers (section 2.3.3; Brydson, 1972), the starch hydrolysates were re-analysed after being debranched with a purified pullulanase preparation. As shown in table 11, the oligosaccharide profile of most of the starch hydrolysates was altered only to a small degree by the pullulanase treatment, indicating that these samples were relatively free of α -1,6 linkages in their native state. Furthermore, as illustrated in figure 28, debranching did not significantly affect the linear relationship between T_g' measured and T_g' predicted values ($y = 1.18x - 50.23$; $r = 0.94$, $p < 0.001$) As well, as was the case for the native samples, the composite glasses of the debranched small molecular weight hydrolysates vitrified at a much lower temperature than theoretically predicted. Therefore, differences between measured and predicted values of T_g' appear to be due exclusively to the effect of solute molecular weight rather than a combined effect of solute molecular weight and structure.

TABLE 11. Oligosaccharide composition¹ of various debranched² commercial starch hydrolysates³

Sample	Composition (%)							>DP ₇ ⁴
	DP ₁	DP ₂	DP ₃	DP ₄	DP ₅	DP ₆	DP ₇	
Amaizo 42	18.53±0.33	12.24±0.19	9.85±0.24	8.11±0.24	6.58±0.27	5.70±0.22	3.90±0.64	35.09
Star-Dri 42F	17.08±0.40	12.47±0.26	10.07±0.16	8.38±0.16	6.98±0.09	5.45±0.12	5.27±1.50	34.30
Amaizo 36	15.45±0.19	10.64±0.13	8.70±0.14	7.49±0.11	6.51±0.06	5.54±0.10	4.42±0.29	41.25
Maltrin M365	7.71±0.19	22.48±0.30	14.10±0.16	7.05±0.03	5.56±0.05	4.89±0.08	4.79±0.92	33.42
Star-Dri 35R	14.12±0.75	10.72±0.57	9.26±0.42	8.22±0.45	7.09±0.47	5.99±0.18	5.23±0.48	39.57
Amaizo 24D	10.86±0.15	8.01±0.17	7.41±0.02	7.10±0.01	6.93±0.16	6.19±0.00	2.13±0.00	51.37
Amaizo 24-924	9.66±0.18	7.22±0.06	6.87±0.08	6.84±0.11	6.85±0.09	6.80±0.26	5.67±0.26	50.09
Star-Dri 24R	8.95±0.16	8.46±0.28	8.86±0.28	7.82±0.25	7.64±0.27	9.12±0.27	9.90±0.79	39.25
Maltrin M250	9.96±0.9	8.36±0.35	8.05±0.41	8.12±0.36	7.91±0.39	6.85±0.25	6.00±0.22	44.75
Maltrin M200	4.43±0.20	7.92±0.17	9.08±0.04	7.28±0.08	6.79±0.76	13.37±0.47	14.40±0.45	36.73
Star-Dri 20	4.16±0.34	7.96±0.23	9.61±0.06	7.61±0.22	8.06±0.09	16.87±0.19	15.89±0.22	29.84
Amaizo 15	7.52±0.66	6.03±0.42	5.95±0.61	5.93±0.50	3.38±1.42	5.05±0.00	1.80±0.00	64.34

TABLE 11 cont.

Sample	Composition (%)							>DP ₇
	DP ₁	DP ₂	DP ₃	DP ₄	DP ₅	DP ₆	DP ₇	
Maltrin M150	2.97±0.34	4.12±0.21	5.55±0.33	5.20±0.27	5.37±0.76	7.43±0.65	14.43±0.80	54.93
Star-Dri 15	3.26±0.04	4.40±0.12	6.25±0.32	5.41±0.24	4.85±0.22	10.63±0.70	15.30±2.89	45.90
Amalzo 10	2.72±0.17	3.08±0.05	4.20±0.04	4.00±0.11	4.00±0.09	6.16±0.06	7.78±1.04	68.06
Maltrin M100	2.78±0.20	3.13±0.23	4.35±0.09	4.13±0.06	3.99±0.12	6.12±0.28	7.55±0.82	67.95
Maltrin M500	3.36±0.15	3.17±0.22	4.25±0.14	4.06±0.07	3.89±0.23	5.27±0.23	5.23±0.40	70.77
Star-Dri 10	3.58±0.20	2.67±0.22	3.48±0.06	3.37±0.20	3.28±0.06	5.56±0.22	6.44±0.02	71.62
Maltrin M050	2.60±0.24	0.99±0.10	1.19±0.11	1.53±0.06	1.57±0.01	1.99±0.10	0.35±0.11	89.78
Amalzo 5	3.77±0.18	2.31±0.18	2.84±0.11	2.79±0.17	2.58±0.32	2.69±0.15	4.19±0.27	78.83
Star-Dri 5	3.19±0.08	2.11±0.17	2.02±0.11	1.98±0.08	1.99±0.25	3.05±0.06	3.08±0.10	82.58
Maltrin M040	2.40±0.20	0.98±0.01	1.37±0.04	1.36±0.16	0.69±0.05	-	-	93.20
Avebe 10	2.56±0.08	1.47±0.03	2.67±0.04	2.43±0.08	1.90±0.08	4.15±0.08	5.61±0.28	79.21
Avebe 6	2.39±0.18	0.79±0.06	1.39±0.08	1.33±0.03	1.97±0.07	2.55±0.18	2.89±0.35	86.69

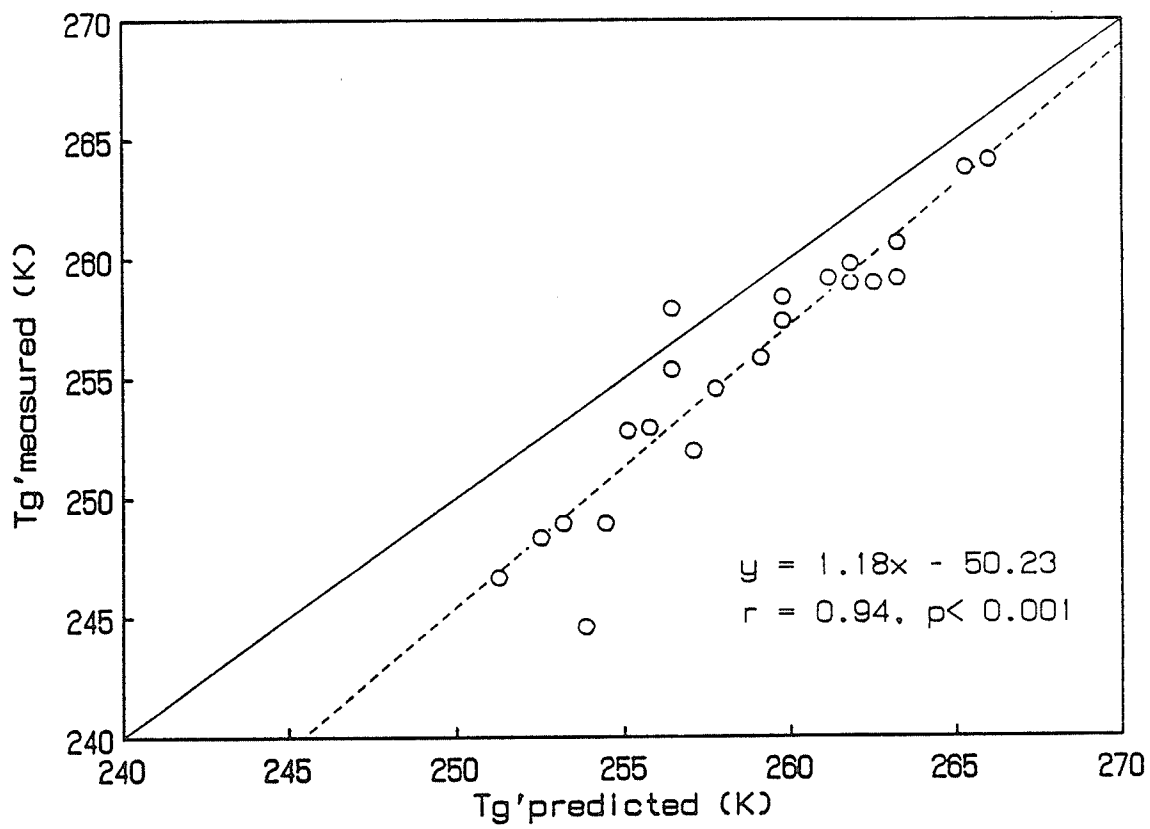
¹ Data are expressed as percentage of total carbohydrate content (\bar{x} ±SD, n=3).

² Debranching conditions as described in section 3.2.1.

³ HPLC analysis of starch hydrolysates as described in section 3.2.1.

⁴ Determined by difference: 100 - Σ (DP_i)

Figure 28. Comparison between T_g' -predicted (Flory-Fox equation) and T_g' -measured (DSC) (shown by broken line) for debranched polydisperse commercial SHPs of varying DE. Solid line refers to the theoretically predicted relationship.



4.2 Technological Implications Of Using Starch Hydrolysates In Food Formulations

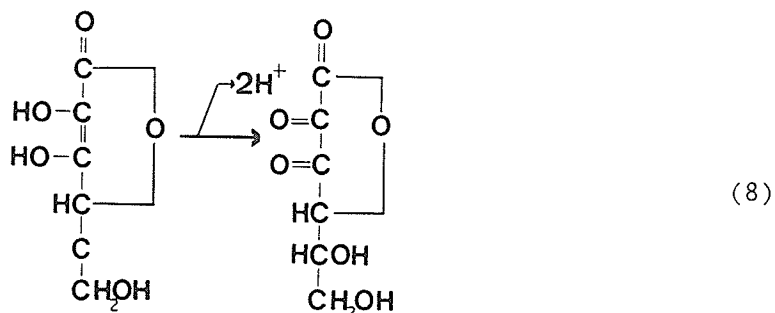
The significance of the phase behaviour of aqueous-carbohydrate systems, as it relates to applied food technology, was examined in the last half of this research program. Two separate studies were performed. One dealt with the effects of incorporating starch hydrolysates in aqueous solutions of ascorbic acid on its oxidation kinetics. In a second study, the antistaling effects of SHPs in starch gels, as monitored by changes in viscoelasticity of the gel network, were examined.

4.2.1 Reaction Kinetics Of Ascorbic Acid Oxidation

The additional cost associated with maintaining foods at subzero temperature environments results in higher overall processing and/or storage costs, or, often, the adoption of improper storage conditions by the processor; i.e. storage at temperatures above T_g' , at which deteriorative reactions and collapse-related phenomena are possible (Karel, 1985). Recently, Levine and Slade (1986) have proposed that inclusion of water soluble carbohydrates into frozen systems, in order to elevate their T_g' and thus retard the rate of physico-chemical deterioration, could be an economical alternative to low temperature processing and storage. Using model food systems, they have demonstrated qualitatively the cryoprotective properties of some commercial starch hydrolysates.

In this study, the performance of SHPs as preservative agents, was quantitatively assessed by monitoring the effects of incorporating starch hydrolysates in frozen aqueous solutions on the oxidation kinetics of ascorbic acid solutions. In the presence of oxygen, ascorbic acid

(vitamin C) is oxidized to dehydroascorbic acid according to the reaction:



Using UV spectroscopy, the disappearance of the enediol can be followed and thus an apparent first order reaction rate constant is determined, as discussed in section 3.2.3.

For the subzero ($^{\circ}\text{C}$) reaction kinetic studies, a series of frozen test aliquots were prepared according to the method described in section 3.2.3 and stored at the specified subzero temperature. At regular time intervals, individual aliquots were removed from the low temperature bath, thawed, and the absorbances of the residual material was measured at 265 nm. Therefore, in figure 29, each point represents the amount of residual ascorbic acid in each particular aliquot drawn at time t . The reaction rate constant, k , was calculated from the steep portion (line AB) of the resulting curve using equation 5 (section 3.2.3). As shown in table 12, the reaction rate constant for all samples containing starch hydrolysate was significantly lower than that observed for the control sample at any given storage temperature. In general, the more concentrated samples (i.e. those prepared in the 40% w/v starch hydrolysate solutions) had lower reaction rates than the more dilute preparations. This can be explained by considering that at the testing temperatures, almost all mixtures were in the rubbery state where the diffusion rates of the reactants, and thus reaction rates, are controlled by the viscosity of the medium. For all samples, the rate of oxidation decreased with

Figure 29. Ascorbic acid oxidation in a solution of acetate buffered (0.02M, pH 5.5) ascorbic acid (2.5 mg mL^{-1}) containing H_2O_2 (1500 ppm) and Maltrin M150 (20% w/v), stored at -4°C ; reaction rate constant, k , was determined from line segment AB.

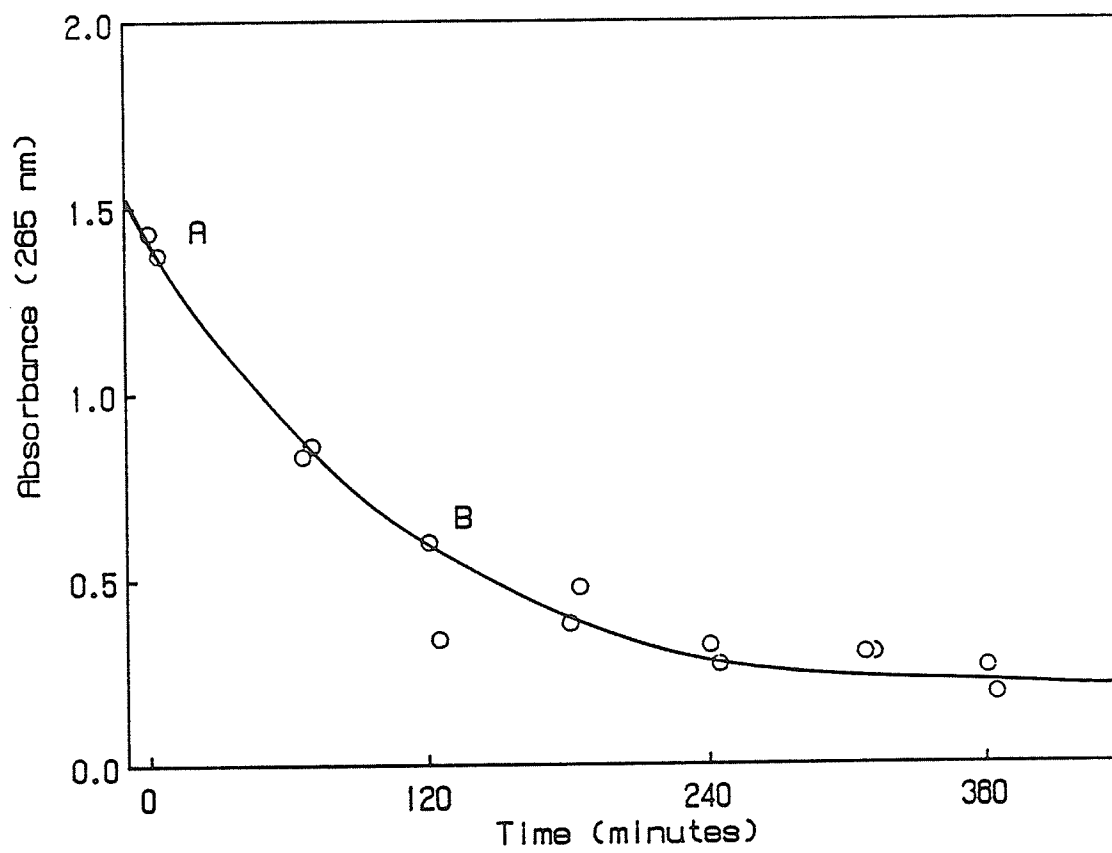


TABLE 12. Effect of SHP incorporation on the oxidation kinetics of frozen ascorbic acid solutions stored at subzero temperatures¹

Sample	$k \times 10^2$ (min ⁻¹)			
	-16°C	-12°C	-8°C	-4°C
Control	2.06±0.10	2.53±0.29	2.83±0.29	2.95±0.65
Star-Dri 42F (20%) ²	0.04±0.01	0.06±0.01	0.11±0.02	0.21±0.02
Maltrin M365 (20%)	0.04±0.01	0.09±0.01	0.16±0.04	0.41±0.07
Maltrin M200 (20%)	0.11±0.03	0.34±0.10	0.37±0.16	0.83±0.21
Maltrin M150 (20%)	0.15±0.01	0.19±0.06	0.53±0.16	0.94±0.28
Star-Dri 42F (40%)	0.01±0.00	0.03±0.01	0.05±0.03	0.27±0.11
Maltrin M365 (40%)	0.02±0.01	0.04±0.01	0.07±0.02	0.21±0.04
Maltrin M200 (40%)	0.05±0.02	0.07±0.02	0.42±0.13	0.77±0.22
Maltrin M150 (40%)	0.05±0.02	0.10±0.03	0.36±0.03	0.48±0.12

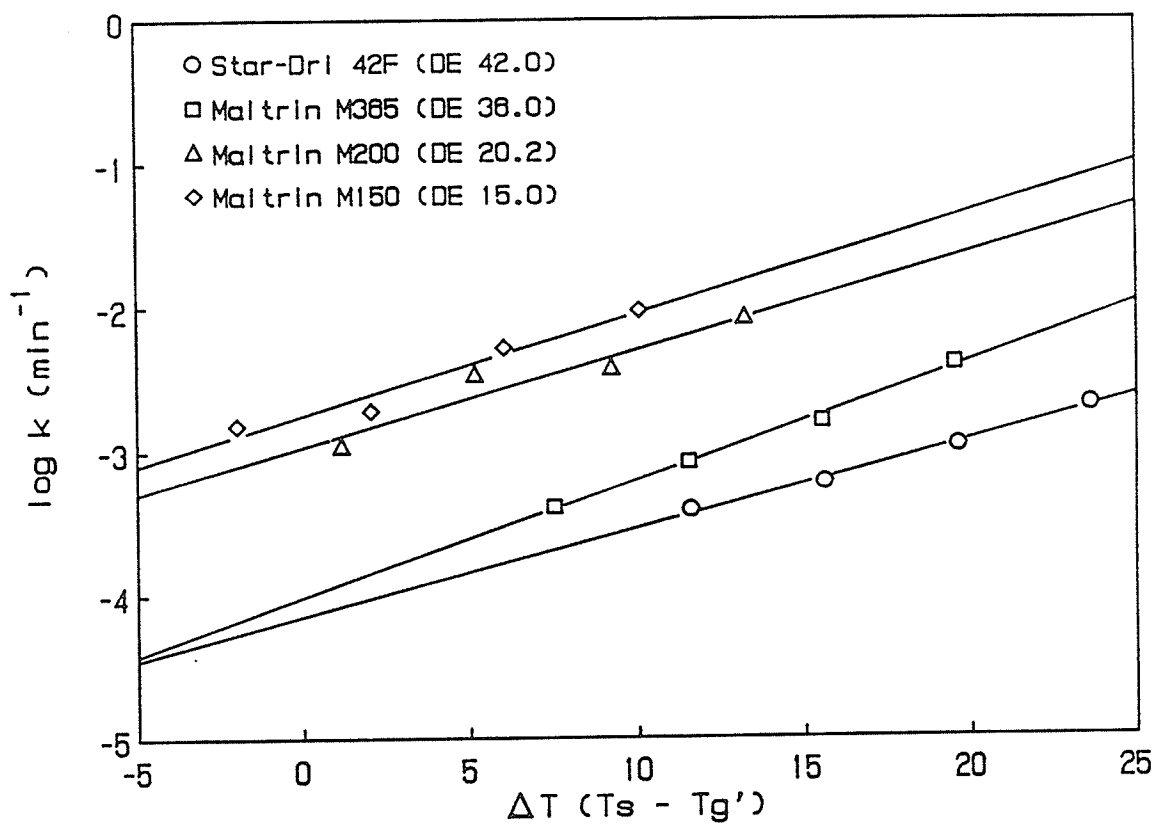
¹ Data are expressed as the reaction rate constant k ($k \times 10^2$ min⁻¹ ±sd; $n=2$), as determined by equation 5, section 3.2.3.

² Percents in parentheses represent the concentration (w/v) of the starch hydrolysate solutions.

decreasing storage temperature. One interesting observation was the increase in the reaction rate with decreasing DE values of the included hydrolysate. This behaviour was observed at all storage temperatures and at both starch hydrolysate concentrations tested. However, due to the sensitivity of k to the medium viscosity, the opposite behaviour was anticipated; i.e. a decrease in reaction rates with decreasing DE. The apparent inconsistency with what the theory predicts (i.e., decreased reaction rates for systems of elevated T_g') might be due to differences in the actual amounts of hydrogen peroxide available for ascorbic acid oxidation in the mixture. The effective concentration of this oxidant would depend on the extent of oxidation of the hydrolysates themselves by hydrogen peroxide. It would appear that, although there is an excess of oxygen in the reaction mixture initially, addition of hydrolysates, particularly those with a high concentration of reducing end groups (i.e. high DE), reduces the effective concentration of the oxidant in the composite system. As a result, samples containing starch hydrolysates of high DE would exhibit lower reaction rates than samples containing SHPs of lower DE.

The results for the effect of storage temperature on reaction kinetics, using the WLF formalism, of 20% w/v samples are illustrated graphically in figure 30. The data are presented as a plot of the log of the reaction rate constant as a function of ΔT ($T_{\text{storage}} - T_g'$ of the incorporated SHP). The linear relationship between these two parameters defines the reaction kinetics of an aqueous system as it approaches its glassy state. For all samples tested, the rate of ascorbic acid oxidation decreased as the storage temperature approached T_g' . This is in accord with the WLF equation (equation 1, section 2.3.1), which de-

Figure 30. Effect of temperature on ascorbic acid oxidation kinetics in frozen aqueous SHPs of varying DE.



scribes the reaction kinetics of synthetic polymers in the rubbery state. In fact, the relationships presented in figure 30 demonstrate the exponential temperature dependence of the rate of any deteriorative diffusion-controlled relaxation process. Though raising the T_g' above T_{storage} may not always be practical, the large energy savings associated with even a small elevation of T_g' can make the incorporation of SHPs into food formulations economically worthwhile.

The measured k values for the control samples (table 12) were consistently higher than those reported in literature. Hatley et al. (1986) recorded an average k value of $1.79 \times 10^2 \text{ min}^{-1}$ at -20°C for ascorbic acid solutions with a concentration of $1.7 \text{ mg } 100\text{mL}^{-1}$. This value seems reasonable when compared to our results ($k = 2.06 \times 10^2 \text{ min}^{-1}$ at -16°C), considering that our experiments were conducted on solutions of slightly higher concentration of ascorbic acid ($2.5 \text{ mg } 100 \text{ mL}^{-1}$). On the other hand, Thompson and Fennema (1971) calculated k values that were 5-6X lower than those that we observed for dilute solutions ($2.5 \text{ mg } 100 \text{ mL}^{-1}$) of ascorbic acid. However, as Hatley et al. (1986) pointed out, these low k values reported by Thompson and Fennema could be a direct consequence of inadequate supply of oxygen. In both our study and that of Hatley et al. (1986), hydrogen peroxide was added to the sample solution to ensure a fresh supply of oxygen throughout the reaction.

Results for the oxidation kinetics study of ascorbic acid solutions stored at temperatures that exceeded 0°C are given in table 13. As was found for the low-temperature samples, the reaction rate constant for each of the above 0°C samples decreased with decreasing temperature. However, although these samples were stored at temperatures well within the range ($T_g' - T_g' + 100^\circ\text{C}$) where WLF kinetics apply, they are still

TABLE 13. Effect of SHP incorporation on the oxidation kinetics of ascorbic acid solutions stored at above 0°C temperatures¹

Sample	$k \times 10^2 \text{ (min}^{-1}\text{)}$				
	5°C	10°C	15°C	20°C	25°C
Control	1.30±0.20	3.90±1.20	8.50±2.30	8.89±0.09	13.90±4.50
Maltrin M365 (20%) ²	0.25±0.06	0.43±0.08	0.50±0.08	0.55±0.09	4.26±0.95
Maltrin M200 (20%)	0.93±0.17	2.53±0.50	2.90±0.73	4.21±0.10	7.70±1.93
Maltrin M150 (20%)	0.67±0.13	1.59±0.19	2.70±0.43	3.39±0.80	7.10±1.85
Maltrin M365 (40%)	0.08±0.02	0.22±0.03	0.23±0.05	0.40±0.12	0.70±0.13
Maltrin M200 (40%)	0.10±0.03	1.48±0.33	3.60±0.90	7.30±1.05	12.01±1.64
Maltrin M150 (40%)	0.84±0.20	1.77±0.53	3.20±1.00	5.35±0.72	10.10±2.63

¹ Data are expressed as the reaction rate constant k ($k \times 10^2 \pm \text{sd}$; $n=2$), as determined by equation 5, section 3.2.3.

² Percents in parentheses represent the concentration (w/v) of the starch hydrolysate solutions.

very fluid due to their relatively low solids content. As a result, Arrhenius kinetics would be expected to govern the reaction rates in this temperature regime. As for the subzero study, at each temperature, the reaction rate constants for samples containing SHPs were lower than those observed for the control sample. Again this may be attributed to differences in the amount of hydrogen peroxide available for ascorbic acid oxidation. In the control sample all of the hydrogen peroxide is available for oxidation of ascorbic acid. Conversely, in the test samples, the hydrolysates themselves may be oxidised by the hydrogen peroxide, so that less oxidant is available to react with the ascorbic acid. Moreover, relationships between sample concentration or DE and rate of ascorbic acid oxidation were less clear. Accurate assessment of the effect of the DE of the hydrolysate on k might also be complicated by the presence of reducing sugars and impurities in the SHPs incorporated into the test mixtures.

The reaction rate constants obtained for the control samples at each temperature (table 13) were much higher (1.5-10X higher) than those reported in literature. In studies by Thompson and Fennema (1971), samples were removed and their absorbance measured after 10 min (time zero) and at subsequent time intervals. Hatley et al. (1986), on the other hand, took samples immediately after the addition of ascorbic acid to the buffer/peroxide mixture (time zero) and at regular time intervals thereafter, but held them at 30°C for 5 min prior to the actual measurement. In our studies we observed that the reaction began to slow down as early as 4 min after the addition of ascorbic acid to the buffer/peroxide mixture (when stored at 25°C). Thus it appears that in the studies of both Thompson and Fennema (1971) and Hatley et al. (1986) only the

"tail-end" of the reaction is observed, and thereby an unrealistic assessment of the rate of ascorbic acid oxidation was made.

In comparing the results between the sub- and above-zero tests (tables 12 and 13) it was observed that, for all samples analysed, the rate of ascorbic acid oxidation increased with increasing temperature from -16 to 25°C. Discrepancies in this pattern were observed only for samples stored at -4 and 5°C and most likely reflect differences in the methodologies used for sample measurements at subzero and above zero temperature regimes.

4.2.2 Antistaling Properties Of Starch Hydrolysates

Since starch gels are composites, in which gelatinized granules are embedded in an amylose gel matrix (Miles et al., 1985), one approach to preventing starch retrogradation would be to interrupt the interchain associations between amylose molecules. In related studies by Welsh et al. (1980) on hyaluronate solutions and by Morris and co-workers (1980) on carrageenan, alginate, and xanthan-galactomannan gels, it has been demonstrated that a form of competitive inhibition can be used to prevent polymer gelation. Results from these studies indicated that short chain segments (of sufficient length to participate in junction zones) are in competition with longer polymer chains for binding sites on the gel network. Since these short chain segments are able to participate in only one stable co-operative junction zone (and not two or more required for establishing a continuous crosslinked network of longer polymer chains), they do not contribute to intermolecular network formation. In this context, we have examined the effect of incorporating soluble starch hydrolysates of varying DE on the gel network development of

gelatinized wheat and waxy maize starches.

Traditionally, starch gels have been examined under large deformations that can cause damage to the gel structure. A better way of probing the structural changes of gels with time is by means of nondestructive rheological methods, such as small amplitude oscillatory tests. Using the oscillatory mode of the Bohlin rheometer, the development of gel strength over time, as manifested by increasing values of the storage modulus (G'), was followed. Starch hydrolysates were added to a level of 20% by weight on a starch basis.

Figure 31 shows plots of storage modulus (G') as a function of time for wheat starch (control) and wheat starch-SHP composite gels. For each sample tested, G' began to level off after 30-40 min of storage. Values for G' within this pseudoplateau region (obtained after 10 hr storage), given in table 14, were between 0.76 (Star-Dri 1 + WS) and 3.27 (Control-WS 24% w/v) kPa. Standard deviations for duplicate analyses were less than 10% of the mean value. In comparing the two control samples (WS 24% w/v and WS 20% w/v table 14; and lines 1 and 2, respectively, figure 31), it is seen that the gel strength increased with increasing polymer concentration. Miles et al. (1985) and Clark et al. (1989) have reported similar findings for less concentrated (1.0-7.0% w/v) amylose gels. According to Miles et al. (1985), amylose gelation involves a phase separation into polymer-rich and polymer-deficient regions, with the development of a three-dimensional network occurring in the polymer-rich phase. Furthermore, they noted that the local composition of the polymer-rich phase appears to be independent of overall polymer concentration. This being the case, the greater gel strength observed for the more concentrated wheat starch gel (control sample 24%

Figure 31. Effect of commercial SHPs on the gel strength (storage modulus, G') of gelatinized wheat starch (WS) samples; starch hydrolysates were added at 4% w/v to 20% w/v wheat starch dispersions resulting in a total solids content of 24% w/v.

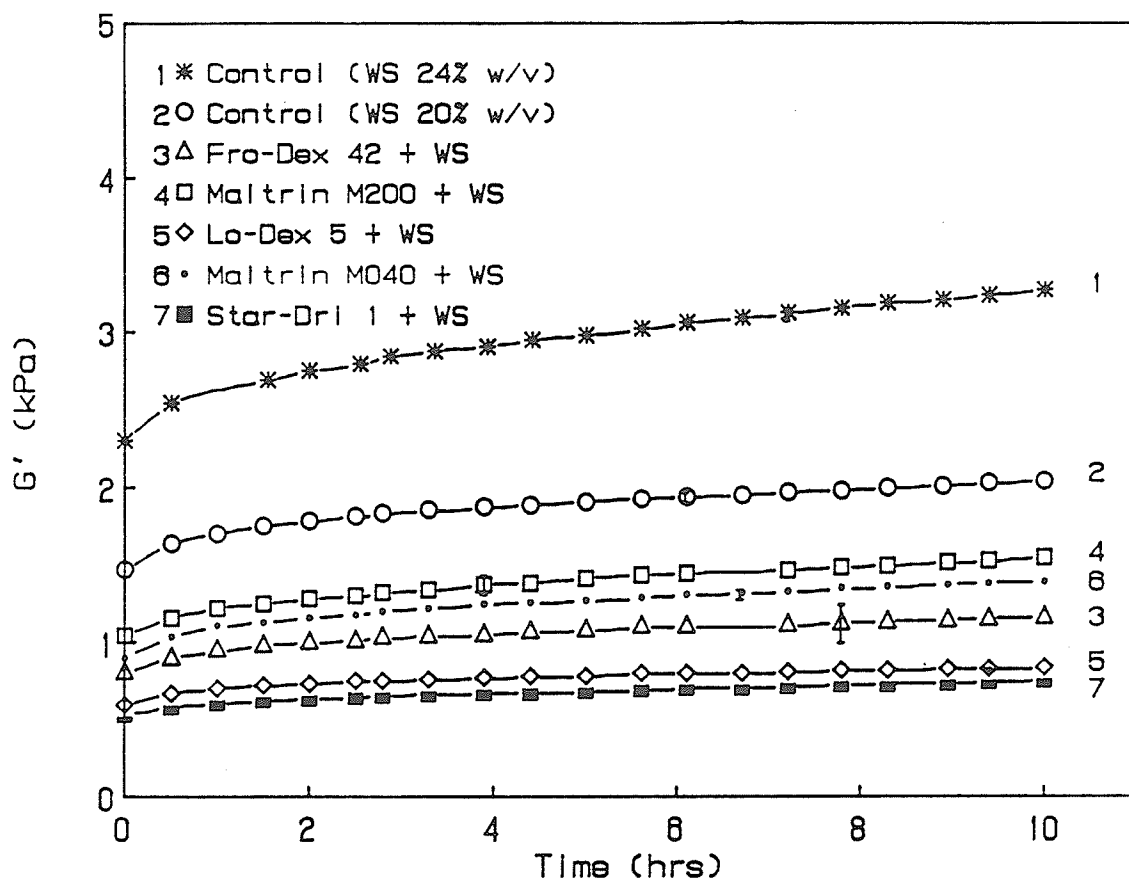


TABLE 14. Effect of SHP¹ on the retrogradation² of gelatinized wheat starch (WS) samples

Sample	G' (kPa) ³
Control (WS 20% w/v)	2.04±0.03 ^a
Control (WS 24% w/v)	3.27±0.05 ^b
Fro-Dex 42 + WS	1.17±0.12 ^c
Maltrin M200 + WS	1.55±0.07 ^d
Lo-Dex 5 + WS	0.84±0.01 ^e
Maltrin M040 + WS	1.40±0.02 ^f
Star-Dri 1 + WS	0.76±0.13 ^e

¹ Starch hydrolysates were added at 4% w/v to 20% w/v wheat starch dispersions resulting in a total solids content of 24% w/v.

² As reflected by increasing storage modulus values (G').

³ Reported G' are those obtained after 10 hr; values followed by the same letter are not significantly different ($p \leq 0.05$).

w/v, line 1, figure 31) may be attributed to a higher concentration of leached amylose in the intergranular regions. For wheat starch, rigidity of the composite gels was greatly reduced when hydrolysates were included (figure 31). With regard to the magnitude of this effect in relation to the DE of the added hydrolysate, there were no clear trends. For example, gels made with Lo-Dex 5 (DE 5) and Star-Dri 1 (DE 1) (lines 5 and 7 respectively, figure 31) exhibited limiting storage modulus values that were approximately 4X lower than that of wheat starch alone (table 14); this can be rationalized in terms of competitive inhibition of amylose chains. Apparently, these low DE starch hydrolysates are of sufficient chain length to participate in junction zones, and thereby inhibit the formation of a continuous network of crosslinked longer amylose chains. However, wheat starch gels that contained Maltrin M040, a starch hydrolysate of comparable DE (4.7), but made by another manufacturer, were much stiffer (line 6, figure 31). Chain polydispersity, degree of branching, as well as differences in the degree of granule swelling and amylose exudation during heating in the presence of each particular hydrolysate are the likely sources of such inconsistency. Clearly, further studies on gels with well characterized fractions are required to reveal specific interactions in the amylose network as well as between the continuous and dispersed phases of the composite gels, and thus establish relationships between structure and gel rheology.

The effect of commercial SHPs on gel development in waxy maize starch systems is illustrated in figure 32. A sigmoidal-shaped gelation curve, characteristic of amylopectin gel development (Ring et al., 1987) was observed for each sample. Limiting values of G' for the waxy maize dispersions analysed, after 18.9 hr storage, were in the range of

Figure 32. Effect of commercial SHPs on the gel strength (storage modulus, G') of gelatinized waxy maize (WM) starch samples; starch hydrolysates were added at 7.6% w/v to 38% w/v waxy maize starch dispersions resulting in a total solids content of 45.6% w/v.

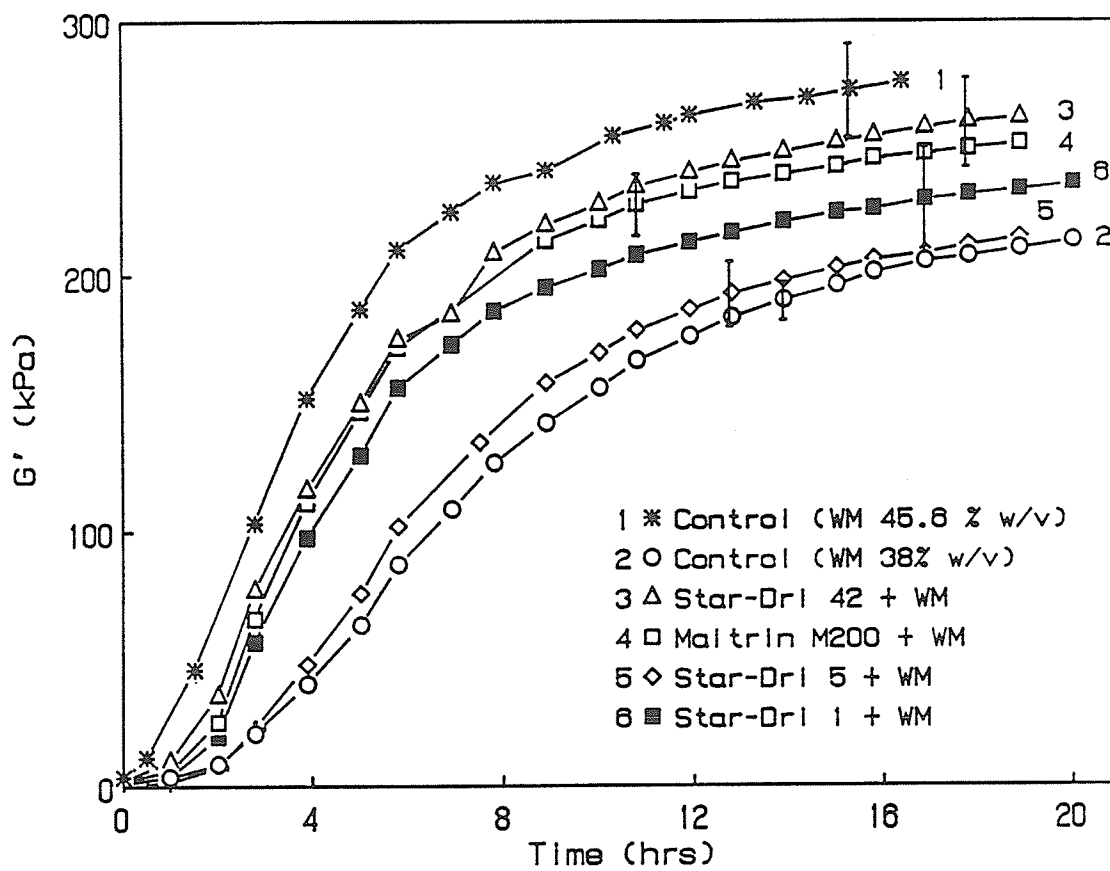


Table 15. Effect of SHP¹ on the retrogradation² of gelatinized waxy maize (WM) starch samples

Sample	G' (kPa) ³
Control (WM 38% w/v)	210.5±6.5 ^a
Control (WM 45.6% w/v)	281.0±12.0 ^b
Star-Dri 42 + WM	262.0±18.0 ^{ab}
Maltrin M200 + WM	252.0±13.0 ^{ab}
Star-Dri 5 + WM	215.0±18.0 ^a
Star-Dri 1 + WM	233.5±19.5 ^{ab}

¹ Starch hydrolysates were added at 7.6% w/v to 38% w/v waxy maize dispersions resulting in a total solids content of 45.6% w/v.

² As reflected by increasing storage modulus values (G').

³ Reported G' are those obtained after 18.9 hr; values followed by the same letter are not significantly different ($p \leq 0.05$).

210.5-281.12 kPa (table 15). Deviations in the modulus values for repeated runs were less than 11% of averaged values. In contrast to wheat starch gels, all composite waxy maize-starch hydrolysate gels exhibited a greater rate of storage modulus development and attained slightly higher limiting G' values, after 20 hr storage at 6°C than the less concentrated (38% w/w) waxy maize control sample (line 2, figure 32). These results imply that depolymerized starch chains have no inhibitory effect on gel network formation involving the branched starch component at high concentrations. For samples that contained SHPs, the increases in modulus values (G'), compared to waxy maize alone (38% w/v), most likely reflect increases in the total solids (up to 45.6% w/w). Waxy maize alone gave a significantly higher G' value (281.0 kPa) at 45% concentration versus the 38% control sample (210.5 kPa). These results, therefore, suggest that, while starch hydrolysates competitively inhibit amylose network formation, they have no apparent effect (aside from increasing the % solids and a possible plasticizing effect) on the amylopectin component of starch gels. The data of figure 31 and 32 are also consistent with the findings of Ring (1987), who reported that: a) amylose and amylopectin become incompatible in concentrated aqueous solutions, leading to formation of separate amylose- and amylopectin-rich phases; and b) amylose and amylopectin form gels by two different mechanisms - amylose, primarily by entanglement coupling of polymer chains leading to three dimensional network formation, and amylopectin, by intra- and intermolecular crystallization.

5 CONCLUSIONS AND RECOMMENDATIONS

The present study was undertaken to investigate the thermophysical and rheological characteristics of commercial starch hydrolysis products (SHPs) in relation to their functionality in food systems.

The SHPs used in this study were from corn and potato starch sources and obtained from various suppliers. High performance liquid chromatography (HPLC) proved to be an effective method of determining the oligosaccharide composition of these materials. It was found that the starch hydrolysates were more accurately characterized by their oligosaccharide composition than by their dextrose equivalent (DE). In general, debranching of the SHPs with a purified pullulanase preparation did not significantly change their oligosaccharide profiles. This result would appear to indicate that, in their native state, the SHPs used in this study contained few α -1,6 branch points.

The thermomechanical behaviour of commercial SHPs at subzero temperatures, as examined by differential scanning calorimetry (DSC), was found to be indicative of sample composition and structure, as well, dependent on the rate of heating and cooling. The glass transition temperature (T_g') of the maximally concentrated solute in frozen aqueous-carbohydrate solutions was between 229.75-259.65 K for monodisperse glucose oligomers and 245.58-267.05 K for polydisperse starch hydrolysates. Moreover, T_g' was found to be inversely correlated with the reciprocal molecular weight in monodisperse systems ($r = -0.990$,

$p < 0.001$), and DE in polydisperse systems ($r = -0.991$, $p < 0.001$). A direct plot of T_g' as a function of molecular weight, for the oligosaccharide standards analysed, revealed a plateau region representing the limit of T_g elevation (257.23 K) and corresponding to the onset of chain entanglement. The importance of these relationships, from a technological point of view, is that the physical properties of food products can be modified, and their stabilities improved, by incorporating SHPs of specific molecular weight or DE in order to elevate T_g' above the storage temperature. Furthermore, these relationships are potentially useful to food processors in selecting the appropriate SHP for a particular food formulation.

For the SHPs tested, T_g' was slightly depressed at higher solute concentrations ($>50\%$ w/v). This finding would seem to indicate that freezing of aqueous-SHPs, under the experimental protocol used, was a non-equilibrium process and, the additional water trapped between ice crystals, as a result of the fast freeze, had a plasticizing effect on the glass. As well, ice recrystallization was observed for all samples exhibiting depressed T_g' values, supporting the claim that these materials were subject to non-equilibrium freezing. In a related experiment, any relationship between the unfreezable water content of frozen aqueous-SHPs and their molecular size was not found. Thus, although DSC can be used to measure physical parameters, such as T_g' and ice melting enthalpies, that characterize phase transitions at subzero temperatures of aqueous-SHPs, more accurate results would be attained if the rate of cooling could be controlled; i.e. if the rate of cooling was lowered so that freezing of these materials would be an equilibrium process. Furthermore, it was noted that increasing the rate of heating of frozen

aqueous-SHPs raised their apparent T_g' .

A predictive model was derived, using the Flory-Fox theory (Fox and Flory, 1954) describing the thermal properties of polymer composites, which provided estimates of T_g' based on the oligosaccharide composition of starch hydrolysates. For both native and debranched SHPs a linear relationship between T_g' -predicted (calculated from the Flory-Fox equation) and T_g' -measured (determined by DSC) was observed. However, in both sample sets, there appeared to be some deviation of the measured values from what theory predicts, particularly for high DE samples. Further investigation into the factors that affect T_g' in food polymer blends (e.g. intermolecular interactions) are recommended for the development of an equation that would more accurately predict the T_g' of high molecular weight commercial starch hydrolysates.

The viscosity of aqueous-SHP solutions increased with increasing solute concentration and decreasing solute DE. Values of viscosity ranged from 2.90×10^3 - 3.94×10^4 Pa.s for 20% w/v samples and 6.92×10^3 - 2.72×10^6 Pa.s for 40% w/v mixtures at a shear rate of 1.47×10^3 s⁻¹. Based on data from shear rate sweeps, the majority of SHPs analysed exhibited classical Newtonian behaviour; i.e. a constant viscosity over a broad range of shear rates. These results suggested that the thickening and bodying properties of commercial starch hydrolysates in fabricated food formulations can be attributed primarily to their effect of increasing both the total solids content and average molecular weight of the final product. However, data from shear rate sweeps performed on Star-Dri 1 (DE 1), indicated that low DE SHPs further contribute to viscosity development by forming a rubber-like viscoelastic network via

polymer chain entanglement.

Using UV spectroscopy, and working with model systems consisting of aqueous solutions of ascorbic acid, it was demonstrated that starch hydrolysates could be used to effectively inhibit deteriorative reactions in stored food products. Retarded rates of ascorbic acid (vitamin C) oxidation were observed for solutions containing SHP. Reaction rate constants, k , varied between 1.30-13.90 min^{-1} for control samples (containing no SHP) as compared to only 0.04-10.10 min^{-1} for test mixtures (containing SHP). For frozen samples, at each temperature, k was lower in the dilute preparations (20% w/v) as compared to the 40% w/v solutions. This result suggested that at the subzero storage temperatures employed, the diffusion rates of the reactants, and thus the reaction rates, were controlled by the viscosity of the medium. Furthermore, it was found that ascorbic acid oxidation in the frozen solutions appeared to be governed by WLF kinetics. Because of the exponential temperature dependence of the rate of deteriorative reactions in food systems maintained within the WLF temperature regime ($T_g' - T_g' + 100 \text{ K}$), elevation of T_g' by incorporating SHPs can greatly improve product quality and storageability. An attempt to relate ascorbic acid oxidation kinetics to the DE of the incorporated starch hydrolysate produced inconclusive results, presumably due the reaction of the oxidant (hydrogen peroxide) with the SHP. Further investigations using alternate test reactions (possibly an enzymic reaction system) to demonstrate the effect of solute molecular size on the retardation of deteriorative processes in frozen food systems is suggested.

The antistaling properties of SHPs in polysaccharide gels were examined using small amplitude oscillatory tests. This nondestructive

technique measured both the rate and extent of structural development in gelatinized wheat and waxy maize starches. Variability between repeated runs was more likely due to differences in sample composition than limitations of the measuring system. Based on data from gel strength measurements (storage modulus, G'), starch hydrolysates in starch systems appeared to competitively inhibit amylose network formation, but had no apparent influence (aside from a possible plasticizing effect) on the amylopectin component of starch gels. These findings further suggested that amylose and amylopectin become incompatible in concentrated aqueous solutions, thus leading to formation of separate amylose- and amylopectin-rich phases. While amylose molecules appear to gel primarily by entanglement coupling of the polymer chains (a very rapid process), amylopectin gelation is due to crystallization over extended time periods. However, additional development of the dynamic viscosity methodology and further studies on gels with well characterized fractions are required to more accurately assess the antistaling properties of SHPs in gelatinized starch systems.

Overall, the results of the present studies have demonstrated that the functionality of commercial starch hydrolysates is directly related to the thermomechanical and rheological properties of these polymeric materials. The next step in this research area would be to test the theories derived from synthetic polymer science in actual food systems. In this context, sensory analysis and microstructure studies in conjunction with traditional methodologies employed to probe solution properties of polymeric materials (e.g. thermal analysis and rheological measurements) would be required.

REFERENCES CITED

- Allcock, H.R. and Lampe, F.W. 1981. Contemporary polymer chemistry. Prentice-Hall Inc., New Jersey, pp. 423-447.
- Angell, C.A. and Choi, Y. 1986. Crystallization and vitrification in aqueous systems. *J. Microscop.* 141:3:251-261.
- Anonymous. Maltrin maltodextrin and corn syrup solids: Brilliance in food and pharmaceutical technology. Bulletin 11005, Grain Processing Corp., Muscatine, Iowa, p. 14.
- Banks, W., Greenwood, C.T., and Muir, D.D. 1971. Studies on starches of high amylose-content. Part 14. The fractionation of amylo maize starch by aqueous leaching. *Starke.* 23:199-200.
- Banks, W. and Greenwood, C.T. 1975. Starch and its components. Halsted Press, New York.
- Bevilacqua, A.E. and Zaritzky, N.E. 1982. Ice recrystallization in frozen beef. *J. Fd. Sci.* 47:1410-1414.
- Biliaderis, C.G., Page, C.M. and Maurice, T.J. 1986. On the multiple melting transitions of starch/monoglyceride systems. *Food Chem.* 22:279-295.
- Biliaderis, C.G., Page, C.M., Maurice, T.J. and Juliano, B.O. 1986. Thermal characterization of rice starches: A polymeric approach to phase transitions of granular starch. *J. Ag. Fd. Chem.* 34:6-14.
- Biliaderis, C.G. 1989. Thermal analysis of food carbohydrates. In: Thermal analysis of foods, V.R. Harwalkar and C.Y. Ma (Eds.), Elsevier Applied Publ. (In press).
- Billmeyer, F.W. 1984. Textbook of polymer science. Wiley-Interscience, New York.
- Birch, G.G. and Kearsley, M.W. 1974. The fractionation of glucose syrups by reverse osmosis. *Starke* 26:220-227.
- Brooks, J.R. and Griffin, V.K. 1987. Saccharide analysis of corn syrup solids and maltodextrins using high performance liquid chromatography. *Cereal Chem.* 64:4:253-255.

- Brydson, J.A. 1972. The glass transition, melting point and structure. In: Polymer science, A.D. Jenkins (Ed.), North-Holland Publishing Co., London, pp. 193-249.
- Chabot, J.F., Allen, J.E. and Hood, L.F. 1978. Freeze-etch ultrastructure of waxy maize and acid hydrolysed waxy maize starch granules. *J. Fd. Sci.* 43:727-730, 734.
- Clark, A.H., Gidley, M.J., Richardson, R.K. and Ross-Murphy, S.B. 1989. Rheological studies of aqueous amylose gels: The effect of chain length and concentration on gel modulus. *Macromolecules* 22:346-351.
- Cowie, J.M.G. 1973. *Polymers: Chemistry and physics of modern materials.* International Textbook Co. Ltd. London.
- Dziedzic, S.Z. and Kearsley, M.W. 1984. Physico-chemical properties of glucose syrups. In: Glucose syrups: Science and technology, S.Z. Dziedzic and M.W. Kearsley (Eds.), Elsevier Applied Science Publishers, London, pp. 138-168.
- Eisenberg, A. 1984. The glassy state and the glass transition. In: Physical properties of polymers, J.E. Marks (Ed.), American Chem. Soc., Washington, D.C., p. 59.
- Ferry, J.D. 1980. *Viscoelastic properties of polymers.* John Wiley and Sons, New York.
- Flink, J.M. 1983. Structure and structure transitions in dried carbohydrate materials. In: Physical properties of foods, M. Peleg and E.B. Bagley (Eds.), AVI Publ. Co. Inc., Westport, Conn., pp. 473-521.
- Folkes, D.J. and Brookes, A. 1984. Analysis and characterization of glucose syrups. In: Glucose syrups: Science and technology. S.Z. Dziedzic and M.W. Kearsley (Eds.), Elsevier Applied Science Publishers, London, pp. 197-245.
- Fox, T.G. and Flory, P.J. 1954. *J. Polym. Sci.* 14:315. As cited by: J. F. Fuzek 1980. Glass transition temperature of wet fibers. In: Water in polymers, S. Powland (Ed.), ACS Symposium Series, vol. 127, American Chem. Society, Washington, D.C., pp. 515-530.
- Franks, F. 1982. The properties of aqueous solutions at subzero temperatures. In: Water: A comprehensive treatise vol. 7, F. Franks (Ed.), Plenum Press, New York., pp. 215-334.
- Franks, F. 1985. Complex aqueous systems at subzero temperatures. In: Properties of water in foods, D. Simatos and J.L. Multon (Eds.), Martinus Nijhoff Publishers, The Netherlands, pp. 1-23.
- Franks, F. 1986. Metastable water at subzero temperatures. *J. Microscop.* 141:3:243-249.

- French, D. 1984. Physical and chemical organization of starch granules. In: Starch: Chemistry and technology, R.L. Whistler, E.F. Paschall and J.N. BeMiller (Eds.), Academic Press, New York, pp. 183-249.
- Fullbrook, P.D. 1984. The enzymic production of glucose syrups. In: Glucose syrups: Science and technology, S.Z. Dziedzic and M.W. Kearsley (Eds.), Elsevier Applied Science Publishers, London, pp. 65-115.
- Harper, E.K. and Shoemaker, C.F. 1983. Effect of locust bean gum and selected sweetening agents on ice recrystallization rates. J. Fd. Sci. 48:1801-1803.
- Hately, R.H.M., Franks, F. and Day, H. 1986. Subzero-temperature preservation of reactive fluids in the undercooled state. II. The effect on the oxidation of ascorbic acid of freeze concentration and undercooling. Biophys. Chem. 24:187-192.
- Herrington, T.M. and Branfield, A.C. 1984. Physico-chemical studies on sugar glasses. I. Rate of crystallization. J. Food Technol. 19:409-425.
- Hobbs, L. 1986. Corn-based sweeteners. Cereal Foods World 31:12: 852,854,856,858.
- Hood, L.F. 1982. Current concepts of starch structure. In: Food carbohydrates, D.R. Lineback and G.E. Ingel (Eds.), AVI, pp. 217-236.
- Hoseney, R.C., Zeleznak, K.J. and Lai, C.S. 1986. Wheat gluten: A glassy polymer. Cereal Chem. 63:285-286.
- Howling, D. 1979. The general science and technology of glucose syrups. In: Sugar: Science and technology, G.G. Birch and K.J. Parker (Eds.), Applied Sci. Publ., London, pp. 259-285.
- Jin, X., Ellis, T.S. and Karasz, F.E. 1984. The effect of crystallinity and crosslinking on the depression of the glass transition temperature in Nylon 6 by water. J. Polym. Sci., Polym. Phys. Ed. 22:1701-1717.
- Karel, M. 1985. Effects of water activity and water content on mobility of food components and their effects on phase transitions in food systems. In: Properties of water in foods, D. Simatos and J.G. Multon (Eds.), Martinus Nijhoff Publ., Dordrecht, Netherlands, pp. 153-169.
- Karel, M. and Flink, J.M. 1983. Some recent developments in food dehydration research. In: Advances in drying, A.S. Mujumdar (Ed.), Hemisphere Publish. Corp., Washington D.C., pp. 118-129.
- Kassenbeck, P. 1978. Contribution to the knowledge on distribution of amylose and amylopectin in starch granules. Starke 30:40-46.
- Katz, F.R. 1986. Maltodextrins. Cereal Fds. World 31:12:866-867.

- Kearsley, M.W. and Birch, G.G. 1975. Selected physical properties of glucose syrup fractions produced by reverse osmosis I. Specific rotation, average molecular weight, solubility rate. *J. Fd. Technol.* 10:613-623.
- Levine, H. and Slade, L. 1986. A polymer physico-chemical approach to the study of commercial starch hydrolysis products (SHPs). *Carbohydr. Polym.* 6:213-244.
- Levine, H. and Slade, L. 1988. Principles of "cryostabilization" technology from structure/property relationships of carbohydrate/water systems - A review. *Cryo-Letters* 9:21-63.
- Lineback, D.R. 1984. The starch granule organization and properties. *Bakers Digest* March 13, 1984, pp.16-21.
- MacKenzie, A.P. 1977. Non-equilibrium freezing behaviour of aqueous systems. *Phil. Trans. R. Soc. Lond. B.* 278:167-189.
- Marshall, J.J. 1975. Application of enzymic methods to the structural analysis of polysaccharides: Part 1. *Adv. Carbohydr. Chem. and Biochem.* 30:257-371.
- Maurice, T.J., Slade, L., Sirret, R. and Page, C.M. 1985. Polysaccharide-water interaction - thermal behaviour of rice starch. In: Properties of water in foods in relation to quality and stability, D. Simatos and J.L. Multon (Eds.), Martinus Nijhoff Publishers, Dordrecht, pp. 211-226.
- McDonald, M. 1984. Uses of glucose syrups in the food industry. In: Glucose syrups: Science and technology, S.Z. Dziedzic and M.W. Kearsley (Eds.), Elsevier Applied Science Publishers, London and New York, pp. 247-263.
- McNulty, P.B. and Flynn, D.G. 1977. Force-deformation and texture profile behaviour of aqueous sugar glasses. *J. Text. Stud.* 8:417-431.
- Miles, M.J., Morris, V.J., Orford, P.D. and Ring, S.G. 1985. The roles of amylose and amylopectin in the gelation and retrogradation of starch. *Carbohydr. Res.* 135:271-281.
- Moreyra, R. and Peleg, M. 1981. Effect of equilibrium water activity on the bulk properties of selected food powders. *J. Fd. Sci.* 46:1918-1922.
- Morris, E.R., Rees, D.A., Robinson, G. and Young, G.A. 1980. Competitive inhibition of interchain interactions in polysaccharide systems. *J. Mol. Biol.* 138:363-374.
- Murray, D.G. and Luft, L.R. 1973. Low-DE corn starch hydrolysates. *Food Technol.* 17:3:32-33,36,38,40.

- Mussulman, W.C. and Wagoner, J.R. 1968. Electron microscopy of unmodified and acid-modified corn starches. *Cereal Chem.* 45:162-171.
- Nielsen, L.E. 1974. Mechanical properties of polymers and composites (vol. 1), Marcel Dekker Inc., New York.
- Pancoast, H.M. and Junk, W.R. 1980. Handbook of sugars. AVI Publishing Co., Westport, Conn.
- Ring, S.G. 1985. Some studies on starch gelation. *Starke* 37:3:80-83.
- Ring, S.G., Colonna, P., I'Anson, K.J., Kalichevsky, M.T., Miles, M.J., Morris, V.J. and Orford, P.D. 1987. The gelation and crystallisation of amylopectin. *Carbohydr. Res.* 162:277-293.
- Robin, J.P., Mercier, C., Charbonniere, R. and Guilbot, A. 1975. Linterized starches. Chromatographic and enzymatic studies on the insoluble residues remaining after the acid hydrolysis of cereal starches, particularly waxy maize. *Starke* 27:36-46.
- Schenz, T.W., Rosolen, A.M., Levine, H. and Slade, L. 1984. In: Proceedings of the 13th North American Thermal Analysis Society Conference, A.R. McGhie (Ed.), NATAS, Univ. Penn., PA, pp. 57-61.
- Sears, J.K. and Darby, J.R. 1982. The technology of plasticizers. John Wiley and Sons, New York.
- Simatos, D., Faure, M., Bonjour, E. and Couach, M. 1975. In: Water relations of foods, R.B. Duckworth (Ed.), Academic Press, New York, pp. 193-209.
- Slade, L. and Levine, H. 1984. Thermal analysis of starch and gelatin. In: Proceedings of the 13th North American Thermal Analysis Conference, A.R. McGhie (Ed.), NATAS, Univ. Penn., PA.
- Slominska, L. and Maczynski, M. 1985. Studies on the application of pullulanase in starch saccharification process. *Starke* 37:386-390.
- Soesanto, T. and Williams, M.C. 1981. Volumetric interpretations of viscosity for concentrated and dilute sugar solutions. *J. Phys. Chem.* 85:3338-3341.
- Swinkels, J.J.M. Sources of starch, its chemistry and physics. In: Starch conversion technology, G.M.A. van Beynum and J.A. Roels (Eds.), Marcel Dekker Inc., New York, pp. 15-46.
- Tegge, G. 1984. Glucose syrups - the raw material. In: Glucose syrups: Science and technology, S.Z. Dziedzic and M.W. Kearsley (Eds.), Elsevier Applied Science Publishers, London, pp. 9-64.
- Thompson, L.U. and Fennema, O. 1971. Effect of freezing on oxidation of L-ascorbic acid. *J. Agr. Food Chem.* 19:1:121-124.

- To, E.C. and Flink, J.M. 1978a. 'Collapse,' a structural transition in freeze dried carbohydrates. I. Evaluation of analytical methods. J. Fd. Technol. 13:551-565.
- To, E.C. and Flink, J.M. 1978b. 'Collapse,' a structural transition in freeze dried carbohydrates. II. Effect of solute composition. J. Fd. Technol. 13:567-581.
- To, E.C. and Flink, J.M. 1978c. 'Collapse,' a structural transition in freeze dried carbohydrates. Prerequisite of recrystallization. J. Fd. Technol. 13:583-594.
- Tsourouflis, S., Flink, J.M. and Karel, M. 1976. Loss of structure in freeze-dried carbohydrate solutions: Effect of temperature, moisture content and composition. J. Sci. Fd. Agric. 27:509-519.
- Tung, M.A. 1988. Some rheological principles involved in food texture. Dept. of Food Science and Technology, University of Nova Scotia, Halifax, Nova Scotia, pp. 17.
- Welsh, E.J., Rees, D.A., Morris, E.R. and Madden, J.K. 1980. Competitive inhibition evidence for specific intermolecular interactions in hyaluronate solutions. J. Mol. Biol. 138:375-382.
- White, G.W. and Cakebread, S.H. 1966. The glassy state in certain sugar-containing food products. J. Fd. Technol. 1:73-82.
- Yamaguchi, M., Kainuma, K. and French, D. 1979. Electron microscopic observations of waxy maize starch. J. Ultrastruct. Res. 69:249-261.
- Young, R.J. 1981. Introduction to polymers. Chapman and Hall, London.
- Zobel, H.F. 1988. Molecules to granules: A comprehensive starch review. Starke 40:44-50.